

Open Research Online

The Open University's repository of research publications and other research outputs

The Geochemistry of Granitoid Intrusions in Llyn, North Wales.

Thesis

How to cite:

Jones, Gladys May (1989). The Geochemistry of Granitoid Intrusions in Llyn, North Wales. MPhil thesis The Open University.

For guidance on citations see [FAQs](#).

© 1989 The Author



<https://creativecommons.org/licenses/by-nc-nd/4.0/>

Version: Version of Record

Link(s) to article on publisher's website:

<http://dx.doi.org/doi:10.21954/ou.ro.0000fc39>

Copyright and Moral Rights for the articles on this site are retained by the individual authors and/or other copyright owners. For more information on Open Research Online's data [policy](#) on reuse of materials please consult the policies page.

oro.open.ac.uk

UNRESTRICTED

The Geochemistry of Granitoid Intrusions in Llŷn, North
Wales.

Submitted by Gladys May Jones, B.A. Hons. (Open)

Offered in the Earth Science Discipline for an M.Phil.
on 31.8.89.

Date of submission: 30th August 1989
Date of Award: 6th November 1989

ProQuest Number: 27758408

All rights reserved

INFORMATION TO ALL USERS

The quality of this reproduction is dependent on the quality of the copy submitted.

In the unlikely event that the author did not send a complete manuscript and there are missing pages, these will be noted. Also, if material had to be removed, a note will indicate the deletion.



ProQuest 27758408

Published by ProQuest LLC (2019). Copyright of the Dissertation is held by the Author.

All Rights Reserved.

This work is protected against unauthorized copying under Title 17, United States Code
Microform Edition © ProQuest LLC.

ProQuest LLC
789 East Eisenhower Parkway
P.O. Box 1346
Ann Arbor, MI 48106 - 1346

Abstract

The Llyn[^] area of North Wales has late Precambrian and Lower Palaeozoic sedimentary and volcanic formations into which are emplaced about twenty intrusions. These vary in composition from microtonalite to microgranite and are closely associated with Caradocian volcanic rocks which include andesitic and basaltic lavas.

Major and trace element analyses show that the intrusions can be divided into five groups; a peralkaline group with high Zr/Nb ratios and four intermediate groups. Petrogenetic modelling using the high field strength elements Nb and Zr suggests that the intrusions could result from 50% fractional crystallisation of plagioclase and/or clino/orthopyroxene and/or hornblende from basaltic magmas such as LL142 or LL143. This is consistent with the lavas and the intrusions both being of Ordovician age.

The most likely setting for the lavas and the intrusions is a complex marginal basin environment dominated by E-W extension.

Contents

Chapter 1 Introduction

Chapter 2 Field relations of the intrusions and associated lavas.

Chapter 3 Petrography of the intrusions and associated lavas.

Chapter 4 Mineralogy of the intrusions and associated lavas.

Chapter 5 Chemistry of the intrusions and associated lavas.

Chapter 6 Petrogenetic modelling and discussion.

Chapter 7 Tectonic setting.

Chapter 8 Conclusions

Appendix 1 Microprobe data

Appendix 2 Analytical methods and results of analyses of standard rocks

Appendix 3 Sample localities with brief indication of mineral content

Appendix 4 Analytical data

List of figures

Figure 1. Map showing the geology of Llŷn and the location and distribution of the intrusions and lavas (based on Cattermole and Romano, 1981).

Figure 2. Stratigraphical sections of the geology of Llŷn showing the volcanic succession; a) in the north; b) in the south.

Figure 3. Structural map of the area (after Roberts, 1979).

Figure 4. Suggested faulting events affecting the 'early granodiorite intrusions' according to Tremlett, (1970).

Figure 5. Map of Carreg-y-Defaid area, (Fitch, 1967).

Figure 6. Plate tectonic models a) Fitton and Hughes (1970); b) Croudace (1980); c) Kokelaar (1988).

Figure 7. Photomicrograph of Bwlch Mawr granodiorite LL80. The area of field of view is 15 x 10mm. The section is highly altered and shows very sericitised feldspars (f).

Figure 8. Photomicrograph of Garn Fadron LL104. The area of field of view is 15 x 10mm. The section shows a highly altered plagioclase phenocryst (p) in a groundmass containing apatite crystals (a).

Figure 9. Photomicrograph of Garnfor granodiorite LL1. The area of field of view is 15 x 10mm. The section shows a phenocryst of plagioclase (p) with clusters of amphibole (a) in a fine grained groundmass.

Figure 10. Photomicrograph of Garnfor tonalite LL10. The area of field of view is 15 x 10mm. The section shows a cluster of plagioclase (p) and amphibole phenocrysts (a) (with minor alteration to sericite) in a groundmass coarser grained than Figure 7a.

Figure 11. Photomicrograph of Penrhyn Bodeilas microgranodiorite LL66. The area of field of view is 15 x 10mm. The section shows porphyritic clusters of amphibole (a), pyroxene (p) and feldspar (f). Apatite (e) and zircon (z) can be seen in the groundmass.

Figure 12. Photomicrograph of Gurn Ddu granodiorite LL77. The area of field of view is 15 x 10mm. The section shows feldspar (f), sericitised and clusters of pyroxenes (p).

Figure 13. Photomicrograph of Nanhoron granophyre LL38. The area of field of view is 15 x 10mm. The section shows the granophyric texture.

Figure 14. Photomicrograph of Llanbedrog porphyritic granite LL63. The area of field of view is 15 x 10mm. The section shows the perthitic (p) intergrowth and granophyric texture.

Figure 15. Photomicrograph of Garn Pentyrch granodiorite LL125. The area of field of view is 15 x 10mm. The section shows a cluster of feldspar (f) and altered phenocrysts (p) in a very fine grained matrix.

Figure 16. Photomicrograph of Garn Boduan tonalite LL130. The area of field of view is 15 x 10mm. The section shows phenocrysts of feldspar (f) and pyroxene (p) in a fine grained groundmass which is directional around the clusters.

Figure 17. Photomicrograph of Moel y Penmaen lava LL145. The area of field of view is 15 x 10mm. The section shows plagioclase phenocrysts (p) (sericitised) in a fine grained matrix of sericitised plagioclase, chlorite, Fe-Ti oxide and pyroxene (px).

Figure 18. Photomicrograph of basalt LL142. The area of field of view is 15 x 10mm. The section shows phenocrysts of augite (a) and plagioclase (p) in a fine groundmass of feldspar laths.

Figure 19. The Wo-Fs-En ternary diagram showing the evolutionary trends of minerals in the Llŷn intrusions. The crystallisation trends of ortho- and clinopyroxenes from some Tertiary acid glasses, (Carmichael, 1960) are shown for comparison (dashed lines). Closed and open squares represent phenocryst and groundmass minerals respectively. Squares - Inner Gwynedd tonalite; Open stars - Penrhyn Bodeilas; (based on Croudace, 1981); Closed circles - LL142 basalt (this study).

Figure 20. Ab-An-Or ternary diagram showing the evolutionary trends of minerals in the Llŷn intrusions. (Symbols as in Figure 19). Broken lines from Tertiary acid glasses (Carmichael, 1960). Circles - LL142 basalt (this study).

Figure 21. Plot of SiO_2 against Al_2O_3 for clinopyroxenes from the basalt LL142. The broken lines separate 3 groups of clinopyroxene composition. A, non-alkaline (tholeiitic, high alumina and calc-alkaline); B, alkaline lavas and C, peralkaline lavas (Le Bas, 1962).

Figure 22. Plot of $\text{Na}_2\text{O} + \text{K}_2\text{O}$ against SiO_2 . The intrusions form distinct groups which fall in fields identified as monzonites, granites, granodiorites, syenites and diorites. The volcanic rocks fall in fields identified as basalt, basaltic andesite and andesite. Only data from this study is plotted.

Figure 23. Harker diagram showing major oxides against SiO_2 . Symbols as in Figure 22. Data from Croudace (1981) included.

Figure 24. Harker diagram showing trace elements against SiO_2 . Symbols as in Figure 22. Data from Croudace (1981) included.

Figure 25. Classification according to Zannettin (1988) showing the fields in which the lavas are contained. Only data from this study is plotted.

Figure 26. Addition - subtraction diagram using LL142 (basalt) and an average Nanhoron composition (LL39).

Figure 27. AFM diagram. The dashed lines separate tholeiitic (TH) from calc-alkaline (CA) associations using the criteria of Irvine and Baragar (1971). Symbols as in Figure 22. Data from Croudace (1981) included.

Figure 28. Plot of Nb against Zr. Symbols as in Figure 22. Data from Croudace (1981) included.

Figure 29. Q-Or-Ab system showing positions of cotectic lines and minima or ternary eutectics for P_{H_2O} of 0.5, 1, 3 and 5 kbars. The positions of temperature minima on the quartz-feldspar cotectic line are indicated by m, and e indicates the position of a ternary eutectic between quartz and two feldspars. Symbols as in Figure 22.

Figure 30. Tremlett (1972) grouping of the intrusions.

Figure 31. Croudace (1981) grouping of the intrusions.

Figure 32. Grouping of the intrusions according to this study.

Figure 33. Zr against Y diagram with vectors for 10% partial melting of shale. Symbols as in Figure 22. Data from this study only.

Figure 34. Plot of Y against Zr. The vectors are for 50% fractional crystallisation. Symbols as in Figure 22. Data from this study only.

Figure 35. Plot of Nb against Zr. The vectors are for 50% fractional crystallisation. Symbols as in Figure 22. Data from this study only.

Figure 36. Plot of Sr against Ba. The vectors are for 50% fractional crystallisation. Symbols as in Figure 22. Data from this study only.

Figure 37. Plot of Rb against Sr. The vectors are for 50% fractional crystallisation. Symbols as in Figure 22. Data from this study only.

Figure 38. Plot of Nb against Y. The vectors are for 50 % fractional crystallisation. Symbols as in Figure 22. Data from this study only.

Figure 39. Plot of Zr against TiO_2 showing fields of arc and within-plate lavas (Pearce, 1980). Line A-B separates basalts from acid and intermediate rocks.

Figure 40. Plot of Y against Nb showing fields of arc, ocean ridge and within-plate granites. (Pearce et al, 1984). Symbols as in Figure 22. Data from this study only is plotted.

Figure 41. Plot of Y + Nb against Rb showing fields of syn-collision, within-plate, arc and ocean ridge granites (Pearce et al, 1984). Symbols as in Figure 22. Data from this study only is plotted.

Chapter 1

Introduction

The Llŷn area comprises late Precambrian and Lower Palaeozoic sedimentary and volcanic formations into which over twenty granitoid intrusions have been emplaced (Figure 1).

The oldest rocks of Llŷn are referred to as the Monian Supergroup of low-grade metasedimentary rocks, which are of Late Precambrian to early Cambrian age. Definite Cambrian rocks crop out in three areas, the most complete Cambrian sequence occurring around St. Tudwal's Road (Figure 1). Ordovician rocks are believed to underlie most of Llŷn. In the east, near Criccieth, Lower Ordovician Arenig sediments unconformably overlie Upper Cambrian rocks and in the west, they progressively overstep Cambrian beds. Rocks of Middle Ordovician Llandeilo age seem to be absent in the Llŷn but the Caradocian and Ashgillian are well represented. Volcanic rocks are abundant within the Ordovician. Lavas and pyroclastic rocks were erupted during the Caradocian throughout Llŷn. Caradocian volcanic rocks consist mainly of andesitic and rhyolitic lavas, ignimbrites and air-fall tuffs and minor basalts (Figure 2). Silurian

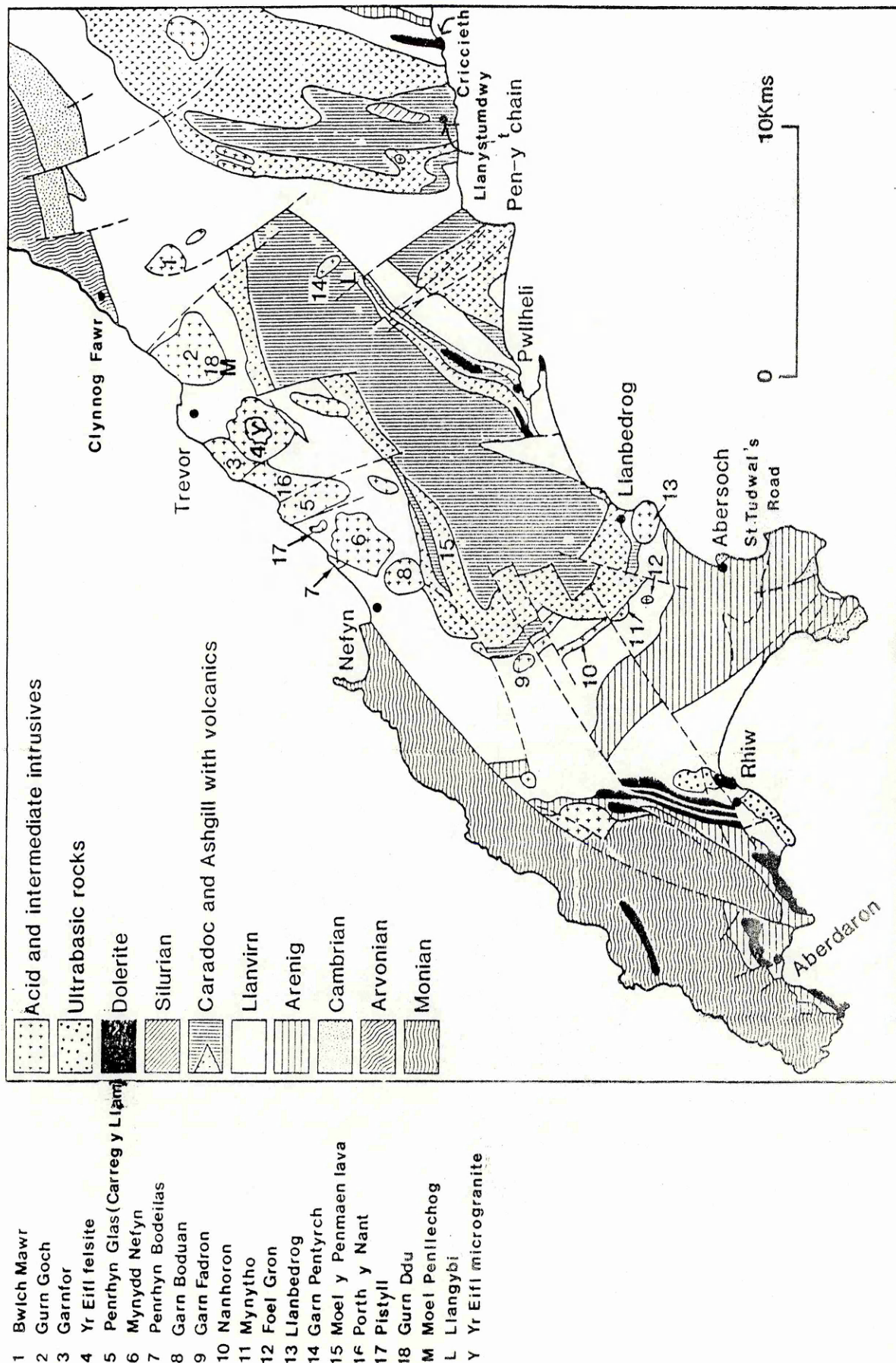


Figure 1. Map showing the geology of Llyn and the location and distribution of the intrusions and lavas (based on Cattermole and Romano, 1981).

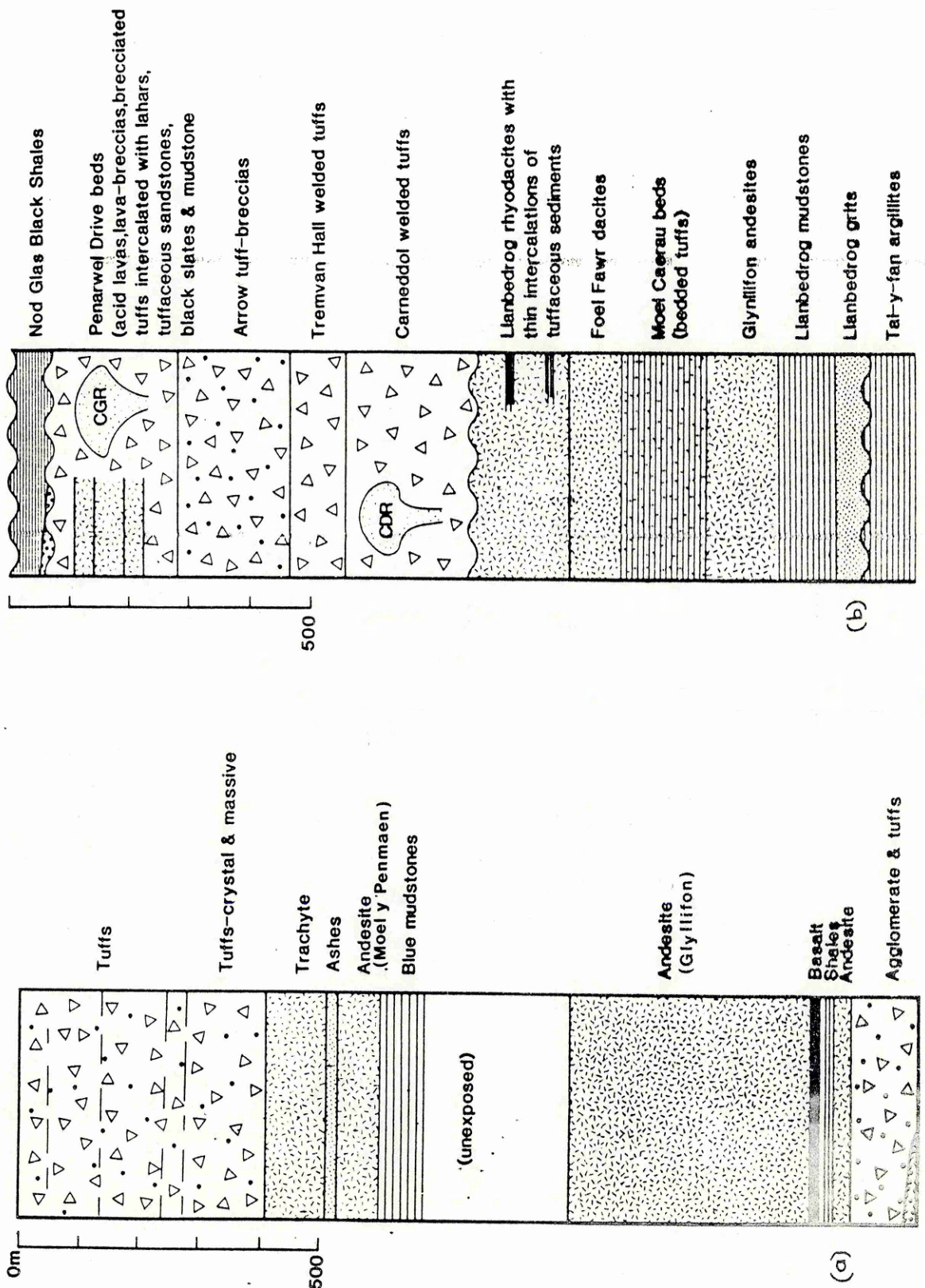


Figure 2. Stratigraphical sections of the geology of Llyn showing the volcanic succession; a) in the north; b) in the south.

CGR: Castell-grug intrusion
CDR: Carreg y defaid rhyolite

rocks are sparsely represented and can only be found near Llanystumdwy where Llandovery sediments occupy the core of a syncline. The Ordovician and Silurian rocks have experienced episodes of Caledonian folding and faulting (Figure 3). There were two main episodes of faulting; one post-Ordovician — pre-Silurian and the other post-Silurian — pre-Devonian.

The granitoid intrusions are fine-grained quartz-plagioclase alkali-feldspar +/-biotite +/-hornblende +/-pyroxene microtonalites, and sub- and peralkaline microgranites. They are now generally regarded as Ordovician in age, and form stocks of less than five square kilometres in outcrop area. The intrusions may be divided into two geographic groups:

On the north coast a line of intrusions form prominent hills between Clynnog Fawr and Nefyn: (Figure 1) 1. Bwlch Mawr; 2. Gurn Goch; 3. Garnfor; 4. Yr Eifl; 5. Penrhyn Glas; 6. Mynydd Nefyn; 7. Penrhyn Bodeilas; 8. Garn Boduan; 16. Porth y Nant, 17. Pistyll and 18. Gurn Ddu.

To the south of Nefyn, a second group of intrusions form another line of hills trending NW-SE: 9. Garn Fadron; 10. Nanhoron; 11. Mynytho; 12. Foel Gron; 13. Llanbedrog; and 14. Garn Pentyrch.

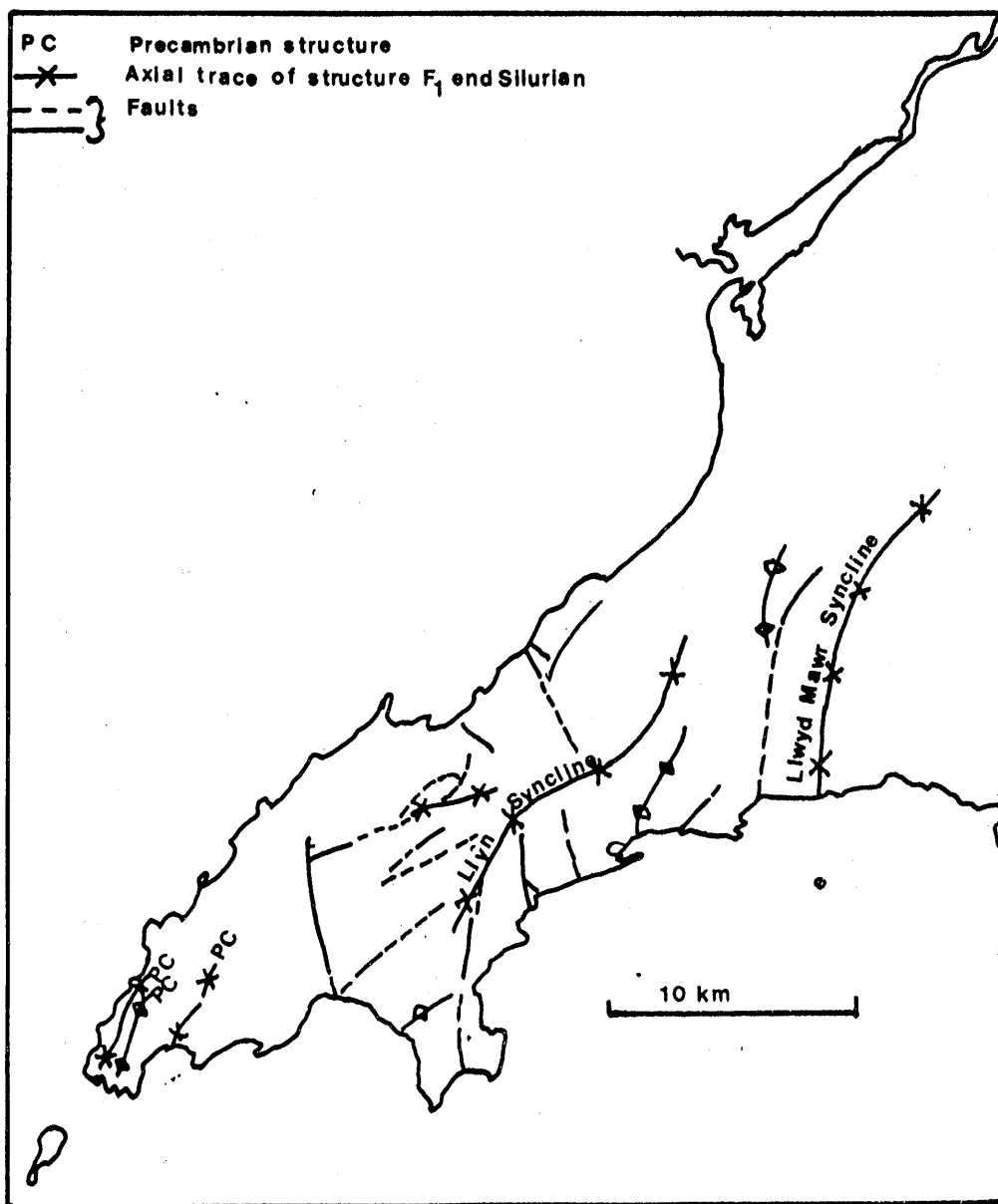


Figure 3. Structural map of the area (after Roberts, 1979).

There has been considerable research on the geology of the Llŷn region since the early work of such eminent geologists as Harker and Sedgwick in the 1880's. Matley (1938), Matley and Heard (1938) mapped several areas including the whole of the Precambrian outcrop, describing the rocks in detail and presenting some geochemical data. Further detailed mapping and petrography was carried out by Tremlett (1962, 1964, 1965, 1970, 1972), Fitch (1967) and Roberts (1981), while Croudace (1981) undertook a more detailed geochemical study of the intrusions and the andesitic lavas in the area of Moel y Penmaen, (15 on Figure 1). The possible ages of these intrusions have been discussed by Tremlett (1962, 1964, 1970, 1972), Thomas and Briden (1976) and Croudace (1981). Over a period of time (1962 - 1972) Tremlett examined both the volcanic and plutonic rocks of the area. It is difficult to summarise his work clearly because of the terminology he used to classify the intrusions; e.g. his 'early' granodiorite suite he stated to be Caledonian in age. However an attempt has been made to summarise his findings.

On the basis of geochemical and structural information Tremlett recognised two distinct groups of granitoids (numbers in brackets refer to Figure 1):-

1. Ordovician in age:

Gurn Goch(2), Mynytho(11), Llanbedrog(13),
Nanhoron(10) and Foel Gron(8);

2. Caledonian (early Devonian) in age:

Mynydd Nefyn(6), Penrhyn Bodeilas(7),
Porth-y-Nant(16), Penrhyn Glas (Carreg-y-yLlam)(5),
Garn Fadron(9), Gurn Ddu(18), Bwlch Mawr(1), Yr
Eifl(4), Garnfor(3) and Garn Boduan(8).

He stated that there were significant geochemical differences between the intrusions which led him to discriminate between those of Ordovician age and those emplaced during the early Devonian, i.e. they were emplaced after the main Caledonian deformation of the area and in close association with, or after, episodes of late Caledonian faulting.

Tremlett further sub-divided the Caledonian intrusions into an 'early' suite of granodiorites and the Garnfor/Yr Eifl complex, mainly on the basis of faulting evidence but also including major element chemistry and petrography. He suggested the following time relationships (Figure 4):-

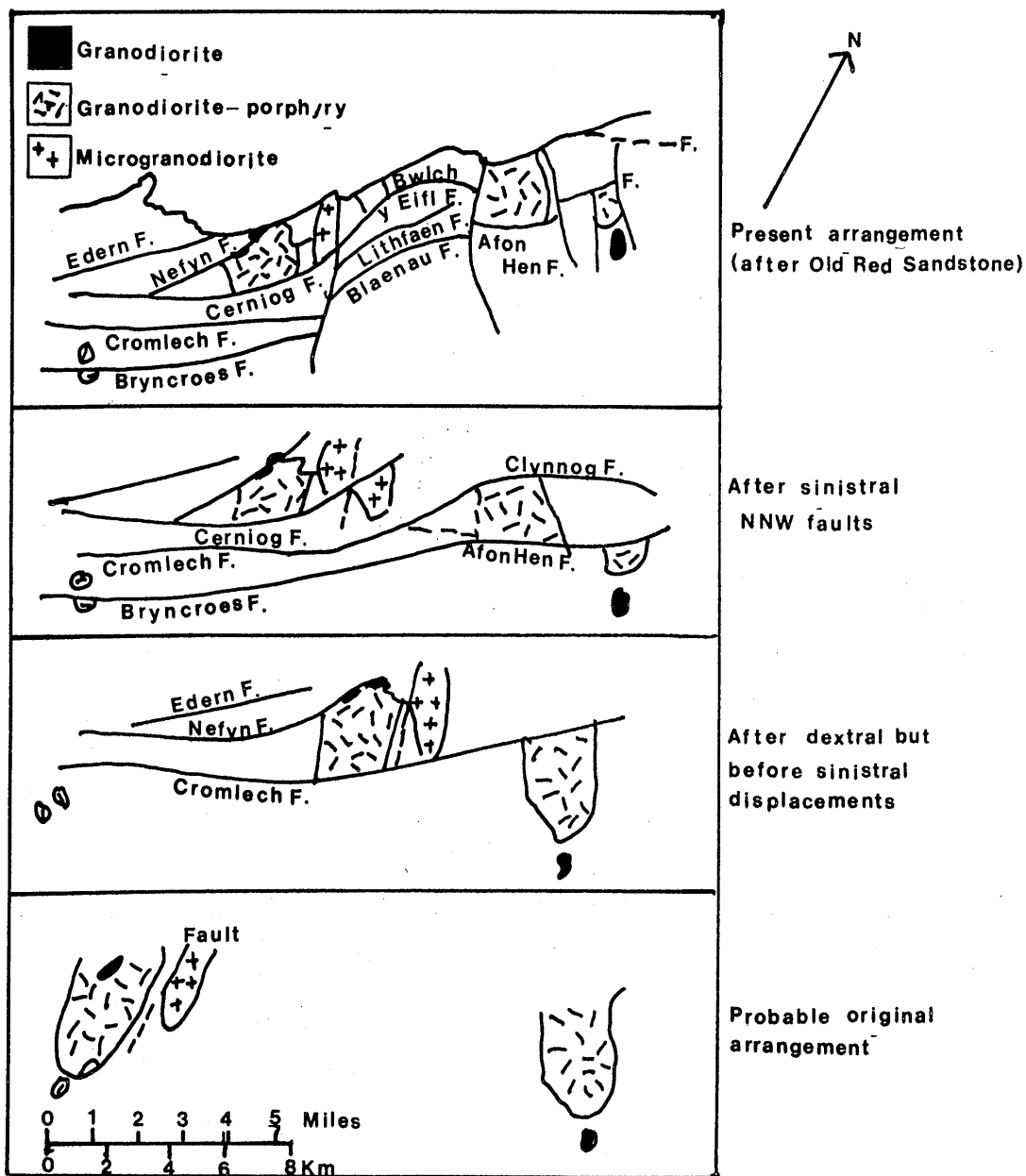


Figure 4. Suggested faulting events affecting the 'early granodiorite intrusions' according to Tremlett,(1970)

1. Emplacement of granodiorite suite (Garn Fadron, Gurn Ddu, Penrhyn Glas (Carreg-y-Llam), Porth y Nant, Mynydd Nefyn) (Figure 4a);
2. Dextral strike-slip movements E-W (Figure 4b);
3. Sinistral faulting disrupting some intrusions (Carreg-y-Llam, Gurn Ddu, Mynydd Nefyn)(Figure 4c);
4. Disruption of the earlier faults (Figure 4d) by NNW sinistral movements. Emplacement of felsites (Yr Eifl) up NNW-SSE sinistral faults followed by intrusion of the Garnfor suite. Dip-slip movements along Silurian or Devonian faults.

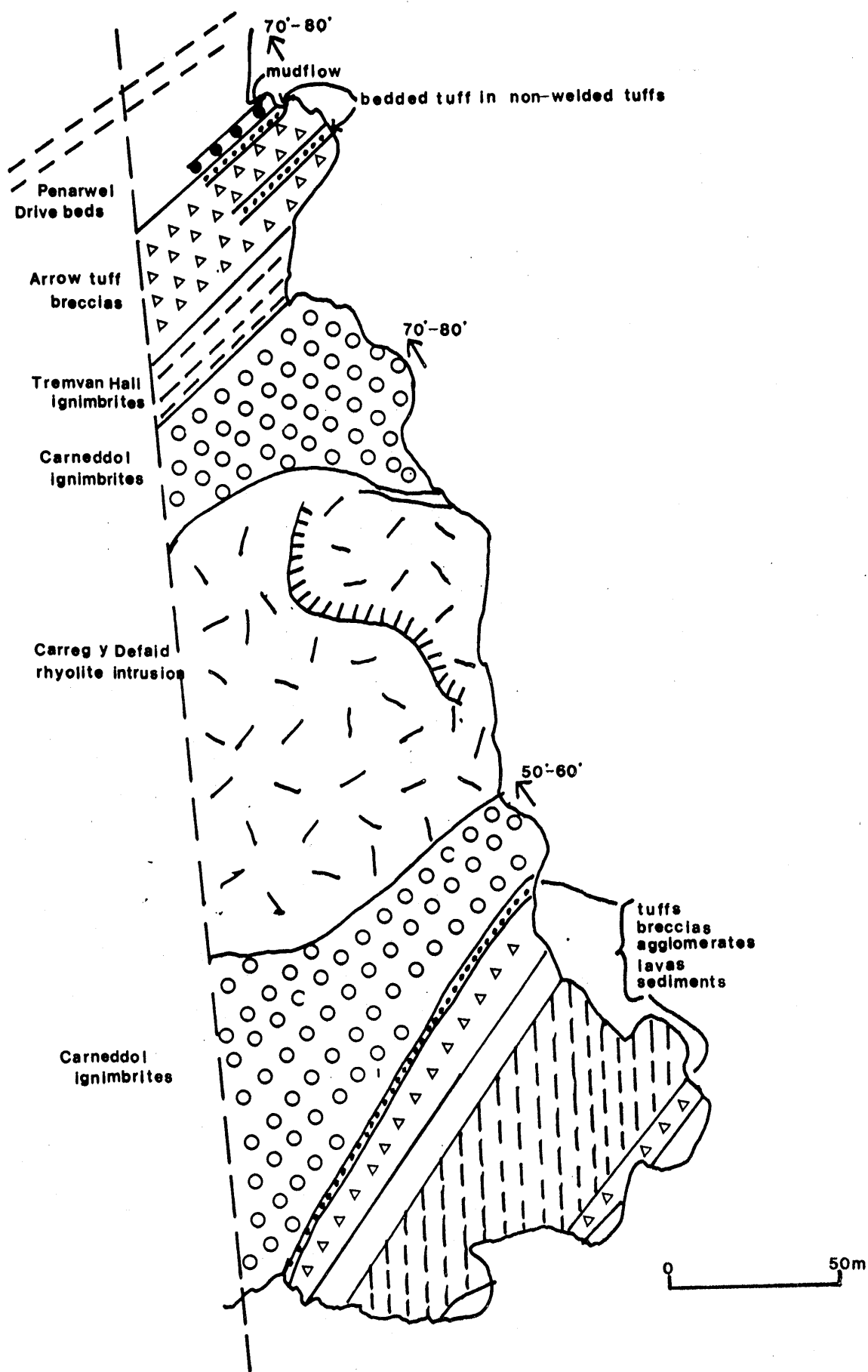
Tremlett (1970) considered that the 'early' suite and the Garnfor suite displayed a chemical evolution which developed at depth. He suggested that the chemical evolution was caused by the progressive contamination of an acid magma by a basic rock at depth. He based this view on the apparently increasing abundance of dolerite xenoliths from the microgranodiorite to tonalite rocks and on good correlations on the Harker diagrams for samples ranging from basic to acid in chemical composition.

By contrast, Croudace (1981) concluded that the all granites were contemporaneous with the Ordovician

lavas, and that the geochemical variations are consistent with the formation of the Caradocian andesitic lavas of the Moel y Penmaen area and the granitic intrusions from a parental tholeiitic magma by crystal fractionation of olivine, pyroxene and plagioclase. He suggested that apatite fractionation strongly controlled REE and Sr abundances and that the Garnfor suite clearly shows the role played by minor mineral fractionation. Croudace concluded that the Llyn^A granitoids are all mid-Ordovician because they are geochemically related to the Caradoc Moel-y-Penmaen lavas. He also concluded that the geochemical similarity of these lavas to the intrusions is consistent with an Ordovician (Caradoc) age.

Thomas and Briden (1976) investigated paleomagnetic remanence directions for samples from six intrusions. Five had declination / inclination directions which corresponded to a paleomagnetic pole at 108° east, 68° south. One sample gave directions deviant to this and was interpreted as being a result of later faulting. The calculated pole position is nearly 90° away from the published Ordovician-Devonian pole for Britain. Thomas and Briden concluded that this was due to an anomalous geomagnetic field occurring in late Ordovician times, the intrusions being of Ordovician age, as their remanence directions were similar to those of the proven Ordovician Cader Idris lavas.

Figure 5. Map of Carreg-y-Defaid area, (Fitch, 1967).



The petrogenesis of the intrusions and Caradocian volcanics has also been considered by Fitch (1967). Fitch examined a sequence of Caradocian andesites, rhyodacites, ignimbrites and acid intrusions in the area of Carreg-y-Defaid (Figure 5) and he used these to model the formation of other Caradocian magmas. He considered the basaltic rocks to have been derived from the mantle, while the basaltic andesites, rhyodacites, ignimbrites and calc-alkaline type granites were formed by the melting of the continental crust which had been heated by the basaltic magma.

A large number of plate tectonic theories have been put forward to explain the evolution of the British Isles, some of which deal specifically with the petrogenesis of Ordovician lavas from Wales and the Lake District. Fitton and Hughes (1970) suggested that the Ordovician volcanics from the Lake District and Wales demonstrated a variation which could be interpreted as being related to a south-eastward dipping subduction system (Figure 6a). Stillman et al (1974) suggested that the Ordovician volcanics in east and south-eastern Ireland were produced in an island arc environment associated with a south-eastward dipping subduction system.

Stillman and Williams (1978) modified the model providing evidence that the Upper Ordovician volcanic rocks of east and south-east Ireland were erupted on the

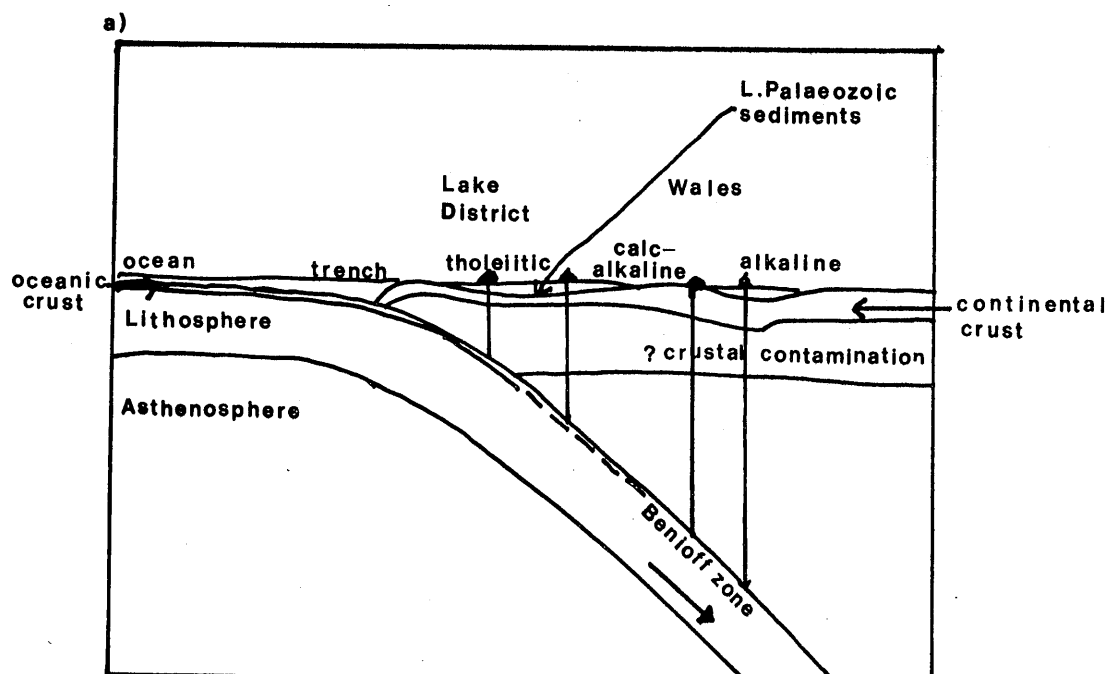


Figure 6. Plate tectonic models a) Fitton and Hughes (1970); b) Croudace (1980); c) Kokelaar (1988).

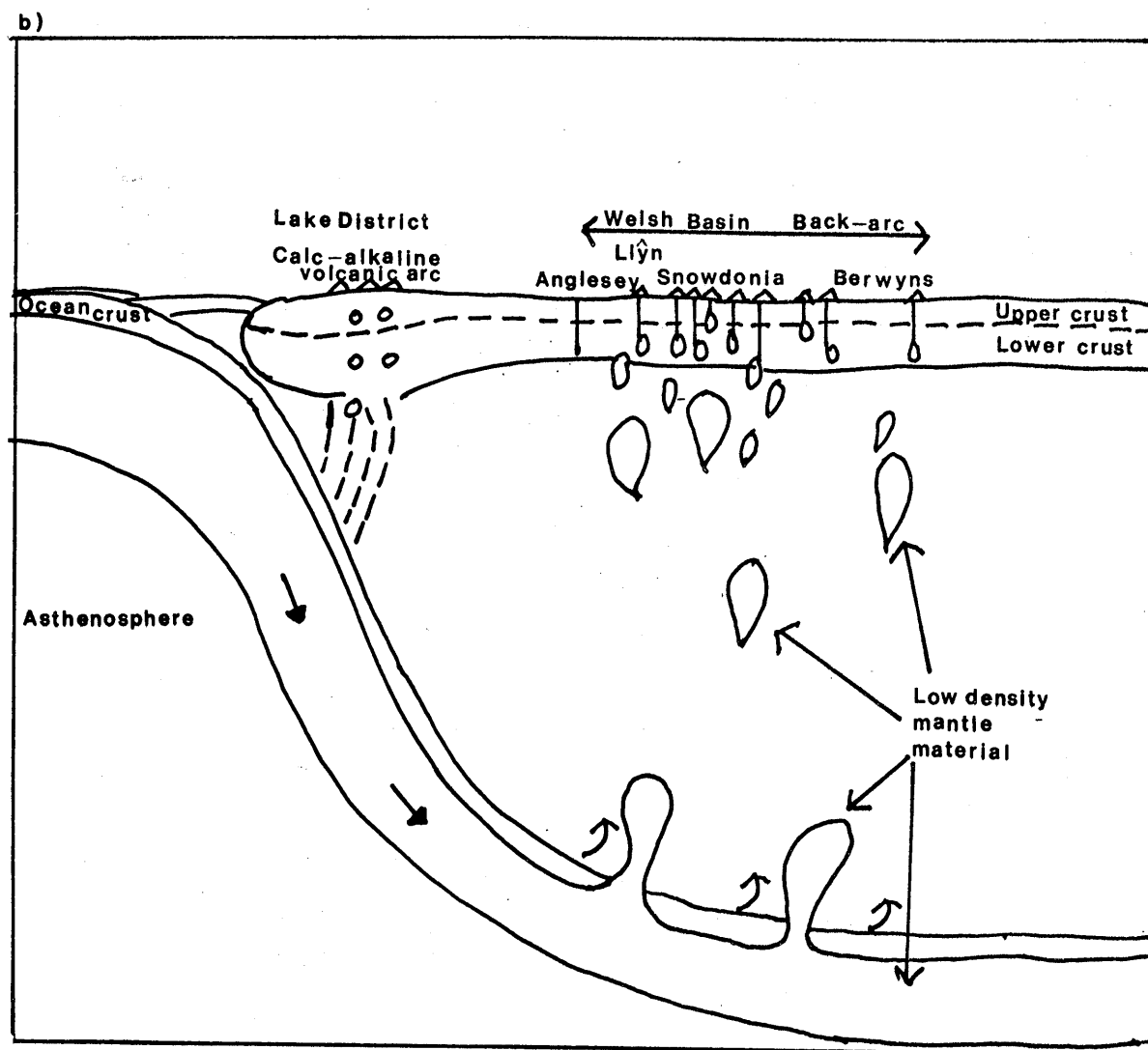
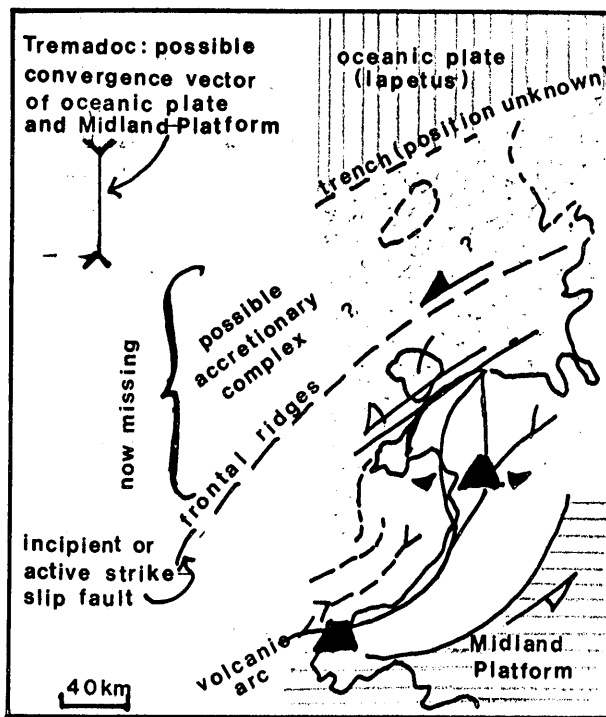


Figure 6c



A plate-tectonic model to explain late Tremadoc tectonism in Wales. (Kokelaar, 1988)

Half-arrows indicate possible shear sense; small arrows the local extension, and topped triangles the location of arc volcanoes.

margin of a continental plate that thickened towards the south-east, above a subduction system dipping to the east-south. Stillman and Francis (1979) proposed the following scheme:-

1. Lithospheric plate destruction, giving rise to transitional island-arc tholeiites, calc-alkaline rocks and alkaline rocks;
2. Associated mantle melting to produce many of the basaltic rocks;
3. Partial melting of the crustal basement to produce the acidic rocks.

The general consensus is that the suture of the Iapetus Ocean ran north-east to south-west through Ireland and Britain (Shannon-Solway line) but that during ocean closure subduction directions dipped from the north-west towards the south-east under Wales. Croudace (1981) proposed that Llŷn was an area of crustal tension and supported his model by the association of peralkaline granites and tholeiites (Figure 6b). Geophysical evidence suggests that the region was ensialic and Croudace therefore proposed that the North Wales area may have been an incipient back-arc basin or a volcano-tectonic rift zone.

Leat and Thorpe (1986) interpret the volcanic rocks as having been erupted into a complex, rapidly evolving, active continental margin dominated by crustal

tension. Recent research by Kokelaar (1988) has supported the theory of crustal tension and considers that faulting greatly influenced both volcanism and sedimentation.

The aim of this study was to investigate the mineralogy and geochemistry of each intrusion and the associated volcanic rocks (especially the basalts and andesites) with a view to establishing whether or not there were petrogenetic links between intrusive and extrusive igneous rocks. Croudace studied only one andesitic lava. In order to confirm Croudace's work a wider range of basic volcanic rocks was studied. In particular a range of trace elements including the immobile elements Zr and Nb were to be used as discriminatory elements. Microprobe work on the pyroxenes and plagioclases from one basalt (LL142) was undertaken to complement previous work by Croudace. Petrogenetic modelling has also been carried out to determine the relationships between the intrusions.

Chapter 2

A. Field relations of the volcanic rocks.

The numbers in brackets refer to Figure 1 and the asterisks indicate those rocks sampled for further investigation.

a. Moel-y-Penmaen (15) *GR336386

Moel-y-Penmaen forms a small hill ca.300 x 150m,300m NNE of Penmaen Farm.The hill is composed of NE-SW striking pyroclastic rocks and lavas.The northern part of the hill is composed of andesitic lava and has been quarried.Samples were collected from the disused quarry.

b. Basalt LL142 * GR315386,Andesite LL143 *GR314385

A small outcrop of the basalt can be found at the side of the road in the bushes near Boduan.It is near to LL143,but separate from it,and consists of a large craggy outcrop.

c. Basaltic andesite LL153 * GR292335

A tiny quarry in the bushes is the only outcrop found of this particular rock.

d. Basaltic andesite LL154,LL155 * GR298371

Small rocky outcrops can be found in the wood near Ffridd Farm.

e. Basalt LL156 * GR311360

There are several small rocky outcrops on the edge of the marsh near Bodgadle.

B. Field relations of the intrusions

Introduction

Most of the granitoid intrusions form prominent hills. Many of them, notably Garnfor, Mynydd Nefyn, Penrhyn Bodeilas, Gurn Ddu, Nanhoron, Foel Gron and Llanbedrog have been quarried and are therefore reasonably well exposed despite extensive weathering. The other intrusions consist mainly of series of craggy outcrops, extensively weathered. There is a lack of exposures where contacts with the country rock can be observed, and outcrops of country rock are scarce due to the proximity of the intrusions to the sea. The aim of this chapter is to attempt to describe such field relations as can still be

observed. (Not all the intrusions described here were sampled and analysed; many samples were not suitable for analysis due to extensive weathering).

(The intrusion numbers are as shown on Figure 1 and those with an * are those which have been sampled for more detailed investigation.)

The intrusions are discussed in geographical groups.

a. Bwlch Mawr * (GR 432478), Gurn Goch, (GR 408475) and Gurn Ddu * (GR 401468)

The intrusion of Bwlch Mawr (1) is exposed as a series of crags on top of a prominent hill. Jointing can be seen, forming long rectangular blocks inclined steeply to the east. Gurn Goch (2) is between Bwlch Mawr and Gurn Ddu, the three hills forming a ridge. It was not sampled as the exposures formed steep cliffs and were difficult to reach. A series of quarries high up in the hill provide excellent exposures of Gurn Ddu (18). Marginal chilled facies can be seen along the eastern contact. The intrusions are emplaced into Llanvirn shales.

b. Garnfor * (GR 360460) and Yr Eifl (GR 365448)

Garnfor (3) intrusion is still being quarried and therefore the exposed surfaces change from month to

month. At the western end of the quarry, the intrusion is grey in colour, but changes to pink and then grey again towards the east. The matrix of the inner type is finer-grained towards the contact with the outer type. The inner type is pink and contains more xenoliths. It appears to have been intruded into the outer grey intrusion. Two dolerite dykes intrude the granite. At the higher level, low angle joints can be seen in the grey rock. Both types include many xenoliths of both igneous and sedimentary origin. Steep cliffs and craggy outcrops expose the microgranite and the felsite of Yr Eifl(4). The microgranite (Y) is well jointed and has a chilled margin against the felsite. It appears that the microgranite has been intruded into the felsite. The country rocks are mudstones and siltstones of Llanvirn age.

c. Penrhyn Glas (Carreg-y-Llam) GR 335438, Mynydd Nefyn (GR 322415) and Penrhyn Bodeilas (GR319441)

A small quarry provides good exposures of Penrhyn Glas (5). Many xenoliths can be seen, some large ones which form long streaks and appear to be igneous in origin. The intrusion of Mynydd Nefyn (6) is well exposed in a series of quarries. Metamorphism can be seen in the NE and SE part of the quarry. High in the quarry columnar cooling joints are exposed. Xenoliths, both igneous and sedimentary are plentiful and faint layering can be seen in the large blocks lying on the quarry floor, the

colour changing from light to dark grey. A small quarry on the coast provides a good exposure of Penrhyn Bodeillas (7). Xenoliths, mainly of sedimentary origin, are common and show various stages of digestion and alteration. They range in size from a few mm to several centimetres. Aplite veins run nearly vertical in a NNE direction and some have a chilled margin. The intrusion is well jointed with some epidotisation along the joints.

d. Garn Boduan *(GR 311387)

Garn Boduan (8) forms a prominent hill with rock outcrops on the top. The rock is extremely weathered and good samples are difficult to find. No trace of contact with the underlying Nefyn shales or lavas can be found although exposures showing such contacts have been seen previously. The lava LL142 was collected about 100 metres from the base of Garn Boduan.

e. Garn Fadron *(GR 278352)

Rocky outcrops on top of a hill provide the only exposures of this intrusion. (9) The rock is grey and very weathered. The occasional xenolith of sedimentary material can be found. The country rock is shale of Llanvirn age.

f. Nanhoron * (GR 330287), Mynytho (GR 298318) and Foel Gron (GR 301311)

A working quarry provides good exposures of the Nanhoron intrusion (10). The intrusion varies from very fine to coarse grained and veining can be seen giving evidence of a faint layering. There are no xenoliths. Contact-altered shales of Llanvirn age can be seen at the northern edge of the quarry. Mynytho Common (11) is formed from a ridge of riebeckite-granite. There are outcrops of rock on the western side of the common running on 330° strike. Fluxion banding can be seen and riebeckite can be seen with a hand lens. Small quarries on the roadside and on the slopes leading to the summit of the hill of Foel Gron (12) provide reasonable exposures. Contact with the Llanvirn shales can no longer be seen but shales are exposed in the footpath at the bottom of the hill.

g. Llanbedrog * (GR 329305)

Good exposures are provided by two fairly large disused quarries. Rock in the higher levels is a slightly darker grey than that found in the lower levels. A common feature of the rock is the presence of miarolitic cavities containing quartz and chlorite crystals. The intrusion is emplaced into Llanvirn shales although no actual contact can be seen.

h. Garn Pentyrch * (GR 425418) /

Small rocky outcrops form the exposures on the summit of the hill. It is intruded into sediments of Llanvirn age.

Conclusions

Although exposures of many of the intrusions are excellent there are no localities where contacts with the surrounding rock can be seen. The intrusions vary in colour from light grey to pink and xenoliths, both of igneous and local sedimentary material are common in some intrusions but not in others. Field evidence alone does not contribute to any hypothesis concerning the relationships between the intrusions or their origin. However, the intrusions are mainly emplaced into Llanvirn sediments, and are therefore younger than Llanvirn but there is no direct structural evidence of their upper age limit.

Chapter 3

Petrography of the intrusions and associated lavas.

Introduction

The rock names used in this study are those used by Tremlett and Croudace.

The texture of a granite may provide some information concerning its origin, its water content and its depth of origin. Granophyric intergrowth for example, is generally regarded as the product of eutectic crystallisation; perthite may have developed as a result of sub-solvus exsolution under late magmatic and/or metamorphic conditions while zoned crystals show rapid cooling when equilibrium between solid and liquid has not been fully established.

Short petrographic descriptions are provided for samples of the granitic intrusions and basic rocks from the area studied. Previous detailed petrographic studies have been made by Tremlett (1962, 1964, 1965) and Croudace (1981). The intrusions range in size from ca. 1km to 3km across. Some intrusions contain xenoliths, of both igneous and sedimentary origin.

The main minerals in the intrusions are alkali feldspar, plagioclase and quartz. Minor minerals include amphibole, orthopyroxene, clinopyroxene and biotite. Accessory minerals are Fe-Ti oxide, apatite, zircon, allanite, epidote and sphene.

The intrusions generally comprise phenocrysts of alkali feldspar, plagioclase and amphibole. Granophyric texture is seen in three of the intrusions (Nanhoron, Llanbedrog and Gurn Ddu).

There is no relationship between the mineralogy of the intrusions and geographical situation (Figure 1). All samples show alteration of plagioclase to sericite and/or epidote, and of pyroxene to chlorite. There is therefore mobility of some elements in these minerals.

A. Intrusions

a). Bwlch Mawr and Gurn Ddu (1 and 18 on Fig. 1)

All the samples of the granodiorite Bwlch Mawr are highly altered. The main minerals are alkali feldspar (heavily sericitised), plagioclase (altered to epidote and/or chlorite) and quartz. The groundmass is very fine grained and no individual constituents can be picked out. The whole sample is extensively altered to carbonate. (Figure 7). Gurn Ddu is a porphyritic microgranodiorite consisting of clusters of amphibole

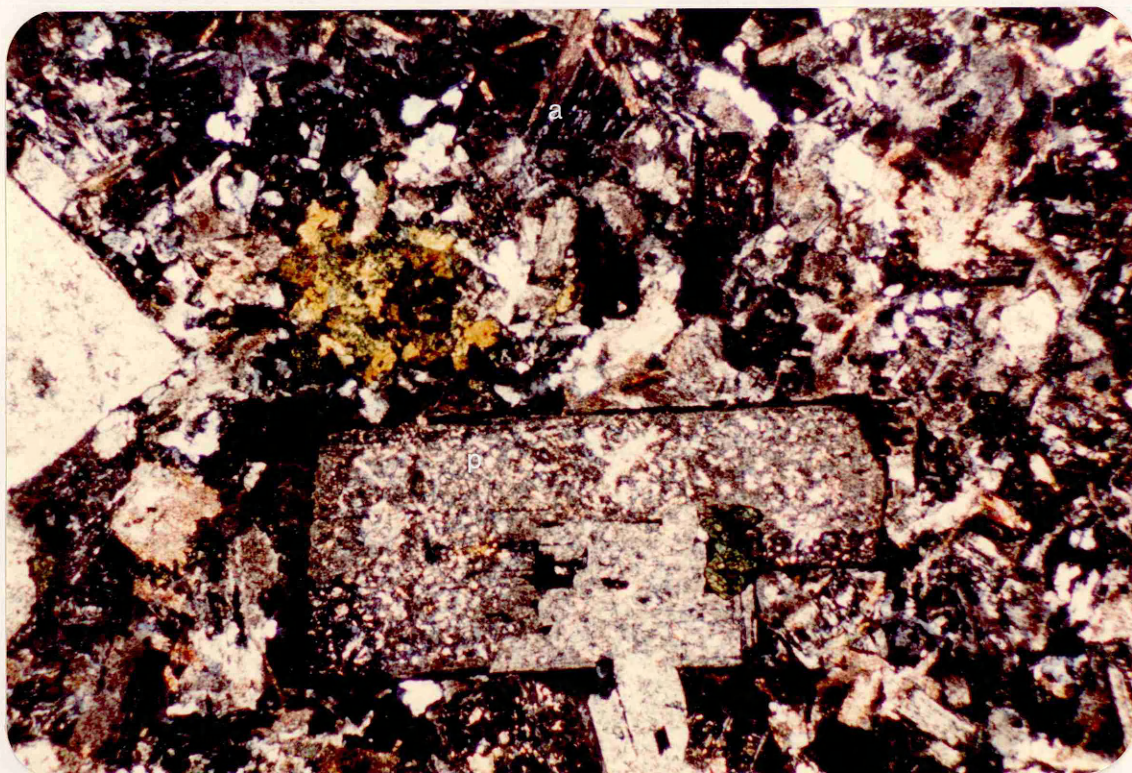


Figure 8. Photomicrograph of Garn Fadron LL104. The area of field of view is 15 x 10mm. The section shows a highly altered plagioclase phenocryst (p) in a groundmass containing apatite crystals (a).

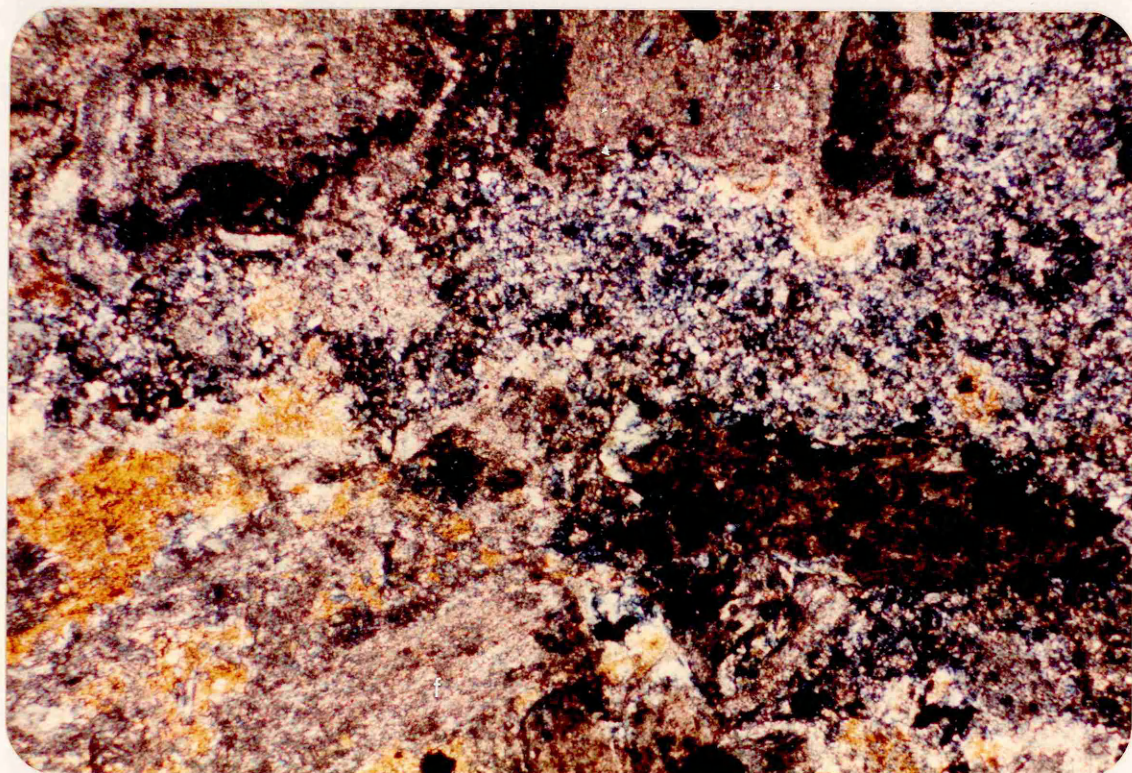


Figure 7. Photomicrograph of Bwlch Mawr granodiorite LL80. The area of field of view is 15 x 10mm. The section is highly altered and shows very sericitised feldspars (f).

crystals which are usually altered to epidote and /or chlorite. These clusters occasionally contain zircon crystals. There are also large phenocrysts of alkali feldspar which are often sericitised. The fine grained groundmass consists of quartz, feldspar and amphibole. Fe-Ti oxide and apatite are accessory minerals. (Figure 12). Some of the samples contain pyroxenes rimmed with epidote and/or hornblende. Crystals of allanite are occasionally seen.

b). Garnfor (3 on Fig.1)

There are two distinct varieties in this intrusion. In hand specimen, one is pink medium grained porphyritic microgranodiorite (a) and the other is a light grey porphyritic tonalite (b).

i) The major minerals are plagioclase, alkali feldspar and quartz. The plagioclase form laths up to 12mm long, generally fresh but locally altered to epidote and sometimes intergrown with alkali feldspar which is more altered to sericite. Amphibole and clinopyroxene phenocrysts form clusters, the pyroxene having rims of chlorite. A few small biotite crystals can be seen. The groundmass consists of plagioclase feldspars, some small clinopyroxenes and interstitial quartz. Apatite needles are scattered throughout. Fe-Ti oxide is an accessory mineral. (Figure 9).



Figure 9. Photomicrograph of Garnfor granodiorite LL1. The area of field of view is 15 x 10mm. The section shows a phenocryst of plagioclase (p) with clusters of amphibole (a) in a fine grained groundmass.

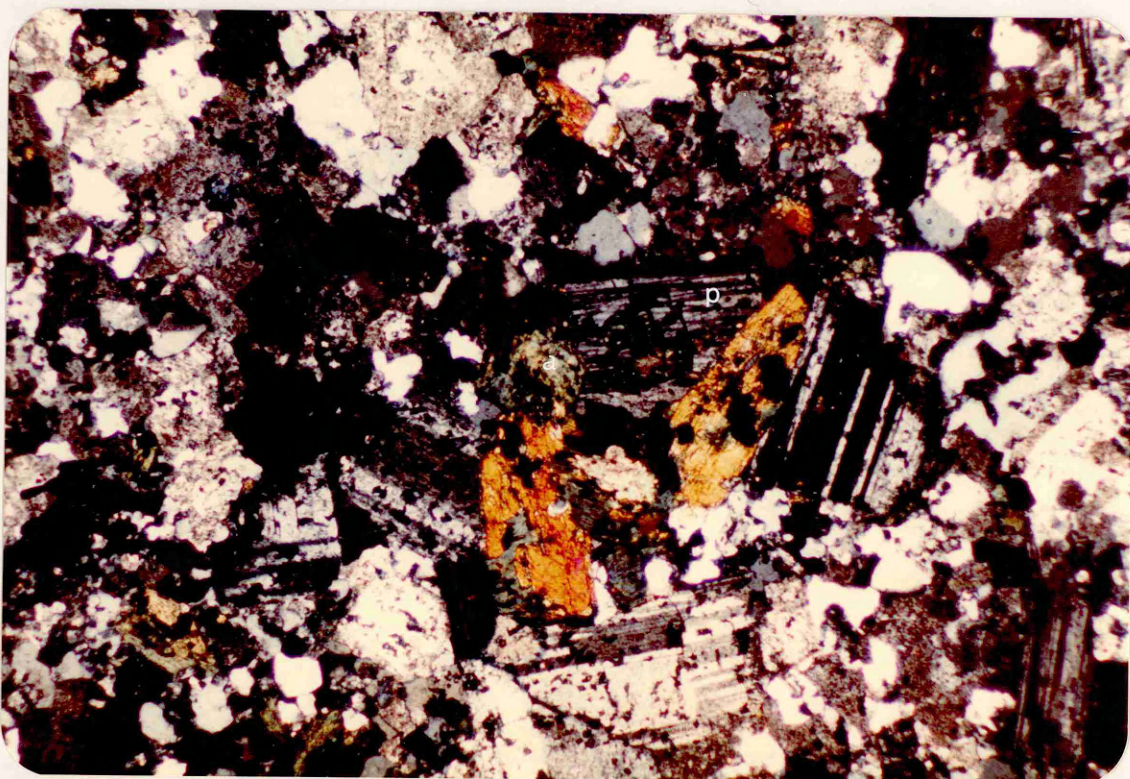


Figure 10. Photomicrograph of Garnfor tonalite LL10. The area of field of view is 15 x 10mm. The section shows a cluster of plagioclase (p) and amphibole phenocrysts (a) (with minor alteration to sericite) in a groundmass coarser grained than Figure 7a.

ii) The major minerals are plagioclase, alkali feldspar and quartz. The feldspars are highly altered to sericite. Pyroxene and biotite phenocrysts are altered to chlorite. Plagioclase and pyroxene form clusters, some of which are completely epidotised. The groundmass of feldspar and interstitial quartz is coarser grained than that of (a). Apatite and Fe-Ti oxide are accessory minerals. (Figure 10).

c). Penrhyn Bodeillas (7 on Fig.1)

This is a porphyritic microgranodiorite with large clusters of amphibole and pyroxene, some completely replaced by chlorite, others partially replaced by hornblende. There are also large feldspar phenocrysts, up to 4mm in size, with sericitic alteration. The groundmass consists of plagioclase, alkali feldspar and quartz. There is some granophyric texture. Accessory minerals are zircon, apatite and Fe-Ti oxide. (Figure 11).

d) Garn Boduan (8 on Fig.1)

All the samples of this tonalite are porphyritic with clusters of plagioclase, pyroxene and alkali feldspar in a fine grained groundmass which appears to be



Figure 11. Photomicrograph of Penrhyn Bodeilas microgranodiorite LL66. The area of field of view is 15 x 10mm. The section shows porphyritic clusters of amphibole (a), pyroxene (p) and feldspar (f). Apatite (e) and zircon (z) can be seen in the groundmass.

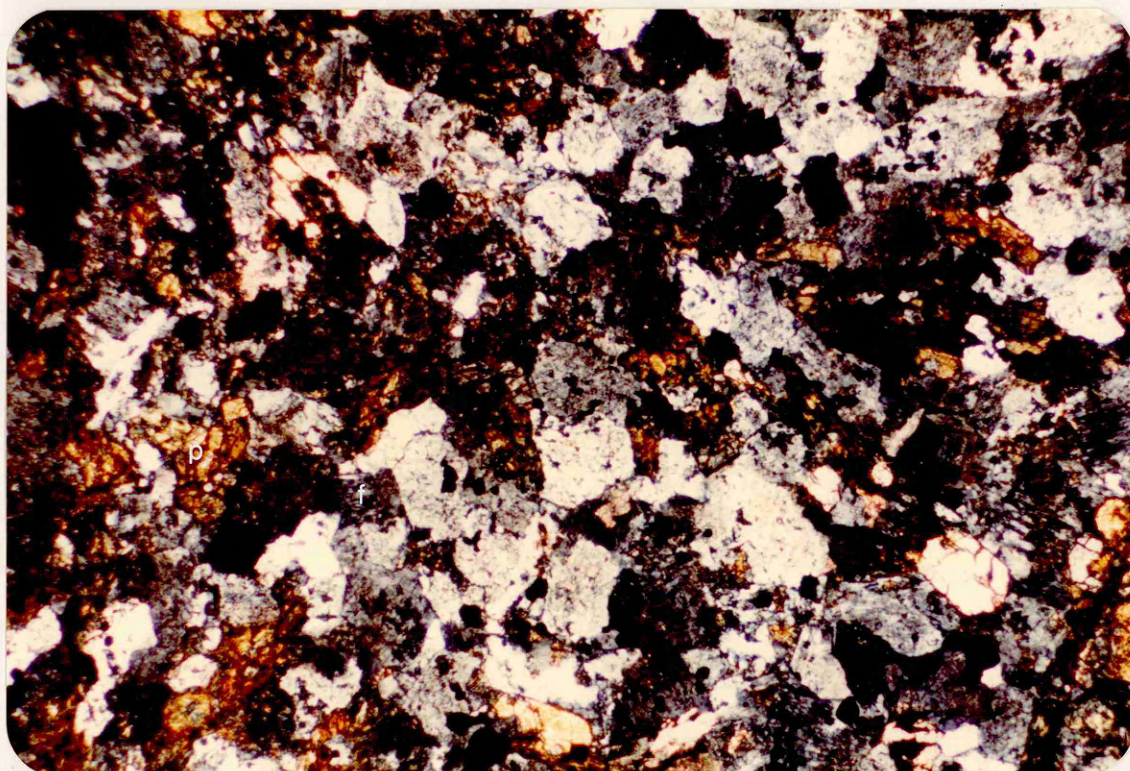


Figure 12. Photomicrograph of Gurn Ddu granodiorite LL77. The area of field of view is 15 x 10mm. The section shows feldspar (f), sericitised and clusters of pyroxenes (p).

directional around the clusters. (Figure 16). Fe-Ti oxide and zircon are accessory minerals.

e). Garn Fadron (9 on Fig.1)

Some of the samples of this granophyre are extensively altered to carbonate. Apatite and zircon crystals can be seen in the fine groundmass which contains highly altered plagioclase phenocrysts. (Figure 8). Those less altered show granophyric intergrowth and crystals of apatite.

f). Nanhoron (10 on Fig.1)

All the samples of this granite consisted of equigranular crystals, 1mm in size, of microperthitic feldspars intergrown with quartz. All the feldspars are turbid in plane polarized light. There are many areas of granophyric intergrowth. One zircon crystal was found in a total of eleven samples. Minor epidotisation also occurs locally. (Figure 13).

g). Llanbedrog (13 On Fig.1)

This is a porphyritic granite consisting of clusters of amphibole, some of which are chloritised and clusters of



Figure 13. Photomicrograph of Nanhoron granophyre LL38. The area of field of view is 15 x 10mm. The section shows the granophyric texture.

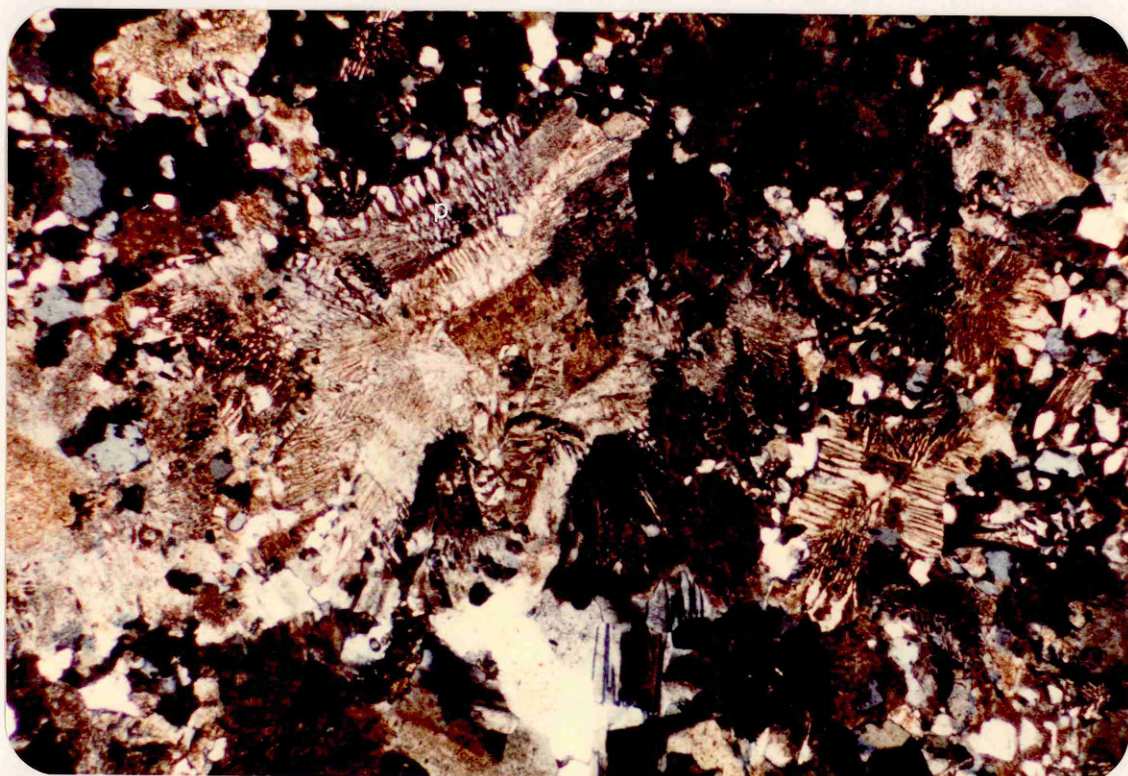


Figure 14. Photomicrograph of Llanbedrog porphyritic granite LL63. The area of field of view is 15 x 10mm. The section shows the perthitic (p) intergrowth and granophyric texture.

phenocrysts which are sericitised in a fine grained groundmass of microperthitic feldspar and quartz with a granophyric texture. An occasional zircon can be seen, some occurring as inclusions in the amphibole clusters (Figure 14).

h) Garn Pentyrch (14 on Fig.1)

Large alkali feldspar and plagioclase phenocrysts form clusters with some altered pyroxenes in this granodiorite. These are surrounded by a very fine groundmass with the occasional zircon. (Figure 15).

B. Volcanic Rocks

Both acid and basic types of volcanics were erupted during the Lower Ordovician. There were localised accumulations of lavas and pyroclastic rocks during the Arenig and Llanvirn and also during the Caradoc. The younger Caradocian volcanics comprise andesitic lavas and tuffs and rhyolitic lavas, ignimbrites and air-fall tuffs. The lower and upper suites of acidic composition are separated by the andesites.

Study of the thin sections shows that the volcanic rocks



Figure 15. Photomicrograph of Garn Pentyrch granodiorite LL125. The area of field of view is 15 x 10mm. The section shows a cluster of feldspar (f) and altered phenocrysts (p) in a very fine grained matrix.

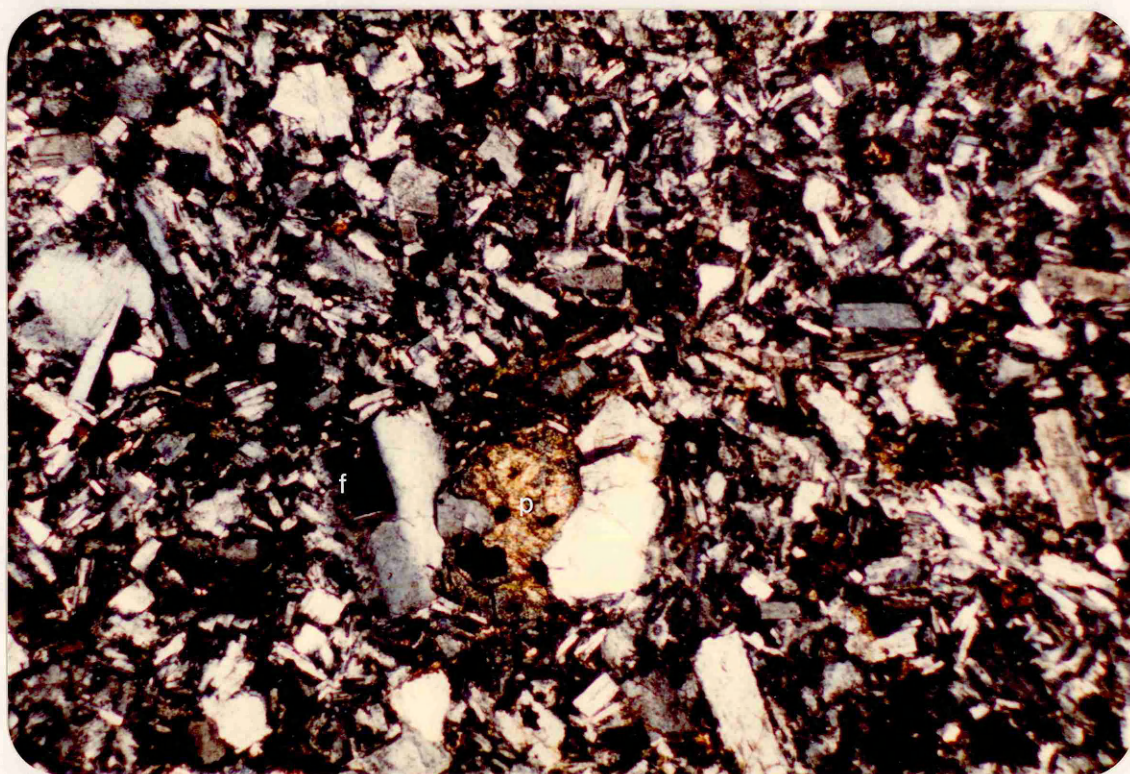


Figure 16. Photomicrograph of Garn Boduan tonalite LL130. The area of field of view is 15 x 10mm. The section shows phenocrysts of feldspar (f) and pyroxene (p) in a fine grained groundmass which is directional around the clusters.

may have been subject to low grade metamorphism.

Short petrographic descriptions of the volcanic rocks now follow.

1. Moel y Penmaen (GR336386) near Boduan

Sparse plagioclase phenocrysts can be seen in a fine-grained matrix of seriticised plagioclase, chlorite, Fe-Ti oxide and pyroxene in this fine-grained andesitic rock. (Figure 17).

2. Basalt (LL142)GR 315386 near Garn Boduan.

Phenocrysts of augite and plagioclase together with much Fe-Ti oxide are surrounded by a groundmass of feldspar laths with granular augite and some epidote. Some chlorite can be seen (Figure 18). The pyroxene is augite and is similar in composition to Garnfor (Croudace 1981).

3. Andesite (LL143)GR 314385 near LL142

Phenocrysts of augite and plagioclase can be seen in a fine-grained groundmass which is too fine to distinguish individual minerals.

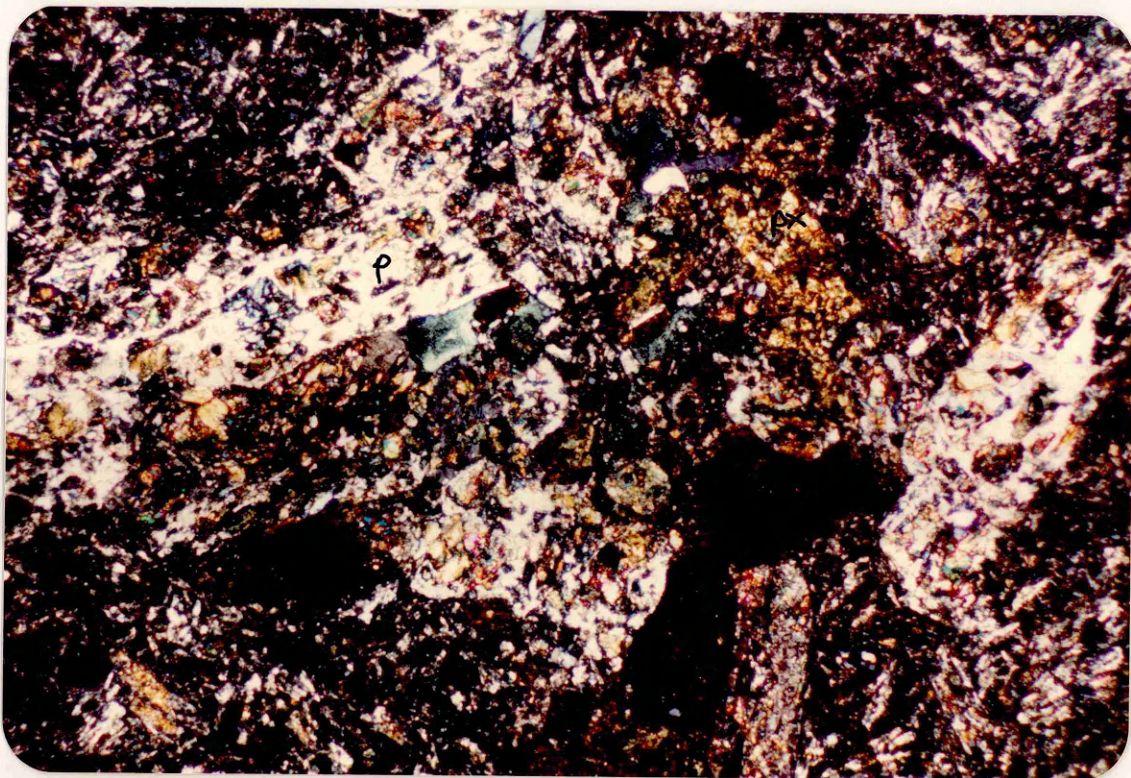


Figure 17. Photomicrograph of Moel y Penmaen lava LL145. The area of field of view is 15 x 10mm. The section shows plagioclase phenocrysts (p) (sericitised) in a fine grained matrix of sericitised plagioclase, chlorite, Fe-Ti oxide and pyroxene (px).



Figure 18. Photomicrograph of basalt LL142. The area of field of view is 15 x 10mm. The section shows phenocrysts of augite (a) and plagioclase (p) in a fine groundmass of feldspar laths.

4. Basaltic andesite (LL153)GR 292335 near Nanhoron.

Phenocrysts of plagioclase feldspar and clinopyroxene can be seen in a very altered groundmass. It is fairly rich in apatite.

5. Basaltic andesite (LL154,LL155)GR 298371 near Ffridd Farm.

Plagioclase phenocrysts (sericitised) are surrounded by a very altered groundmass. The groundmass is fine grained and only feldspar laths can be distinguished.

6. Basalt (LL156)GR 311360 Bodgadle.

A very altered example, consisting of feldspar laths and altered pyroxenes in an unresolvable groundmass.

Chapter 4

Mineralogy of the intrusions and associated lavas

Introduction

Croudace (1981) provided microprobe data on clinopyroxenes, orthopyroxenes and plagioclases from the Llyn[^] granodiorites and tonalites. (Inner Garnfor, Penrhyn Bodeilas and Penrhyn Glas (Carreg y Llam)). Croudace was unable to study the primary mineralogy of the Moel-y-Penmaen lavas because they have been affected by regional greenschist metamorphism. In order to determine the affinities of lavas analysed in this study, and to compare them with the intrusions (Inner Garnfor tonalite, Penrhyn Glas (Carreg-y-Llam) microgranodiorite and Penrhyn Bodeilas), samples of volcanic rocks containing fresh primary minerals were sought for microprobe analysis. Sample LL142 was the only suitable material containing fresh clinopyroxene and plagioclase phenocrysts in a fine-grained matrix, and microprobe analyses are given in Appendix 1.

Summary of previous work by Croudace (1961)

Pyroxene compositions were determined in samples from the three intrusions named above. These were plotted on a Wo-En-Fs diagram and compared with the evolutionary trend of pyroxenes from Tertiary acid glasses (Carmichael, 1960), which are considered to represent rocks derived by crystal fractionation from tholeiitic magmas.

Plagioclase compositions were also determined and shown on the Ab-Or-An diagram. The broad range of compositions from An₂₅ to An₅₅ suggests that some feldspars are xenocrysts derived from another part of the magmas system.

Mineralogy of lavas (this study)

The clinopyroxenes from LL142 are shown in a Wo-En-Fs diagram, (Figure 19). The pyroxenes are of augite composition and vary from Wo₃₇En₄₁Fs₂₂ to Wo₃₉En₄₂Fs₁₅. They plot on the Mg-rich end of the trend reported for Icelandic pitchstones (Carmichael, 1960).

The pyroxene analyses were also plotted to show their SiO₂ and Al₂O₃ content (Figure 21). Le Bas (1962) divided clinopyroxenes into three groups using their SiO₂ and Al₂O₃ contents. His three groups are A, non-alkaline

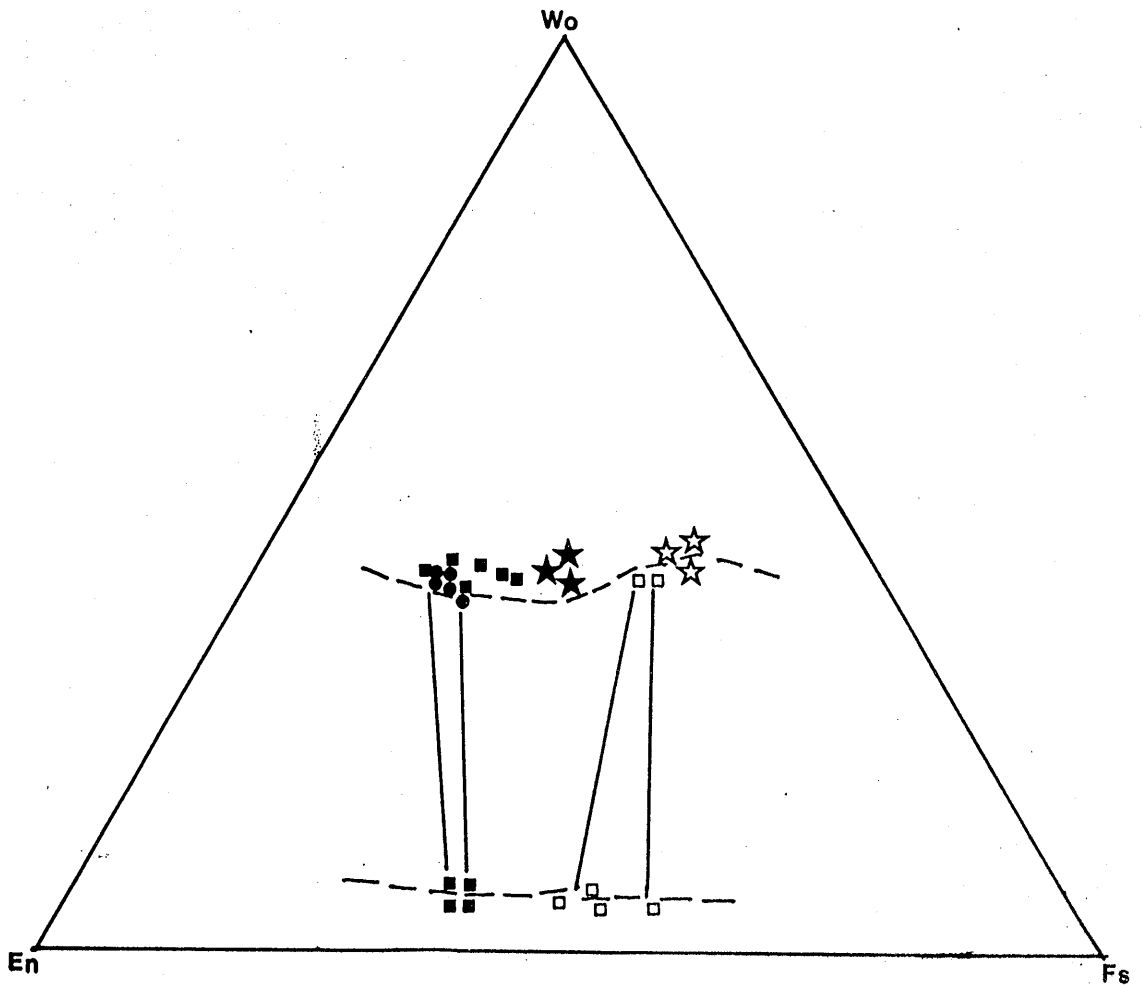


Figure 19. The Wo-Fs-En ternary diagram showing the evolutionary trends of minerals in the Llŷn intrusions. The crystallisation trends of ortho- and clinopyroxenes from some Tertiary acid glasses, (Carmichael, 1960) are shown for comparison (dashed lines). Closed and open squares represent phenocryst and groundmass minerals respectively. Squares - Inner Garnfor tonalite; Open stars - Penrhyn Bodeilas; (based on Croudace, 1981); Closed circles - LL142 basalt (this study).

(tholeiitic, high alumina and calc-alkaline lavas); B, alkaline lavas and C, peralkaline lavas. The pyroxene analyses from this study fall into group A, confirming the supposition put forward by the Wo-En-Fs diagram.

The plagioclases from LL142 are shown in an Ab-Or-An diagram (Figure 20). The plagioclases vary in composition from $Ab_{40}An_4Or_{56}$ to $Ab_{55}An_4Or_{41}$.

Comparison of both sets of data.

Comparison of the pyroxene analyses indicates 1) that the clinopyroxenes (augite) which are similar to those in the intrusions (Garnfor tonalite) studied by Croudace (1981), plot within the field of phenocrysts of the Garnfor tonalite intrusion, 2) they are of tholeiitic or calc-alkaline character, 3) the tonalite and lava LL142 overlap in composition and so may be contemporaneous and therefore 4) the tonalites may have been derived from a magma such as that represented by LL142, 5) and the location of the LL142 pyroxenes and the tonalite at the basic end (i.e. Mg-rich end of the pyroxene fractionation trend) is consistent with the more acid intrusions and lavas being derived from such basic/intermediate magma.

Comparison of the plagioclase analyses indicates 1) that

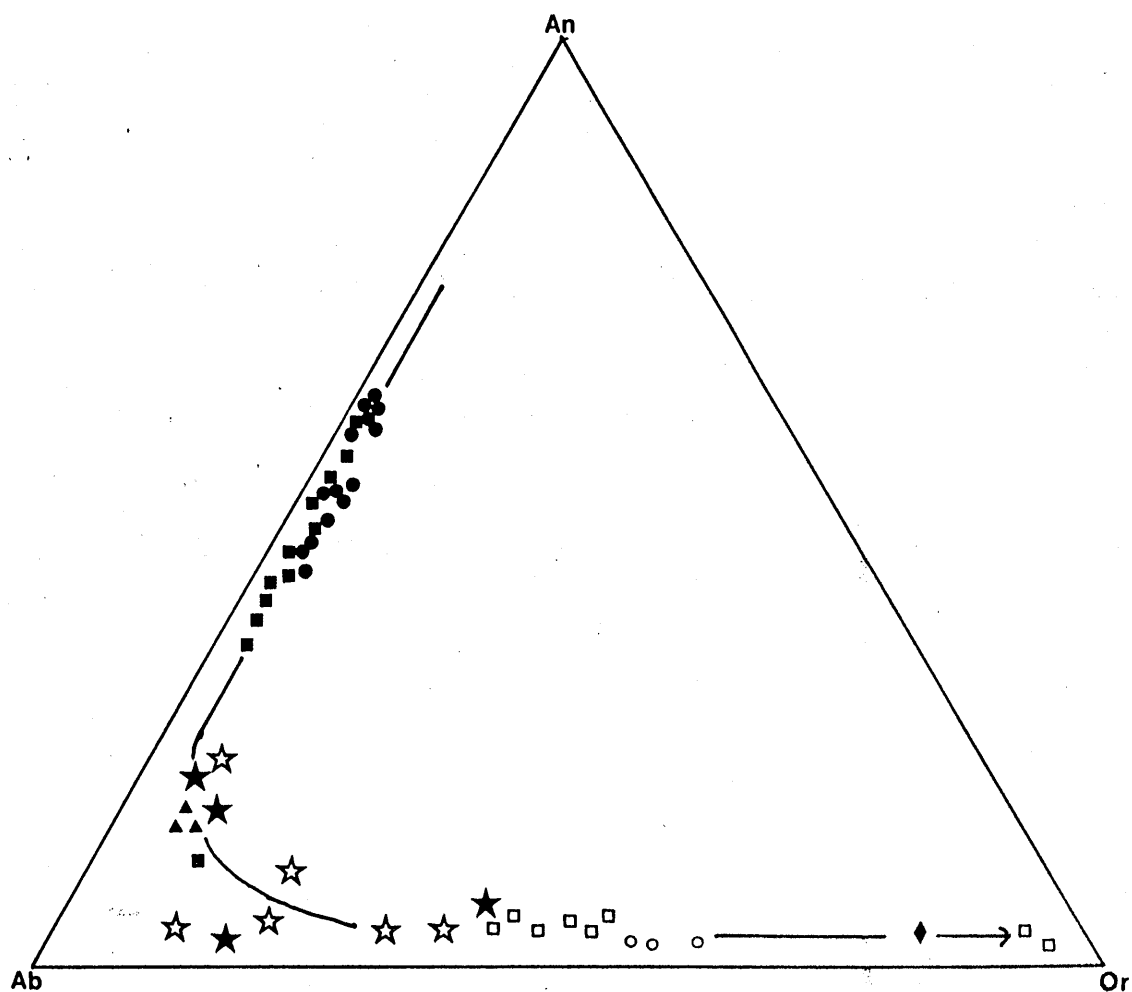


Figure 20. Ab-An-Or ternary diagram showing the evolutionary trends of minerals in the Llŷn intrusions. (Symbols as in Figure 19). Broken lines from Tertiary acid glasses (Carmichael, 1960). Circles - LL142 basalt (this study).

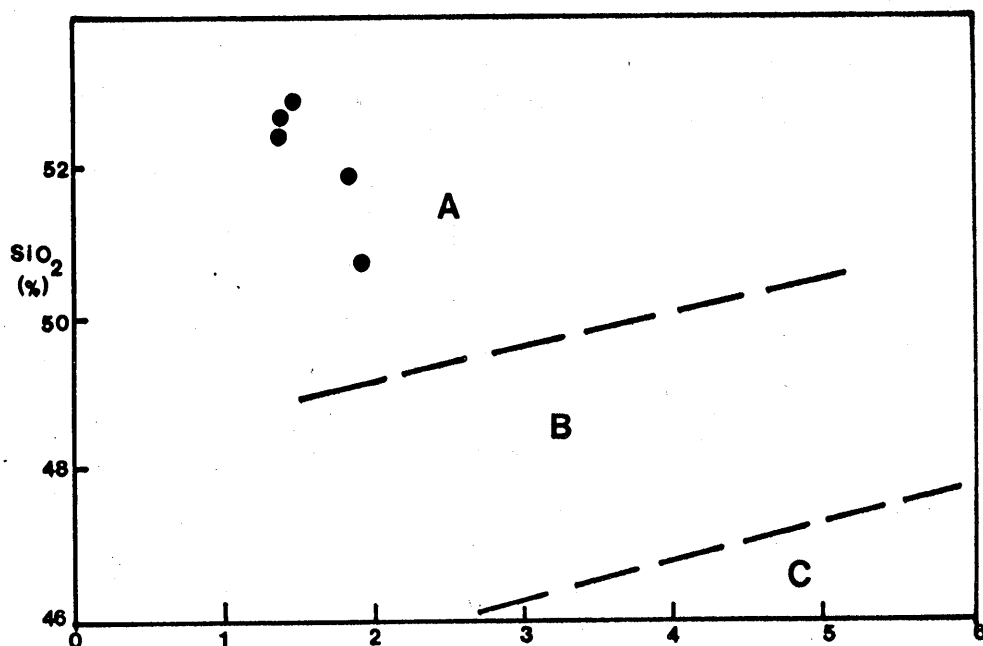


Figure 21. Plot of SiO_2 against Al_2O_3 for clinopyroxenes from the basalt LL142. The broken lines separate 3 groups of clinopyroxene composition. A, non-alkaline (tholeiitic, high alumina and calc-alkaline); B, alkaline lavas and C, peralkaline lavas (Le Bas, 1962).

the plagioclases are similar to those in the intrusions (Garnfor tonalite) studied by Croudace (1981), 2) the tonalite and lava LL142 overlap in mineral composition and so may be contemporaneous and therefore 3) the tonalite may be derived from a lava such as LL142, 3) the analysed plagioclase samples plot within the field of the phenocrysts of the Garnfor tonalite intrusions analysed by Croudace (1981)

Chapter 5.

Chemistry of the intrusions and associated lavas

Introduction

The samples of lavas and granitic intrusions collected from the Llyn^A peninsular range from 46 - 75% SiO_2 . The acid rocks are described as microgranites, granophyres, microgranodiorites and microtonalites (Tremlett 1962, 1964) while the basic / intermediate rocks are basaltic or andesitic in composition (Matley and Heard, 1938). 81 samples (67 granites and 14 lavas) were analysed by X-ray fluorescence spectrometry (Appendix 2). This data shows the differences within the sample population. Some of these differences were noted by Tremlett (1972) who separated the intrusions of Llyn into Ordovician and Caledonian (end Silurian-Devonian) dependent on various geochemical parameters. In order to clarify these differences, the samples were plotted onto classification diagrams. (Figures 22 and 25)

Chemistry of the intrusions

Figure 22 shows the intrusions plotted on a SiO_2 v. $\text{Na}_2\text{O} + \text{K}_2\text{O}$ diagram taken from Cox, Bell and Pankhurst (1979). Most of the intrusions plot in discrete fields (Nanhoron, Garnfor (2 groups), Bwlch Mawr, Llanbedrog and Penrhyn Bodeillas) while the others overlap two or even

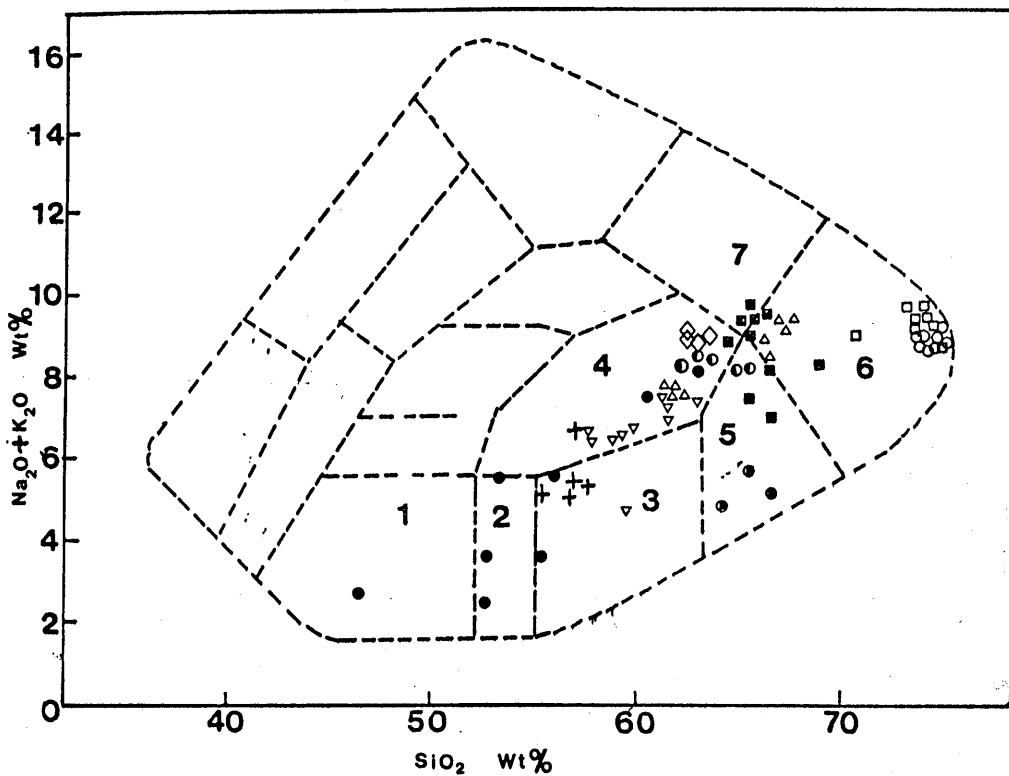


Figure 22. Plot of $\text{Na}_2\text{O} + \text{K}_2\text{O}$ against SiO_2 . The intrusions form distinct groups which fall in fields identified as monzonites, granites, granodiorites, syenites and diorites. The volcanic rocks fall in fields identified as basalt, basaltic andesite and andesite. Only data from this study is plotted.

KEY:	1	Basalt	5	Granodiorite
	2	Basaltic andesite	6	Granite
	3	Andesite	7	Syenite
	4	Monzonite		

Key to Figures 22 to 41

- △ Garnfor
- Nanhoron
- Llanbedrog
- + Moel y Penmaen
- ◇ Penrhyn Bodeillas
- Gurn Ddu
- Bwlch Mawr
- ▽ Garn Fadron
- Garn Boduan
- ▲ Foel Gron
- Lavas

- Mynydd Nefyn
- ◆ Yr Eifl microgranite
- C Penrhyn Glas
- ⊕ Gurn Goch
- ⊖ Llanybi
- M Moel Penllechog

Data from Croudace (1981)

Data from this study

three fields (Garn Boduan, Garn Fadron and Gurn Ddu). Nanhoron, Llanbedrog and one Garnfor group are classed as granites; Penrhyn Bodeilas and the second Garnfor group as monzonite ; Bwlch Mawr as granodiorite . The intrusions which overlap different fields are classed as diorite / granodiorite / granite / syenite.

In order to relate the chemical analyses to mineral composition, the chemical analyses were recalculated into normative minerals. On this basis the intrusions fall into three groups;

- i) peraluminous (those with normative corundum);
Garn Boduan, Bwlch Mawr, Llanbedrog and Garnfor (LL5,6,11);
- ii) metaluminous (those with normative diopside and anorthite); Garnfor (except LL5,6,11), Gurn Ddu, Garn Fadron, Garn Boduan (LL138-141), Penrhyn Bodeilas;
- iii) peralkaline (those with normative acmite);
Nanhoron.

A brief geochemical description of each intrusion follows. Table 1 shows the ranges of oxides and trace elements within each intrusion.

Table 1. Range of oxides and trace elements within each intrusion

	Garnfor	Nanhoron	Llanbedrog	Penrhyn Bodeillas	Gurn Ddu	Bwlch Mawr	Garn Fadron	Garn Pentyrch	Garn Boduan
SiO ₂	a) 60.85- 62.28 b) 66.12 67.22	73.36- 75.06	70.37- 74.63	62.67- 63.22	63.22- 65.39	64.06- 66.42	59.57 63.40	65.52	64.66- 68.89
TiO ₂	0.49- 1.47	0.22- 0.26	0.16- 0.19	0.74- 0.84	0.67- 0.94	0.44- 0.50	0.90 0.98	0.48	0.36- 0.42
Al ₂ O ₃	14.87- 16.23	10.19- 13.07	11.73- 14.26	15.96- 16.49	14.20- 15.26	16.34- 18.11	13.81- 15.46	14.05	16.17- 17.82
Fe ₂ O ₃	3.30- 7.39	3.85- 4.49	1.48- 1.93	5.99- 6.47	6.41- 7.79	5.32- 5.76	9.40- 9.90	6.47	4.15- 6.51
MgO	0.80- 1.83	0.02- 0.07	0.08- 0.17	1.33- 1.56	0.91- 1.13	0.44- 0.50	1.40- 1.69	0.61	0.38- 1.17
CaO	1.66- 3.96	0.18- 0.34	0.18- 1.02	2.50- 2.84	2.23- 2.65	3.38- 4.11	2.33- 5.49	1.06	0.42- 2.33
Na ₂ O	4.55- 5.19	3.52- 5.09	3.82- 4.49	5.63- 5.92	4.70- 5.20	1.88- 4.43	2.63- 4.55	4.51	5.41- 6.31
K ₂ O	3.05- 4.33	3.75- 5.48	4.97- 5.47	3.35- 3.47	3.43- 3.78	1.79- 3.01	2.07- 3.74	4.19	1.63- 3.60

Table 1 (contd.)

	Garnfor	Nanhoron	Llanbeddrog	Penrhyn Bodeillas	Gurn Ddu	Bwlch Mawr	Garn Fadron	Garn Penttyrch	Garn Boduan
Ba	502- 596	37- 67	441- 503	574- 627	599- 759	313- 387	455- 1081	650	220- 797
Ce	76- 104	172- 246	131- 166	102- 129	111- 139	114- 127	110- 129	124	98- 139
Nb	31- 35	76- 97	43- 52	45- 48	44- 50	49- 54	42- 48	51	49- 58
Rb	70- 97	120- 213	152- 171	57- 65	80- 101	52- 88	55- 100	109	44- 64
Sr	206- 391	7- 15	14- 41	293- 323	238- 301	137- 206	177- 411	121	91- 251
Th	2- 14	14- 32	6- 18	2- 5	3- 13	6- 8	4- 10	12	1- 7
Y	36- 45	117- 155	83- 90	49- 53	59- 65	68- 69	63- 70	73	48- 63
Zr	508- 557	881- 1144	210- 252	696- 745	551- 600	532- 559	492- 536	573	773- 856

1. Garnfor

There are two distinct groups within the Garnfor intrusion. The geochemical analyses confirm this with a group of samples around 61% SiO_2 and another group around 66% SiO_2 . The analyses also show that Fe_2O_3 , TiO_2 , MgO , Y and Sr decrease with the increasing SiO_2 and K_2O , Na_2O , Th , Zr , Rb and Nb increase with increasing SiO_2 .

2. Gurn Ddu and Bwlch Mawr

These two intrusions plot close to each other and have close geographical proximity. Their geochemistry is very similar, Bwlch Mawr having slightly more CaO and much less Ba .

3. Nanhoron and Foel Gron

The Nanhoron granophyre is a peralkaline rock with ^hhigh concentrations of Nb and Zr . The SiO_2 content is similar to that of the Llanbedrog intrusion but the Nanhoron granophyre is lower in Al_2O_3 and Ba , but is higher in Fe_2O_3 , CaO , Nb , Rb , Y and Zr . Foel Gron is of similar composition with high Rb , Th , Y , Zr , Nb and low Ba and Sr .

4. Llanbedrog

The samples when plotted on Harker diagrams show a linear relationship with each other, decreasing in Fe_2O_3 and K_2O with increasing SiO_2 and increasing in TiO_2 and Na_2O with increasing SiO_2 and Sr . The intrusion has a

high K_2O content and is low in Zr and Sr but high in Y and Rb.

5. Penrhyn Bodeilas

These samples form a small cluster on Harker diagrams. They have high Zr and Ba and are similar in chemistry to Garn Fadron.

6. Garn Fadron

This intrusion also has high Zr and Ba content but the Zr content is not as high as in Penrhyn Bodeilas. Al_2O_3 is also lower but Fe_2O_3 is higher.

7. Garn Boduan

This intrusion is high in Al_2O_3 and Zr relative to the other intrusions except Nanhoron.

Discussion

Variation diagrams such as Figures 23 and 24 are useful devices for investigating the origin of differences in chemical composition between members of a rock series presumed to represent stages in the evolution of a magma. With the aid of the diagram, one can simulate graphically the subtraction of mineral phases (crystal fractionation, liquid unmixing) or addition of rock materials or magmas (assimilation or hybridism) to ascertain how closely these processes might be able to account for the observed chemical differences between members of the rock series.

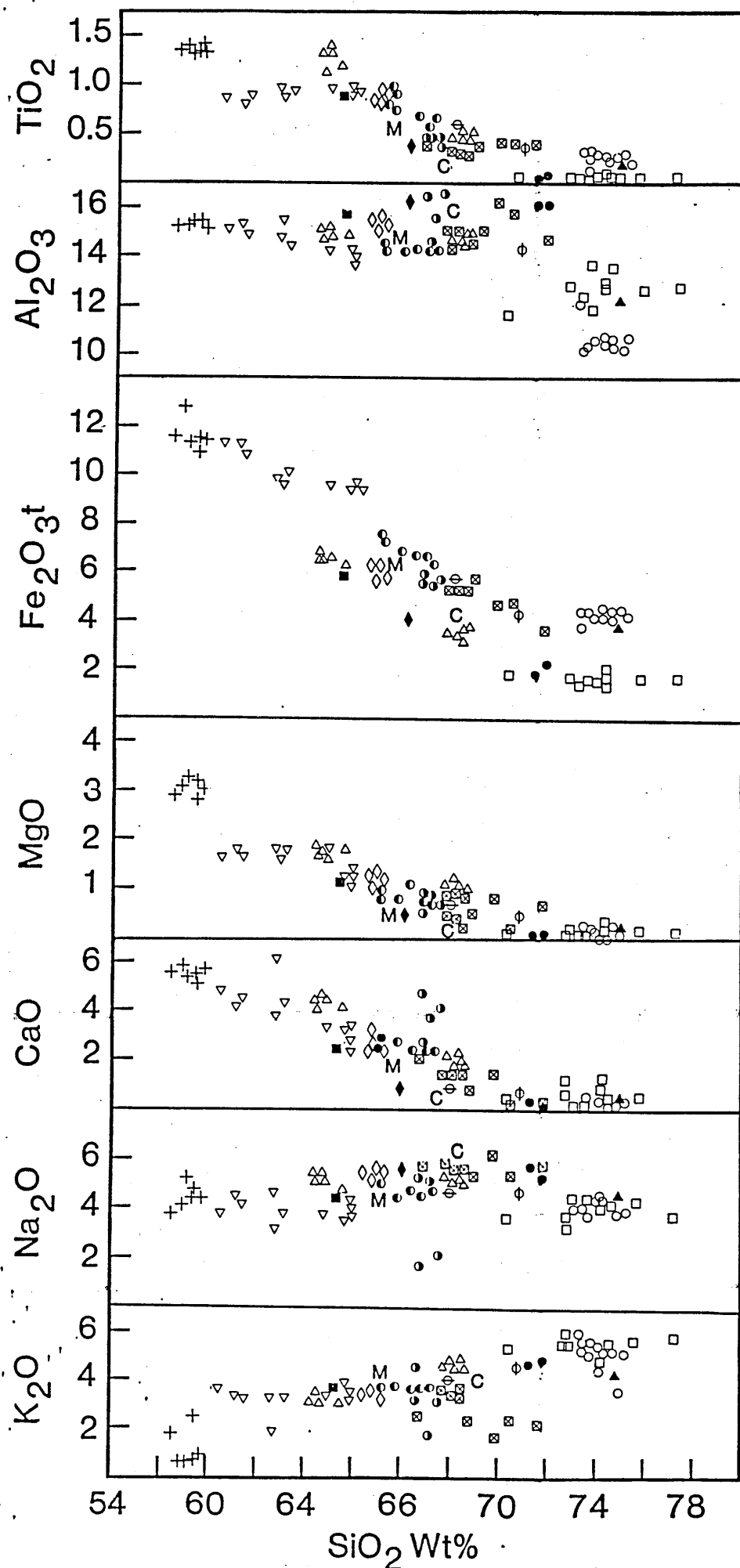


Figure 23. Harker diagram showing major oxides against SiO₂. Symbols as in Figure 22. Data from Croudace (1981) included.

Figure 23 shows a plot of major oxides against SiO_2 . There is a steady decrease in Fe_2O_3 against increasing SiO_2 . TiO_2 , MgO and CaO also decrease against increasing SiO_2 but in a less steady way, more in a series of apparent steps. K_2O increases with increasing SiO_2 in a similar sort of way. Na_2O and Al_2O_3 both increase with increasing SiO_2 until 70% SiO_2 is reached and then decreases as SiO_2 increases. Although the Nanhoron and Llanbedrog intrusions have similar amounts of SiO_2 , this figure shows that their Al_2O_3 ,

TiO_2 , Fe_2O_3 and CaO contents are significantly different. The scatter may be due to the fact that some of the intrusions are very porphyritic (see Appendix 1) (Garnfor, Llanbedrog, Penrhyn Bodeilas, Gurn Ddu, Bwlch Mawr and Garn Boduan), and this can affect the overall chemical analysis; i.e. in a very porphyritic sample the composition of the phenocrysts would affect the overall composition when analysed. In this case this is not of great importance.

Figure 24 is a plot of selected trace elements against SiO_2 . Sr decreases with increasing SiO_2 but there is a large element of scatter. This may be due to the fact that Sr is a mobile element and the intrusions have been subject to alteration. Rb increases with increasing SiO_2 but also has a large element of scatter, probably for the same reason as Sr. Y stays at a fairly steady concentration until rising sharply between 70 - 74%

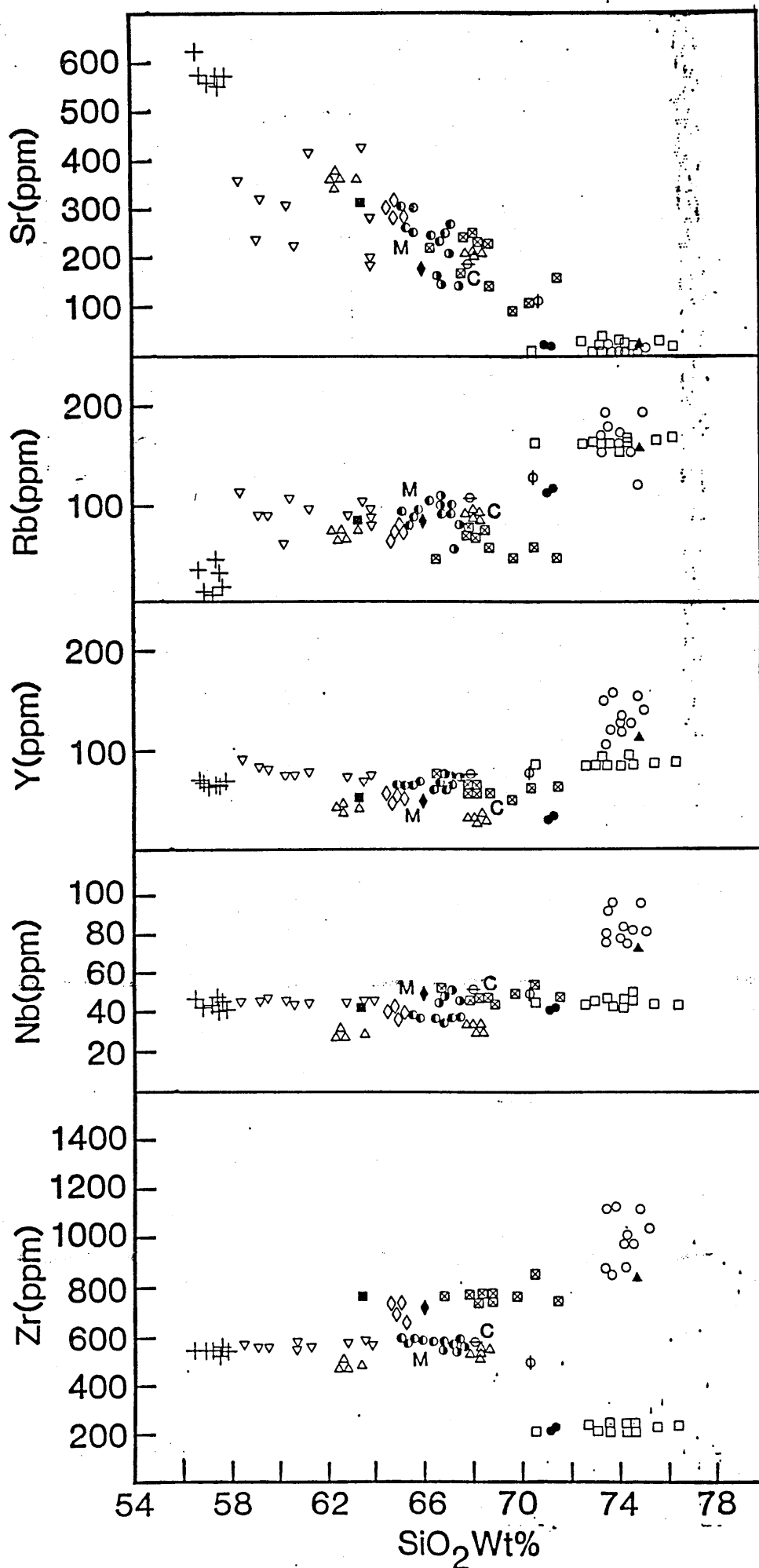


Figure 24. Harker diagram showing trace elements against SiO_2 . Symbols as in Figure 22. Data from Croudace (1981) included.

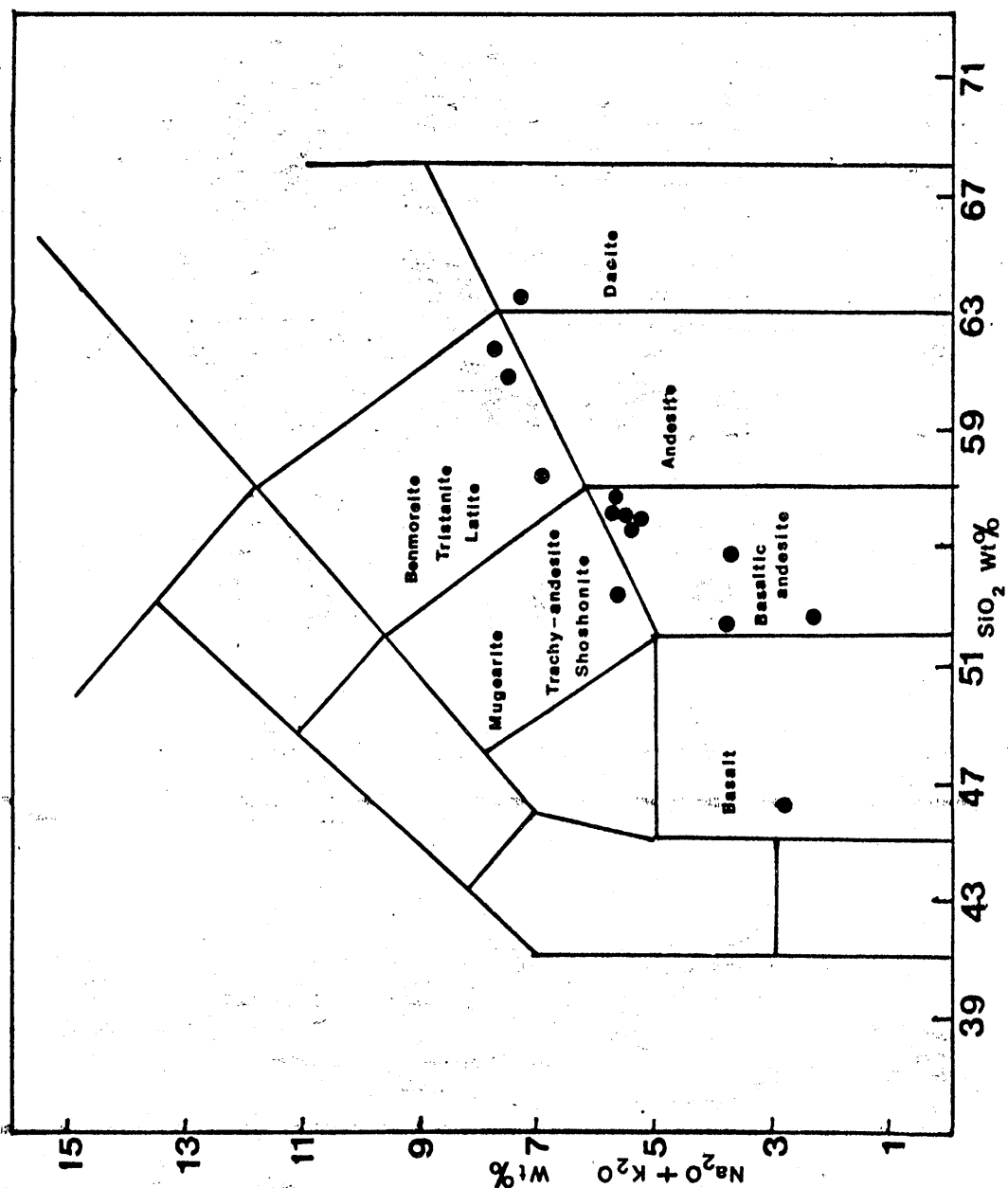


Figure 25. Classification according to Zannettin (1988) showing the fields in which the lavas are contained. Only data from this study is plotted.

SiO₂. Nb has a similar trend to Y. Zr increases steadily with increasing SiO₂ until 70% SiO₂, then from 66% SiO₂ to the low Sr intrusion (Llanbedrog) forming two separate groups. The increase of Sr content could be caused by plagioclase crystallisation.

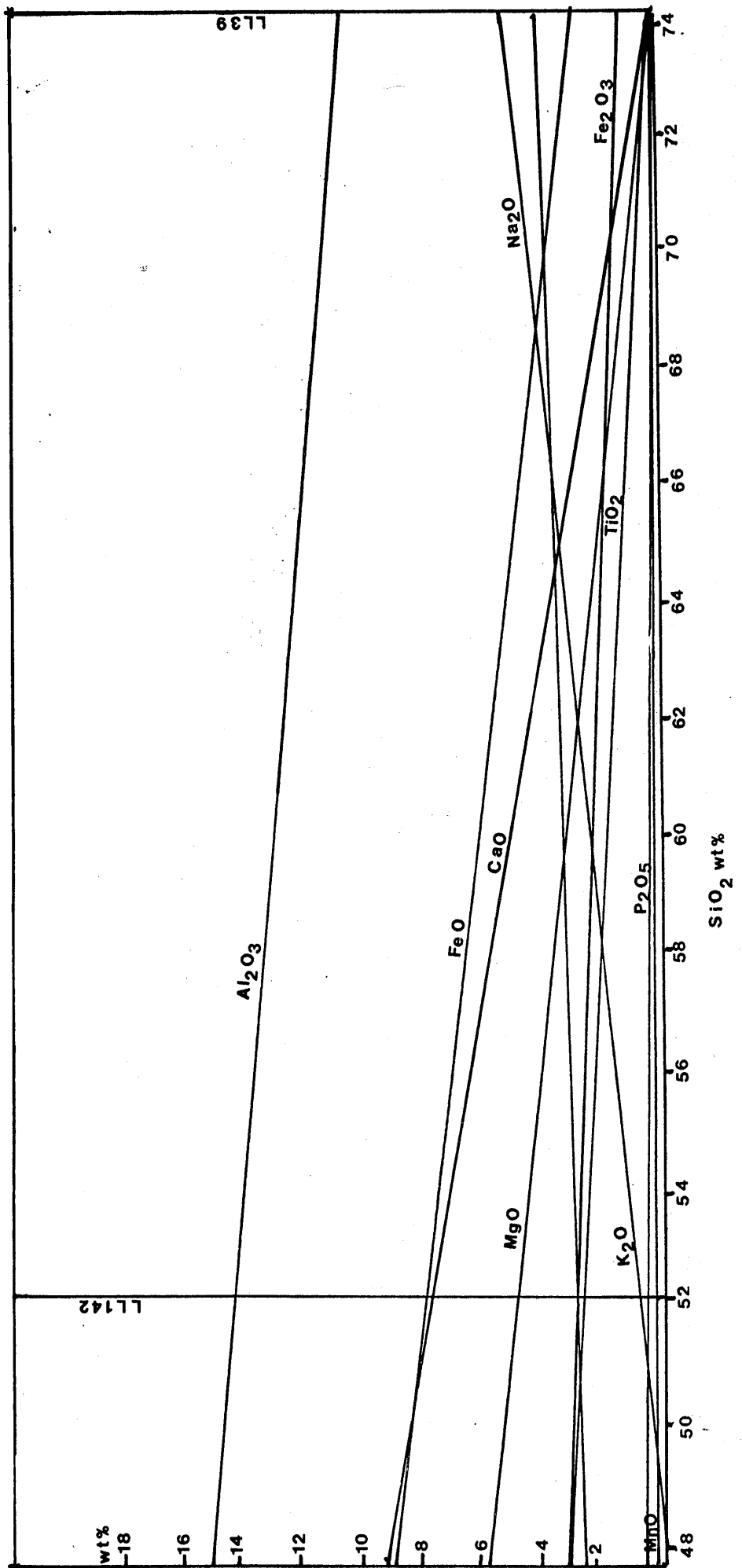
Chemistry of the lavas

On Figure 22 the lavas plot as basalt, basaltic andesite, andesite and trachyandesite.

Figure 25 is a plot of the lavas onto a Total Alkali-Silica diagram which has been proposed as a definitive classification for volcanic rocks (Zanettin, 1984). Here the lavas are classed as basalt, basaltic andesite, trachyandesite, dacite and benmoreite.

When the chemical analyses were recalculated into normative minerals it was clear that LL142 is a tholeiitic basalt; i.e. it has normative quartz and hypersthene despite a relatively high FeO/Fe₂O₃. The Moel y Penmaen andesite, LL155, LL143, LL153 and LL154 also have quartz and hypersthene and may therefore be related to LL142.

Figure 26. Addition - subtraction diagram using LL142 (basalt) and an average Nanhoron composition (LL39).



Discussion of lavas and their relationship to the intrusions

Figure 26 shows an addition - subtraction diagram where the basalt, LL142 and an average Nanhoron composition, LL39 are plotted, the points joined together by a line which is extrapolated backwards to the more basic end of the plot. LL142 was chosen because it is an unusually fresh basalt and also to test the hypothesis that the granitic intrusions could have been generated from a basaltic magma. From this it can be seen that the most basic possible crystal extract that can be removed from LL142 to yield Nanhoron is of composition at which K_2O becomes zero, i.e. SiO_2 48%, Al_2O_3 15%, CaO 9%, MgO 5.8%, TiO_2 3.1%, Fe_2O_3 3.05%, FeO 8.8%, Na_2O 2.8%, P_2O_5 0.5% and K_2O 0.0%. The most likely mineral composition of this extract would be plagioclase, orthopyroxene and clinopyroxene. LL142 contains phenocrysts of plagioclase and altered pyroxene so is therefore a possible parent magma. The amount of granite produced by removal of such a crystal extract as that above from LL142 can be calculated as follows:

Amount of granite produced

$$\begin{aligned} & \frac{\text{SiO}_2 \text{ in LL142} - \text{SiO}_2 \text{ in crystal extract}}{\text{SiO}_2 \text{ in LL39} - \text{SiO}_2 \text{ in crystal extract}} \times 100 \\ &= \frac{52.25 - 48}{74.00 - 48} \times 100 \\ &= 16.35\% \end{aligned}$$

This is the maximum amount of granite which could be produced as some crystals might not be completely removed from the melt and some substitution of K for Na would occur in plagioclase.

The percentage of intermediate magma of 62% SiO₂ produced

$$\begin{aligned} &= \frac{\text{SiO}_2 \text{ in LL142} - \text{SiO}_2 \text{ in crystal extract}}{62 - \text{SiO}_2 \text{ in crystal extract}} \times 100 \\ &= \frac{52.25 - 48}{62 - 48} \times 100 \\ &= 30.36\% \end{aligned}$$

This again is a maximum figure. Figure 26 shows that fractional crystallisation could easily have produced the intrusions and should produce a range of basic to acidic rock types with about twice as much intermediate as acidic rock.

The normative analysis of the possible crystal extract was calculated, the following composition being obtained:

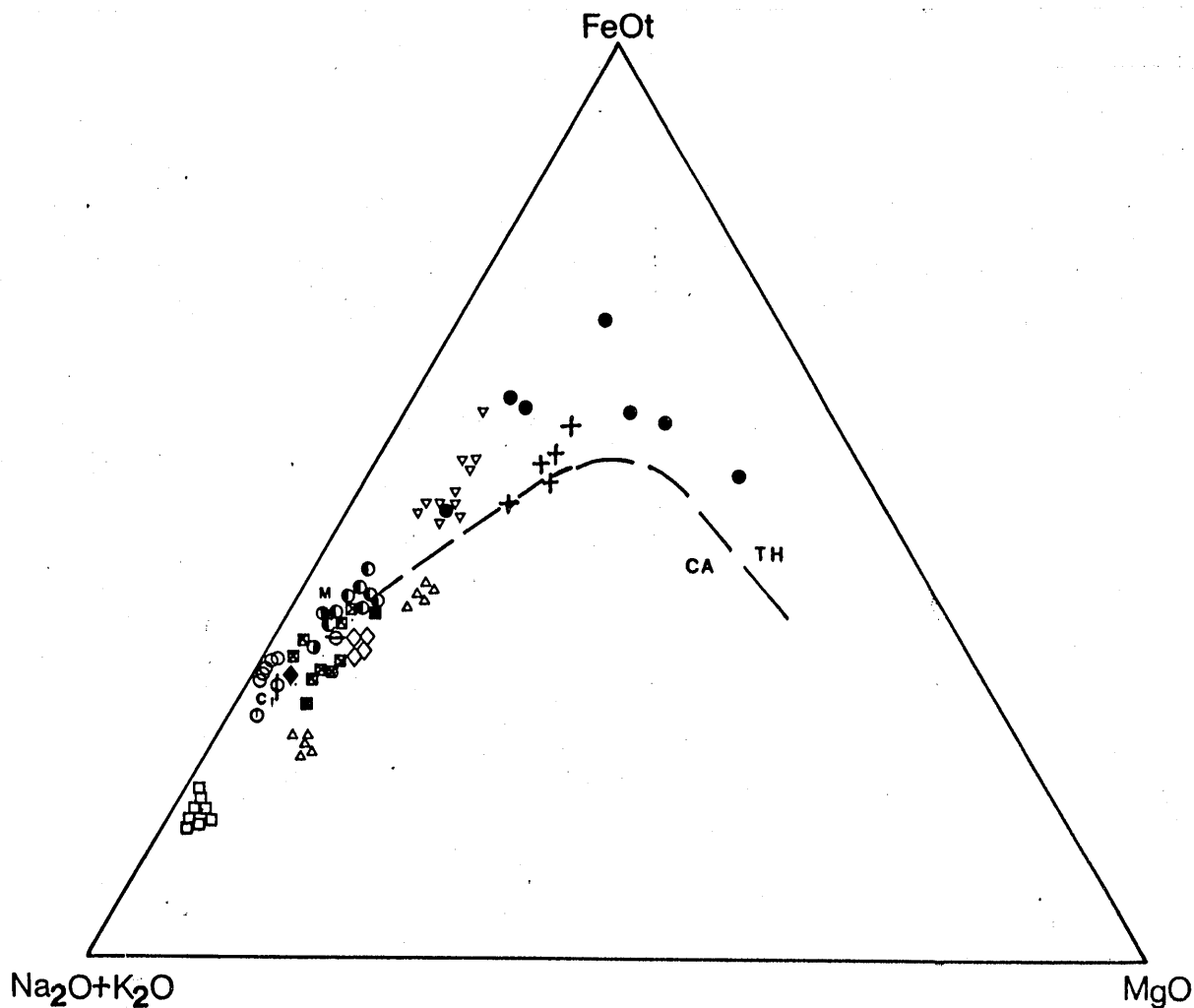


Figure 27. AFM diagram. The dashed lines separate .. tholeiitic (TH) from calc-alkaline (CA) associations using the criteria of Irvine and Baragar (1971). Symbols as in Figure 22. Data from Croudace (1981) included.

Quartz	4.47%
Ilmenite	6.15%
Anorthite	29.74%
Albite	21.22%
Magnetite	4.55%
Diopside	10.66%
Hypersthene	19.04%
Apatite	1.16%

This normative composition is typical of a tholeiitic basalt, confirming the trend suggested by the microprobe and bulk chemical data.

In order to confirm the tholeiitic characteristics suggested by the microprobe and normative analyses, the lavas and intrusions were also plotted on an AFM diagram (Figure 27) which confirms that some of the intrusions at least are tholeiitic while the others are calc-alkaline. The criteria of Irvine and Baragar (1971) was used to draw in the trend lines. All the lavas, including Moel y Penmaen, the intrusions of Garn Fadron, Gurn Ddu and Nanhoron plot on the tholeiitic association while the others plot on the calc-alkaline association, although this division is not considered as being of importance here.

From the trace element data plotted in Figure 24, it is clear that the high field strength elements, Zr, Y and Nb

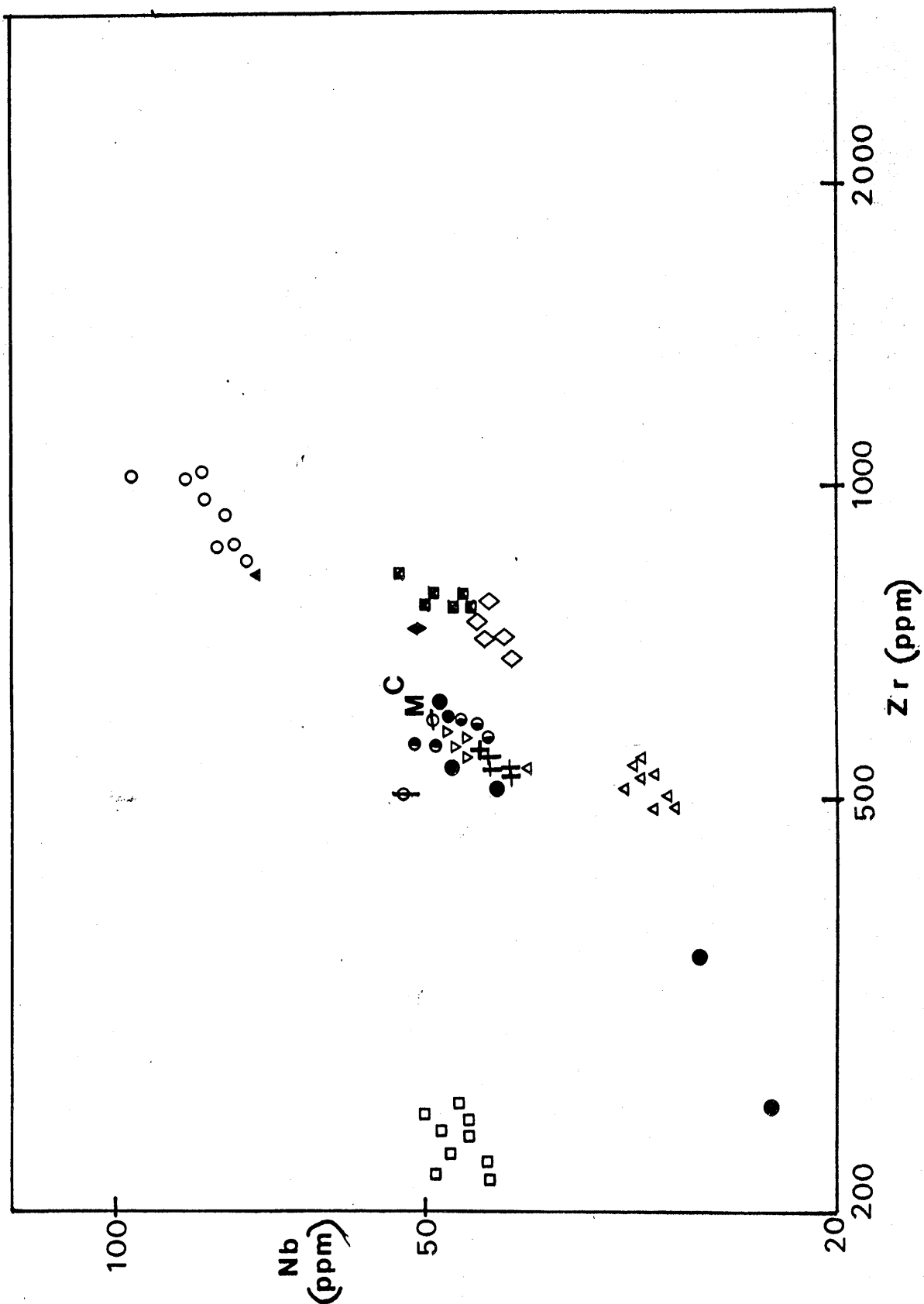


Figure 28. Plot of Nb against Zr. Symbols as in Figure 22. Data from Croudace (1981) included.

are the most powerful means of discrimination between the intrusions. These elements are also believed to be relatively stable during alteration. Although some discrimination is shown by Rb and Sr, the altered character of feldspar discussed earlier indicates that these elements may have been mobile. The lavas and intrusions together with data from Croudace (1981) were plotted on a Zr versus Nb diagram (Figure 28). The intrusions fall into five chemical groups which are not simply geographically related:

- a) Llanbedrog (13) and the Yr Eifl felsite(4)
- b) Nanhoron (10) and Foel Gron(12)
- c) Garnfor(3)
- d) Garn Boduan (8),Penrhyn Bodeilas (7),Mynydd Nefyn (6) and the Yr Eifl microgranite(Y)
- e) Garn Fadron (9),Gurn Ddu (18),Bwlch Mawr (1),Gurn Goch (2),Llangybi (L),Moel Penllechog (M) and Penrhyn Glas (Carreg-y-Llam) (5).

The Moel y Penmaen andesite is quite high in Zr and plots with group 5. The basalt,LL142 and the andesite,LL143 plot separately on the diagram showing trends which will be discussed later.LL154,155 and 163 plot with the intrusions and LL156, a primitive basalt plots on its own. LL156 poses interpretation problems. Leat and Thorpe (1986) consider it not to be chemically related to any of the other Caradocian volcanic rocks of the Llyn[^].

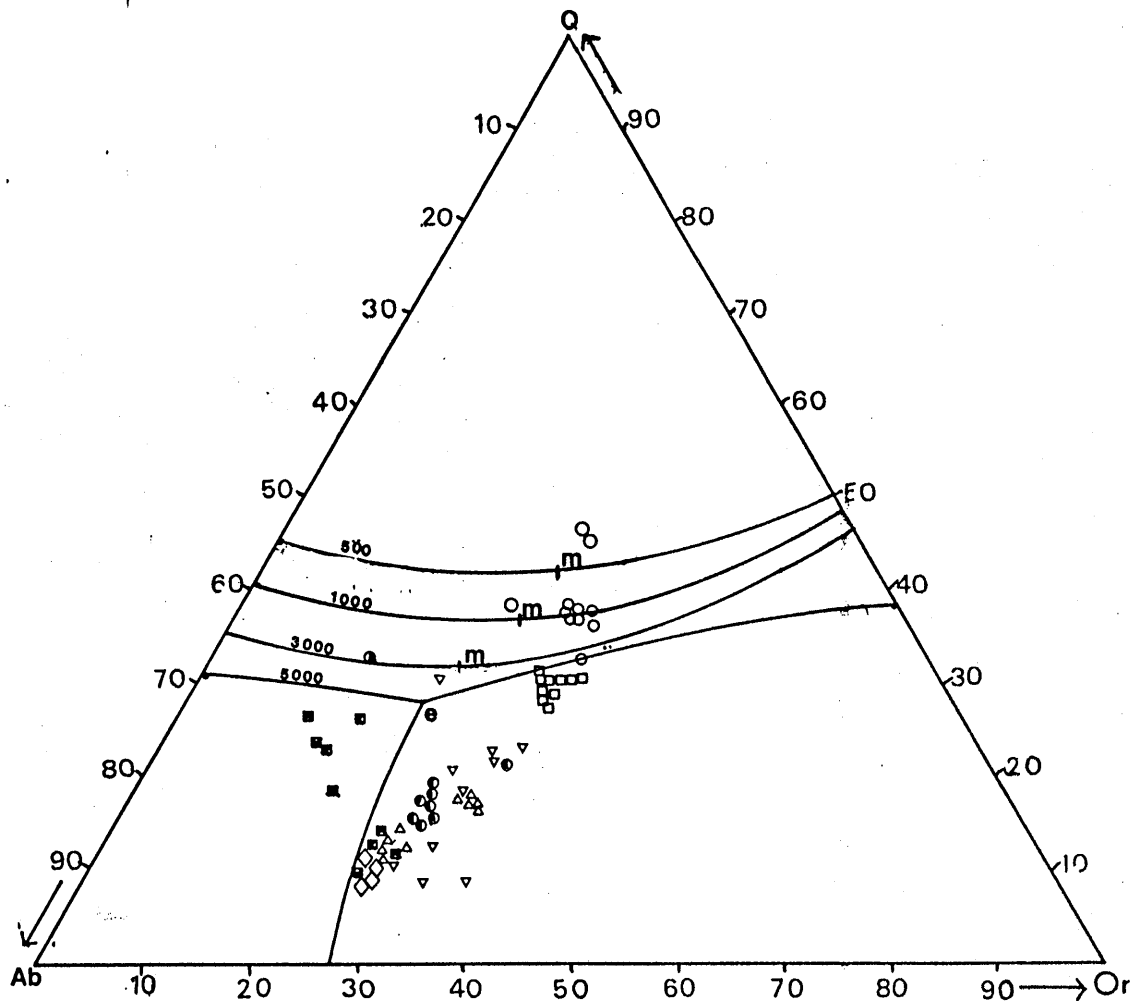


Figure 29. Q-Or-Ab system showing positions of cotectic lines and minima or ternary eutectics for P_{H_2O} of 0.5, 1, 3 and 5 kbars. The positions of temperature minima on the quartz-feldspar cotectic line are indicated by m, and e indicates the position of a ternary eutectic between quartz and two feldspars. Symbols as in Figure 22.

To see what information could be derived concerning the crystallisation of the granitic intrusions, the sum of normative Q, Ab and Or and their percentages relative to that sum were calculated. The composition of each intrusion in terms of these three normative minerals was then plotted on the granite system phase diagram (Figure 29). Two of the Garn Boduan analyses plot in the quartz field for all values of P_{H_2O} . All of the other analyses except one of the Bwlch Mawr and five of Garn Boduan could be considered to plot in the quartz or alkali feldspar field, depending on their assumed pressure of crystallisation; but all except those previously mentioned plot in the alkali feldspar field for values of P_{H_2O} less than 0.5 kbar.

The Q-Ab-Or plot indicates that since the intrusions form a trend from near the Ab-Or sytem to the minimum at $P = 1000$ kbar, some of the intrusions crystallised at a low pressure (about 1 kbar) and may therefore have crystallised beneath volcanoes. (A pressure of 1 kbar is equivalent to a depth of 2 - 3 kms) The Q-Ab-Or system suggests that under conditions of fractional crystallisation, liquids containing quartz and alkali feldspar will always finish crystallising near the granite minima (marked on Figure 29). Only the Nanhoron intrusion fulfils this criteria (a) (at P_{H_2O} 1 kbar) although Llanbedrog could also be considered to fit. This suggests that these two intrusions could represent the

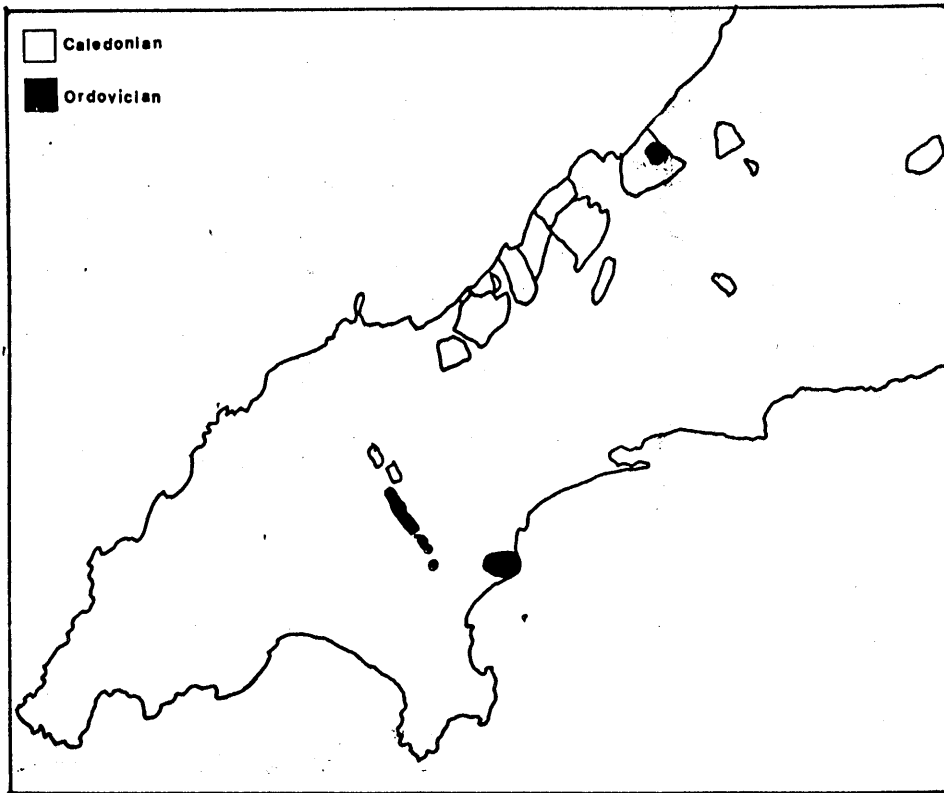


Figure 30. Tremlett (1972) grouping of the intrusions.

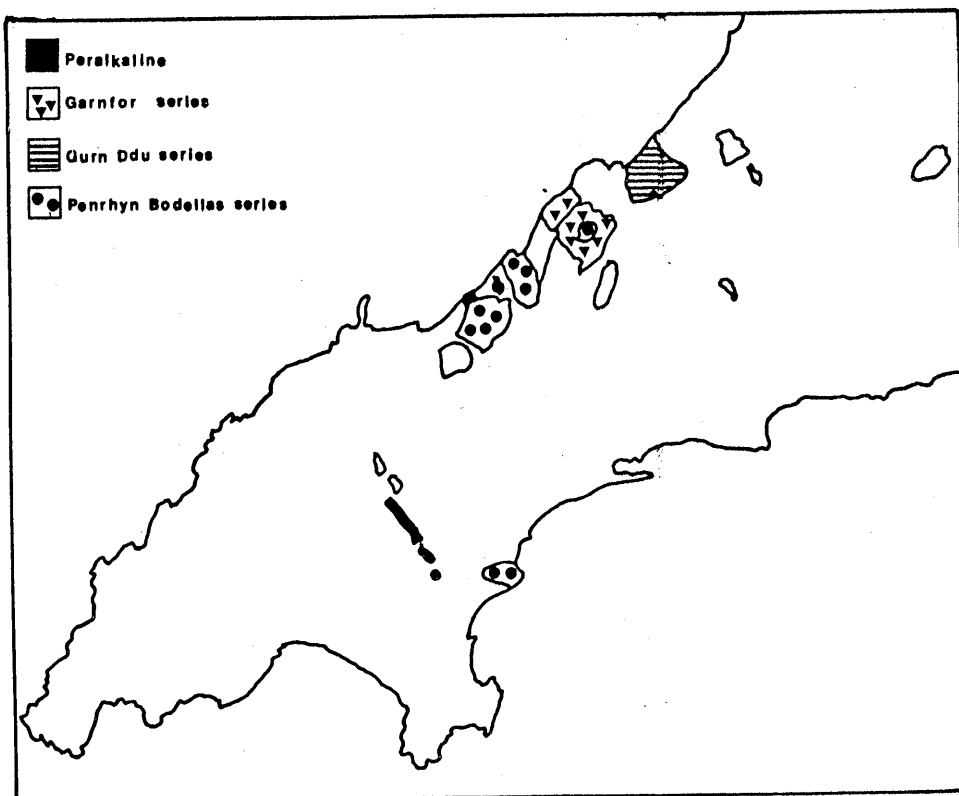


Figure 31. Croudace (1981) grouping of the intrusions.

extreme end product of fractional crystallisation process. This is consistent with calculations made earlier using Figure 26 etc.

Conclusions

This study enables the granites to be classified using chemical criteria. Tremlett (1972) divided the intrusions into two groups according to their geochemistry; his groups were divided into distinct ages: Ordovician and Silurian-Devonian. He stated that the Ordovician intrusions were higher in SiO_2 , lower in Al_2O_3 and CaO and had a lower $\text{Na}_2\text{O}/\text{K}_2\text{O}$ ratio than the Silurian-Devonian intrusions. They also occupied different positions on the Q:Or:Ab diagram. He also separated the intrusions by comparing $\text{Ba}/\text{K}_2\text{O}$ and $\text{Rb}/\text{K}_2\text{O}$, Zr and Y, and Li and MgO. Figure 30 shows his grouping of the intrusions.

Croudace (1981) also divided the intrusions into groups according to their geochemistry, although he regarded them as essentially the same age (Ordovician). This subdivision is summarised as follows:

1. Peralkaline group

This includes the intrusions of Nanhoron, Foel Gron and Mynytho.

2. Subalkaline group

a. Garnfor series:- Inner and outer Garnfor and the Yr Eifl felsite.

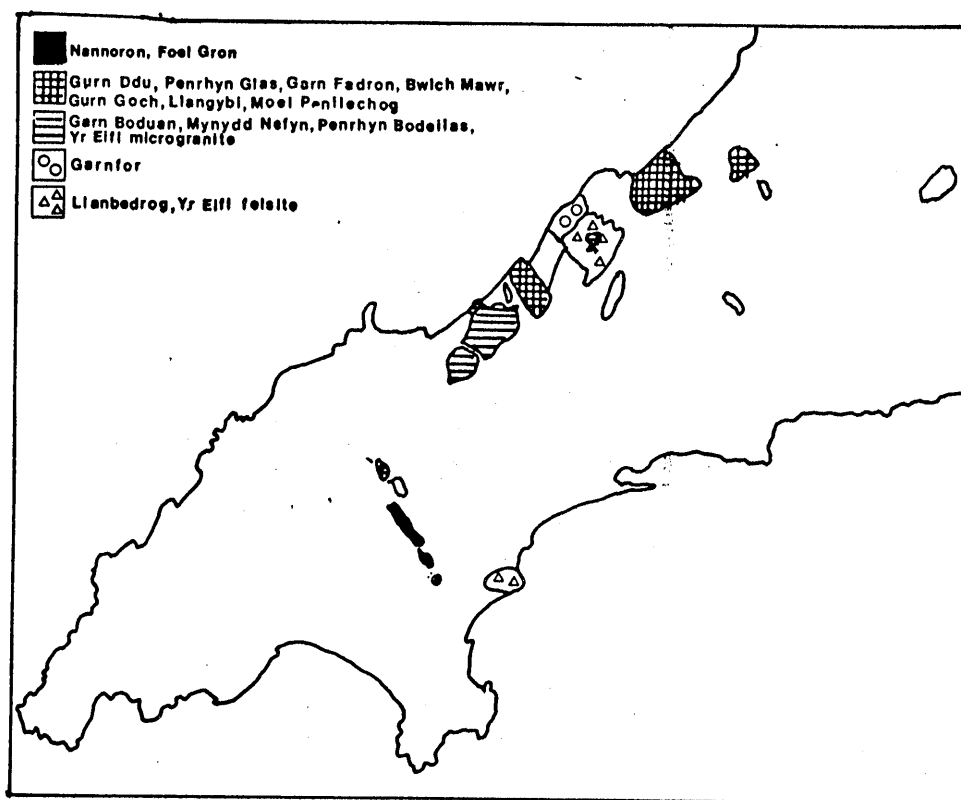


Figure 32. Grouping of the intrusions according to this study.

b. Penrhyn Bodeilas series:- Penrhyn Bodeilas, Mynydd Nefyn, Carreg-y-Llam (Penrhyn Glas), Pistyll, Yr Eifl microgranite and Llanbedrog.

c. Gurn Ddu series:- Gurn Ddu, Moel Penllechog, Llangybi and Gurn Goch

The subdivision into three evolutionary series of the subalkaline group is based on coherent trends on variation diagrams for the three sub groups with the Moel Y Penmaen lava at the end of each trend.

Figure 31 illustrates this grouping.

This study places the intrusions into five chemical groups using the high field strength elements Zr and Nb.

The five groups are:- (Figure 32)

a. Llanbedrog and the Yr Eifl felsite, the Llanbedrog intrusion plotting near the granite minimum on the Q:Or:Ab diagram at P_{H_2O} 5kbar.

b. Nanhoron and Foel Gron, the Nanhoron intrusion being a peralkaline granite and plotting near the granite minimum on the Q:Or:Ab diagram at 1kbar.

c. Garnfor

d. Garn Boduan, Penrhyn Bodeilas, Mynydd Nefyn and the Yr Eifl microgranite.

e. Garn Fadron, Gurn Ddu, Bwlch Mawr, Gurn Goch, Llangybi, Moel Penllechog and Carreg-y-Llam.

The main difference between Croudace's grouping and the fivefold subdivision presented here is the proposal to

put the Llanbedrog intrusion and the Yr Eifl felsite into a separate category. Penrhyn Glas (Carreg y Llam) is also placed in the Gurn Ddu group, not in the Penrhyn Bodeilas series. This study therefore mainly confirms the grouping of Croudace. The differences are not considered significant at this stage.

It is also concluded that the basalts and andesites appear to have tholeiitic tendencies as shown by their normative composition and Figures 19 and 27. and that the intrusions could be derived from a basalt such as LL142 by fractional crystallisation of plagioclase and clinopyroxene, the relative volume of acid and intermediate intrusions being consistent with such an origin.

Chapter 6

Petrogenetic modelling and discussion

The geochemical results presented in the previous chapter have shown that the intrusions can be divided into groups by their chemical composition and that they may have been derived from a basalt magma by fractional crystallisation of the phenocryst phases (plagioclase and pyroxene). In order to further investigate the relationship between the groups and the fractional crystallisation processes petrogenetic modelling was undertaken.

The use of modelling equations has enabled petrologists to test their evolutionary hypotheses for igneous suites. Rayleigh (1896) first formulated an expression to describe mass fractionation during distillation. This equation was then developed for partial melting equations (Gast 1968), zone refining equations (Harris 1957), magma plumbing (O'Hara 1977) and for other modelling equations (Arth 1976, Hanson 1978).

The application of modelling equations is now widely used but a unique solution can often only be provided by using a large number of models. The fractional crystallisation process comprises two variants. It can either be described by Rayleigh surface - equilibrium crystallisation (Equation 1) or by total equilibrium crystallisation (Equation 2).

Equation 1

$$\frac{C_L}{C_0} = F^{D-1}$$

Equation 2

$$\frac{C_L}{C_0} = \frac{1}{D(1-F)+F}$$

where:

C_L is the concentration of a trace element in the liquid

C_0 is the concentration of a trace element in the original melt

F is the fraction of the melt remaining

D is the crystal-melt distribution coefficient for an element

When a mineral is in chemical equilibrium with a liquid, elements are partitioned between the two phases according to the chemical activity in each. The relationship

$$\frac{\text{Concentration in mineral}}{\text{Concentration in liquid}} = K_D$$

Rayleigh fractionation involves the instantaneous equilibrium crystallisation of a mineral which is completely covered by another layer, thus preventing further equilibration of the covered crystals with the evolving melt. Total equilibrium crystallisation is likely to occur in a slowly cooling magma where the whole crystals equilibrate with the liquid and where the slow rate of cooling allows equilibrium to be maintained by diffusion of the elements. Rayleigh crystallisation is more likely to occur in an upper-crystal magma reservoir where cooling and crystallisation rates are fairly high.

The partial melting process comprises three variants:

- i) Fractional melting where continuous removal of very small quantities of melt are removed from a residual solid;
- ii) Batch melting where the melt and solid are in continual equilibrium until the melt is finally removed from the solid;
- iii) Aggregate melting where the melt is continuously removed from the solid but it collects in a magma reservoir.

Model ii) is the most used as it is a more reasonable geological mechanism. The models considered in this study are

Table 2 Average shale composition (Wedepohl 1971)

SiO ₂	58.9	Rb	140
TiO ₂	0.78	Sr	300
Al ₂ O ₃	16.7	Ba	580
Fe ₂ O ₃	6.9	Zr	160
MnO	0.09	Y	41
MgO	2.6	La	40
CaO	2.2	Ca	95
Na ₂ O	1.6	Th	12
K ₂ O	3.6		
P ₂ O ₅	0.16		

Distribution coefficients were taken from Cox et al (1979) and Pearce and Norry (1979) and are shown in Table 3.

Table 3 Distribution coefficients for rocks of basic composition

	Rb	Sr	Ba	Zr	Y	Nb	Ti
Orthopyroxene	0.001	0.01	0.001	0.03	0.2	0.15	0.1
Clinopyroxene	0.001	0.07	0.001	0.1	0.5	0.1	0.3
Plagioclase	0.07	2.2	0.2	0.01	0.03	0.01	0.04
Amphibole	0.3	0.5	0.4		No data		
Hornblende	No data			0.5	1.0	0.8	1.5
Fe-Ti Oxide	3.1	0.08	1.1	0.1	0.2	0.4	7.5

- a) Partial melting of sedimentary material;
- b) Fractional crystallisation from a basaltic magma.

a) Partial melting of sedimentary material

The melting of sedimentary material has often been put forward to explain the generation of tonalitic-granitic melts (Alberquerque 1977). Using Equation 2 (but relating the terms to partial melt rather than fractional crystallisation) calculations were made for 10% partial melting of an average shale (Wedepohl 1971), the composition of which is given in Table 2, and vectors were calculated in the following manner:

Using the equation 1, C_L was calculated for Zr and Nb values in plagioclase, magnetite, clino and orthopyroxene and hornblende and plotted on the graph (Figure 33). Vectors were then drawn using the values obtained for C_L and C_0 .

Figure 34³ shows a Zr versus Y diagram with vectors for 10% partial melting of shale. The vectors show that much more than 10% partial melting of shale is required to produce the intrusions. Before drawing any conclusions

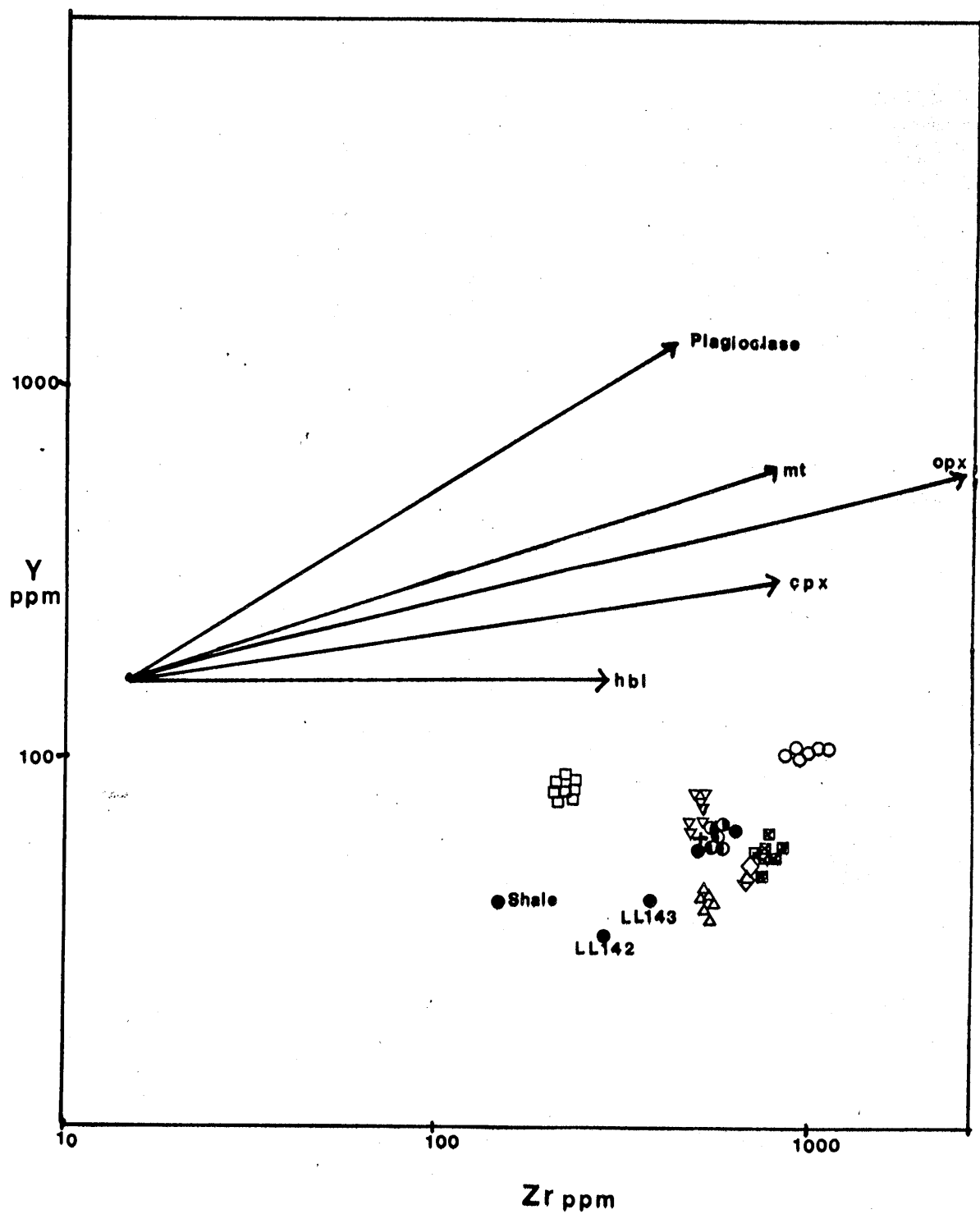


Figure 33. Zr against Y diagram with vectors for 10% partial melting of shale. Symbols as in Figure 22. Data from this study only.

from this, the criteria for S-type granites must be considered.

S-type granites i.e granites derived from sedimentary material have the following characteristics (Chappell and White 1974):

1. Relatively low Na_2O , <3.2% in rocks with 5% K_2O
2. Molar $\text{Al}_2\text{O}_3, \text{Na}_2\text{O} + \text{K}_2\text{O} + \text{CaO} > 1.1$,
3. >1% normative corundum,
4. Restricted range of compositions, dominantly granites,
5. Irregular variation diagrams,
6. High initial $^{87}\text{Sr}/^{86}\text{Sr}$ ratios, >0.708,
7. Magma possesses relatively low oxygen fugacities; ilmenite is a common mineral,
8. Muscovite and biotite are common; hornblende is absent,
9. Monazite, cordierite and garnet are common,
10. Tin mineralisation.

Comparing this criteria with the mineralogy and chemical analyses (Appendix 3) none of the intrusions fulfil the criteria so the result of the modelling shown in Figure 34 is only to be expected. This result is not consistent with the granites being produced by partial melting.

b) Fractional crystallisation from a basaltic magma

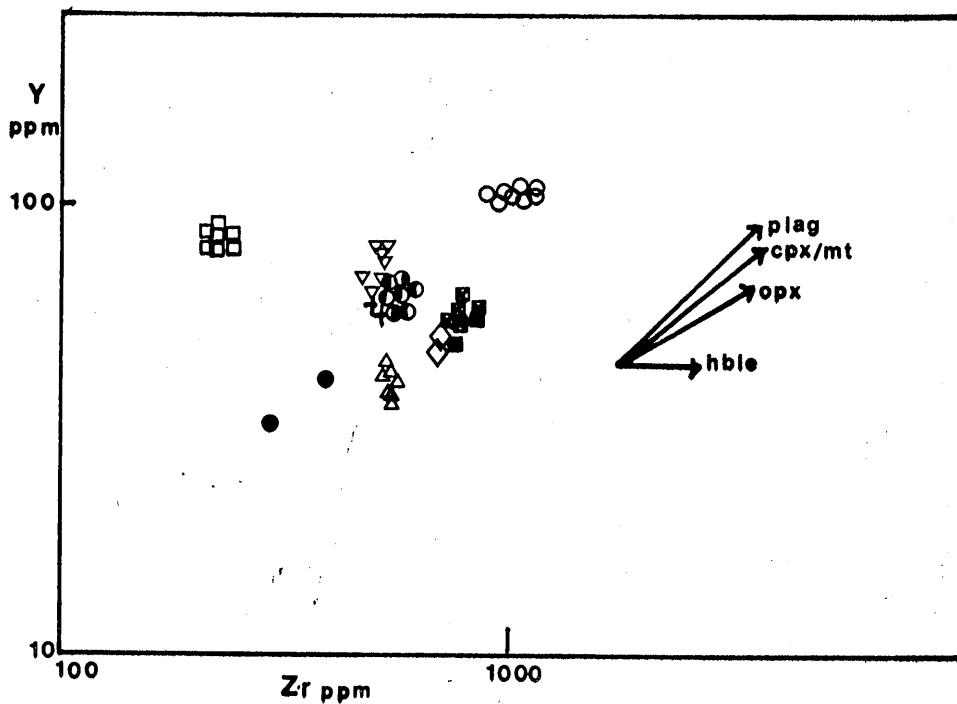


Figure 34. Plot of Y against Zr. The vectors are for 50% fractional crystallisation. Symbols as in Figure 22. Data from this study only.

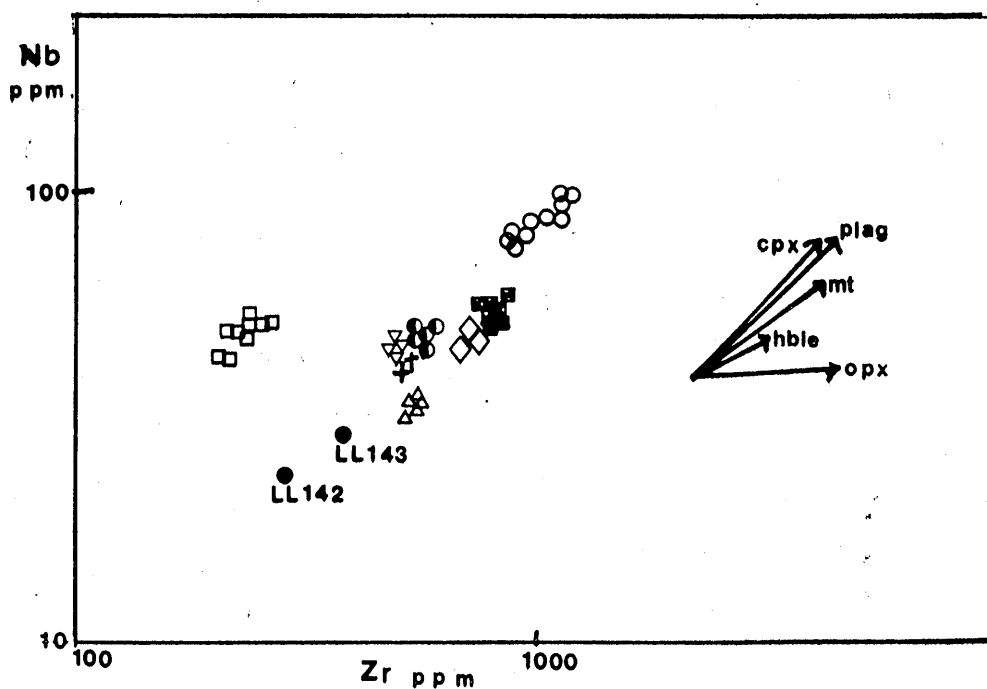


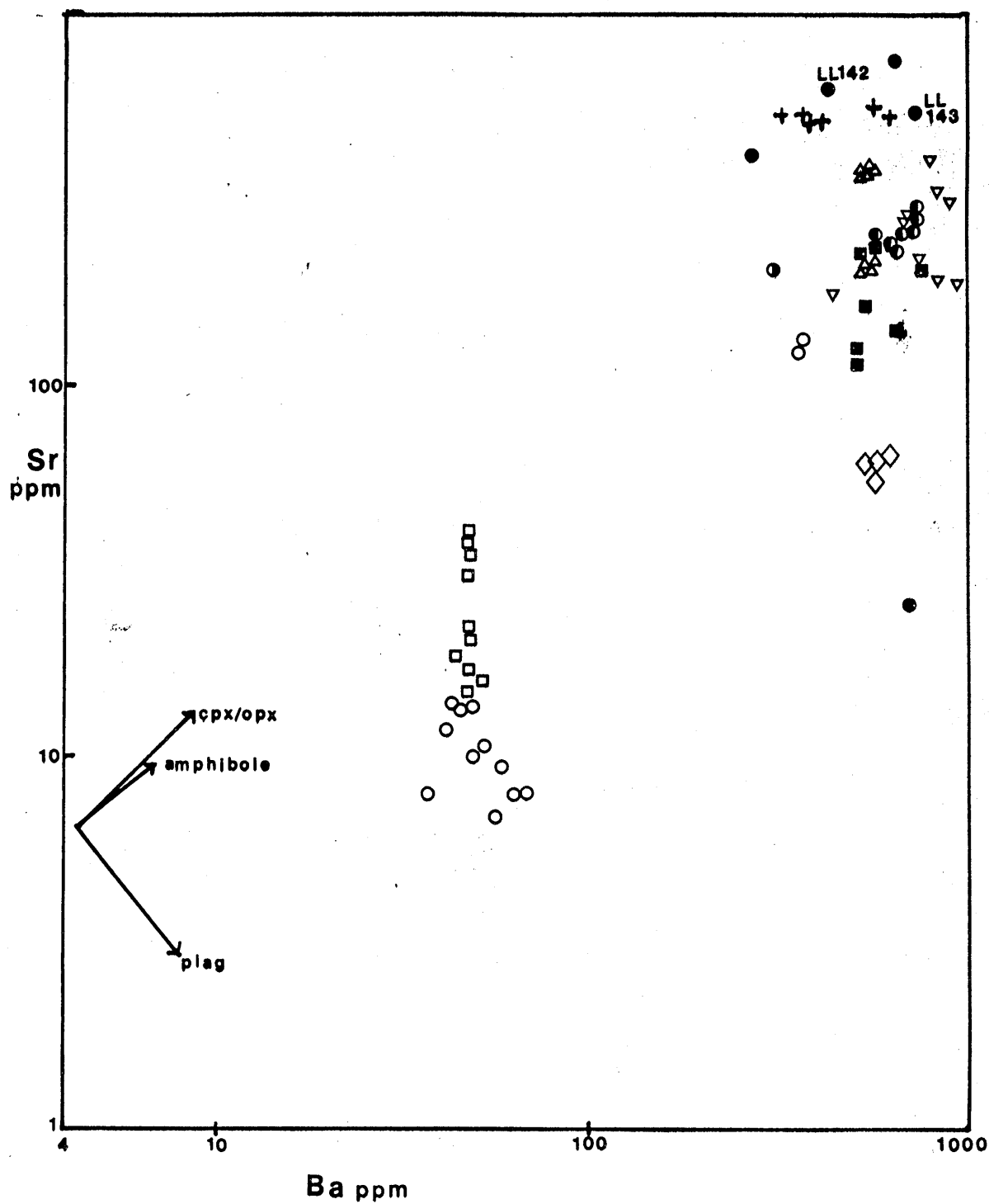
Figure 35. Plot of Nb against Zr. The vectors are for 50% fractional crystallisation. Symbols as in Figure 22. Data from this study only.

In any liquid/solid system the relative abundance in the liquid of a pair of elements such as Nb and Zr will be constant if the bulk distribution coefficients between the crystalline and liquid phases for the two elements are very low (<0.1 ; Weaver et al, 1972). If the abundance of any pair of such elements in the liquids thus derived are plotted against each other the plot will be a straight line. Such a line will project through the origin, with the slope determined by the concentrations of the two elements in the initial liquid. Such elements which are almost completely retained in the liquid phase during any solid/liquid reaction, or at equilibrium are termed incompatible elements.

The variation in the trace element content of a magma undergoing fractional crystallisation can be interpreted in terms of the nature and proportion of crystallising phases. Theoretical fractionation vectors have been drawn for each diagram using the distribution coefficients given in Table 3. A necessary condition for any fractionation trend to be correctly interpreted is that the theoretical trends should match on all variation diagrams.

Using the Y-Zr diagram (Figure 34), the mineral vectors suggest one group of intrusions might result from 50% fractional crystallisation of plagioclase from the basalt lava LL142. This group includes Moel Y

Figure 36. Plot of Sr against Ba. The vectors are for 50% fractional crystallisation. Symbols as in Figure 22. Data from this study only.



Penmaen, Bwlch Mawr, Gurn Ddu and Garn Fadron. Further fractional crystallisation could result in the Nanhoron intrusion. Crystallisation of ortho- and clinopyroxene would increase the Zr and Y content of the residual magma. If there were 50% fractional crystallisation of orthopyroxenes from the basaltic andesite, LL143, the intrusions of Garn Boduan and Penrhyn Bodeilas would result. The intrusion Garnfor could result from 50% fractional crystallisation of hornblende from LL143.

On the Zr-Nb diagram (Figure 35) the mineral vectors suggest that the same group of intrusions (Bwlch Mawr, Gurn Ddu and Garn Fadron and the Moel Y Penmaen lava) might result from 50% fractional crystallisation of plagioclase and/or clinopyroxene from the basalt LL142. Garnfor might be a result of 50% fractional crystallisation of hornblende from the basaltic andesite LL143; Penrhyn Bodeilas as a result of 50% fractional crystallisation of magnetite from LL143.

On the Sr-Ba diagram (Figure 36), the mineral vectors suggest none of the above. The Rb-Sr diagram also suggests none of the above (Figure 37). This is not surprising as Sr is a mobile element and the intrusions may have been subject to alteration, therefore the Sr contents given in the analyses (Appendix 3) may not be the same as the contents at the time of the intrusion.

On the Nb-Y diagram (Figure 38) the mineral vectors

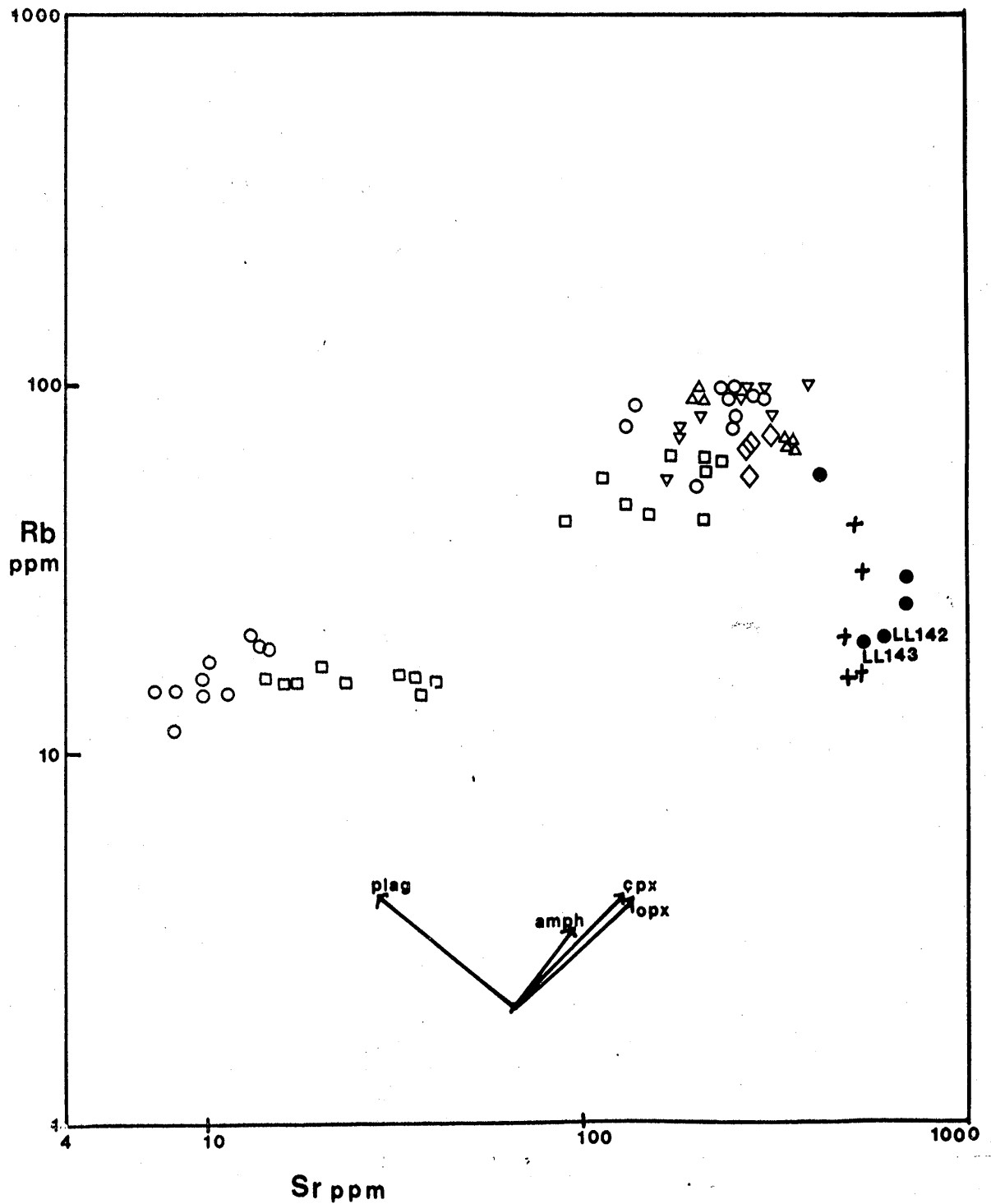


Figure 37. Plot of Rb against Sr. The vectors are for 50% fractional crystallisation. Symbols as in Figure 22. Data from this study only.

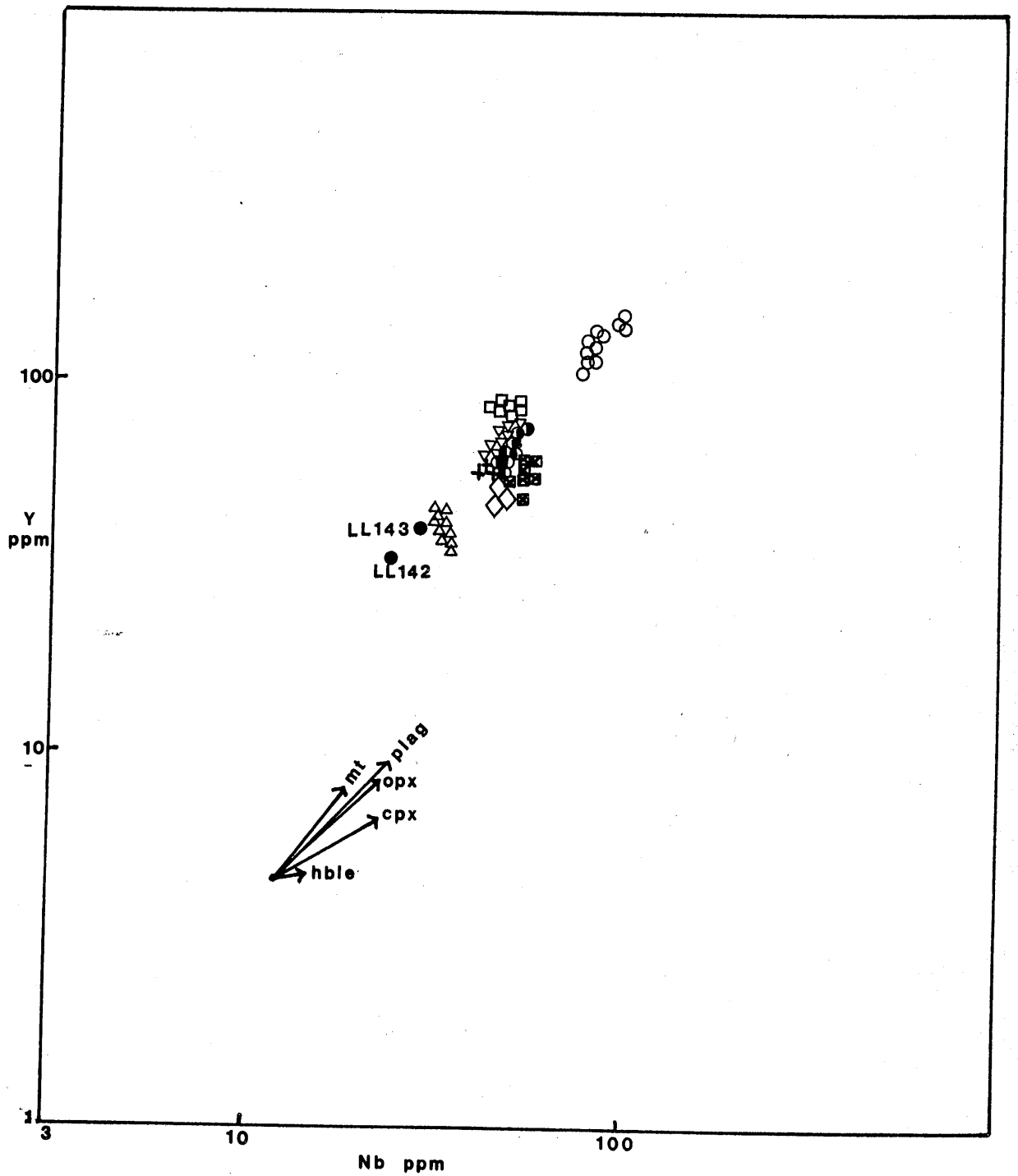


Figure 38. Plot of Nb against Y. The vectors are for 50 % fractional crystallisation. Symbols as in Figure 22. Data from this study only.

again suggest that Gurn Ddu, Bwlch Mawr, Garn Fadron and the Moel Y Penmaen lava could be the result of 50% fractional crystallisation of plagioclase and/or orthopyroxene from the basalt LL142. Garn Boduan could be the result of 50% fractional crystallisation of clinopyroxene from LL143. Garnfor could be the result of less than 50% (probably 30%) fractional crystallisation of hornblende from LL143.

Conclusions

In Figure 35, Nb and Zr have behaved as incompatible elements. This indicates that those intrusions lying with a linear trend may be geochemically related. This almost certainly implies a genetic relationship, since the values of the incompatible element ratios for each intrusion were determined by the composition of the initial liquid or solid from which they are derived. This confirms the previous statement that the group of intrusions (Bwlch Mawr, Gurn Ddu and Garn Fadron) could be genetically related to the basalt LL142.

Those intrusions which do not lie on the trend may have been derived from the basalt or basaltic andesite, LL143 by fractional crystallisation of phases with lower Zr/Nb ratios (e.g. magnetite) or higher Zr/Nb ratios (e.g. zircon). High Zr/Nb ratios are a feature of magmas generated above a subduction zone (calc-alkaline or

island-arc; Wood et al, 1980) and they result largely from the retention of Nb in titanium rich residual phases during hydrous partial melting. Both the basalt LL142 and the basaltic andesite LL143 have high Zr/Nb ratios (>12.0). Crystallisation and removal of ilmenite from a magma may reduce the Nb content and if Zr is not removed at the same time (e.g. in zircon) the Zr/Nb ratios will rise. Nb can also be appreciably accommodated by orthopyroxene, hornblende and magnetite (Pearce and Norry, 1979).

The intrusions of Foel Gron and Nanhoron comprise a peralkaline group. The general consensus for the evolution of peralkaline rocks involves the extensive fractional crystallisation of anhydrous minerals from transitional or alkaline magmas. Most oversaturated peralkaline rocks are found in regions of the crust undergoing tension or extension (Smith et al, 1979) or in stable intra-continental settings (Bowden et al, 1979). They may represent a residual melt from a differentiating body of transitional or mildly alkaline tholeiitic magma (Croudace, 1981). Leat and Thorpe (1986) have attempted to determine the original geochemical character of altered rhyolites, intermediate lavas and basalts of Caradocian age from the Llŷn peninsula using immobile elements. They conclude that the volcanic rocks are chemically similar to the intrusions, which suggests a co-magmatic origin and similar age and confirms the arguments presented here.

To summarise:

1. An attempt was made to model the petrogenesis of the granites by melting of an average shale. This showed that the granites were not derived directly by partial melting.
2. The intrusions of Bwlch Mawr, Gurn Ddu and Garn Fadron and the Moel y Penmaen lavas could result from 50% fractional crystallisation of plagioclase and/or clino/ortho pyroxene from the basalt LL142.
3. The intrusions of Garn Boduan and Penrhyn Bodeillas could result from 50% fractional crystallisation of clino/orthopyroxene from the basaltic andesite LL143.
4. The Garnfor intrusion could result from 50% or less fractional crystallisation of hornblende from the basaltic andesite LL143.
5. The volcanic rocks provide suitable parent magmas from which granite may be derived by fractional crystallisation. This is consistent with lavas and intrusions both being Ordovician in age.

Chapter 7

Tectonic setting

There has been much recent discussion of the tectonic setting of volcanic rocks and associated intrusions in Wales (Bevins et al, 1984, Campbell et al, 1988, Kokelaar, 1988, Kokelaar et al, 1989). The work of Kokelaar is considered to be the most relevant to this study.

Summary of the setting of Ordovician volcanism in Wales.

Ordovician volcanism in Wales occurred on continental crust at a destructive plate margin. Its location and development was controlled by a network of crustal discontinuities. These are characterised by their considerable extent, repeated tectonic activity, channelling of magmas and generally steep structures at shallow levels. They appear to have separated relatively stable blocks. The common occurrence of relatively uniform basaltic magmas, indicates easy access to the surface, without obvious deep entrapment or substantial contamination within the continental crust, suggesting that the fractures were steep and penetrated to the base of the crust.

From these features, it is inferred that the crustal discontinuities were originally major strike-slip faults or shear zones, which cannot have been formed by simple

extension. Kokelaar proposed that the fracture pattern reflects a strike-slip fault or shear zone complex, formed by early Cambrian times. Deep in the crust the fractures were steep, ductile zones and these passed into discrete faults, or narrow fault or shear zones, in the upper crust. Grabens, half-grabens, folds, monoclinical flexures and alignments of volcanic centres reflect upward propagation through the cover of steep splay faults or flower structures. During extension, the crust was attenuated and pierced by magmas, mainly along the fractures, while complex, volcanically active grabens, formed in the overlying cover. During compression and transpression these same sites were marked by relatively intense shortening and shear strain.

Kokelaar (1977, 1979 1986) proposed that the Tremadoc arc volcanism marked the onset of the phase of subduction of oceanic lithosphere, that led to the closure of the Iapetus Ocean. Late Tremadoc tectonic development (see Figure 6c), pre-Arenig uplift in N-W, was that of a fore-arc frontal ridge system responding to the thrust of oceanic lithosphere beneath the NE-SW continental plate margin. Arenig to Caradoc developments reflect evolution of a marginal basin where tectonism was dominated by E-W extension.

Kokelaar (1988) put forward a more detailed tectonic model for North Wales: based on the evidence that a destructive plate margin volcanism persisted in Wales

from Tremadoc to Caradoc times. In North Wales the late Tremadoc uplift and erosion is attributable to the onset of subduction and development of a frontal ridge system. Further south, near the Harlech Dome area, localised uplift was associated with a volcanic front and the development of arc volcanoes. In North Wales, the arc volcanism occurred in a regime of E-W crustal extension and was centred on a deep crustal discontinuity. Marine conditions prevailed from Arenig to Caradoc time, with episodes of marginal basin volcanism. The volcanism occurred mainly along complex and relatively narrow grabens which were sites of repeated channelling of magmas and pronounced subsidence. Changing sites of volcanism were due to transfer of active extension from one fracture to another. The fracture pattern indicates that they may represent part of a complicated deep-crustal strike-slip system. The volcanically active grabens trended roughly N-S in N. Wales, and E-W extension dominated throughout the Ordovician volcanism. Ordovician plate tectonics configurations are uncertain but the extension can be explained by a N-S convergence vector between oceanic and over-riding microcontinental plates.

Kokelaar (1988) considered that the granitic intrusions and associated lavas in the Llyn are coeval and show geochemical characteristics typical of emplacement at an ensialic destructive plate margin dominated by extension. The extrusive rocks are interbedded with

mudstones and sandstones indicating a mainly shallow marine environment with local emergence.

Leat et Thorpe(1986) considered that the Upper Ordovician (Caradoc) volcanic rocks in Llyn[^] and Snowdonia were erupted within a complex setting transitional between a destructive plate margin and a within-plate environment. The lavas were alkaline/within plate in character and may have erupted under tensional conditions during Caledonian subduction.

Croudace (1982) proposed that the N.Wales area may have been an incipient back-arc basin or a volcano-tectonic rift zone in a region of ensialic crustal tension.

Trace element discrimination diagrams.

Trace element discrimination diagrams can be used to determine the tectonic setting of eruption of basic volcanic rocks(Pearce and Cann,1973).The chemical analyses are interpreted with caution because they may have been modified by low-grade regional metamorphism. Therefore geochemical interpretation has been restricted mainly to those elements (Ti,Zr,Y and Nb) which are regarded as most immobile during metamorphism.

A. Lavas

Four major groups of tectonic regimes related to plate

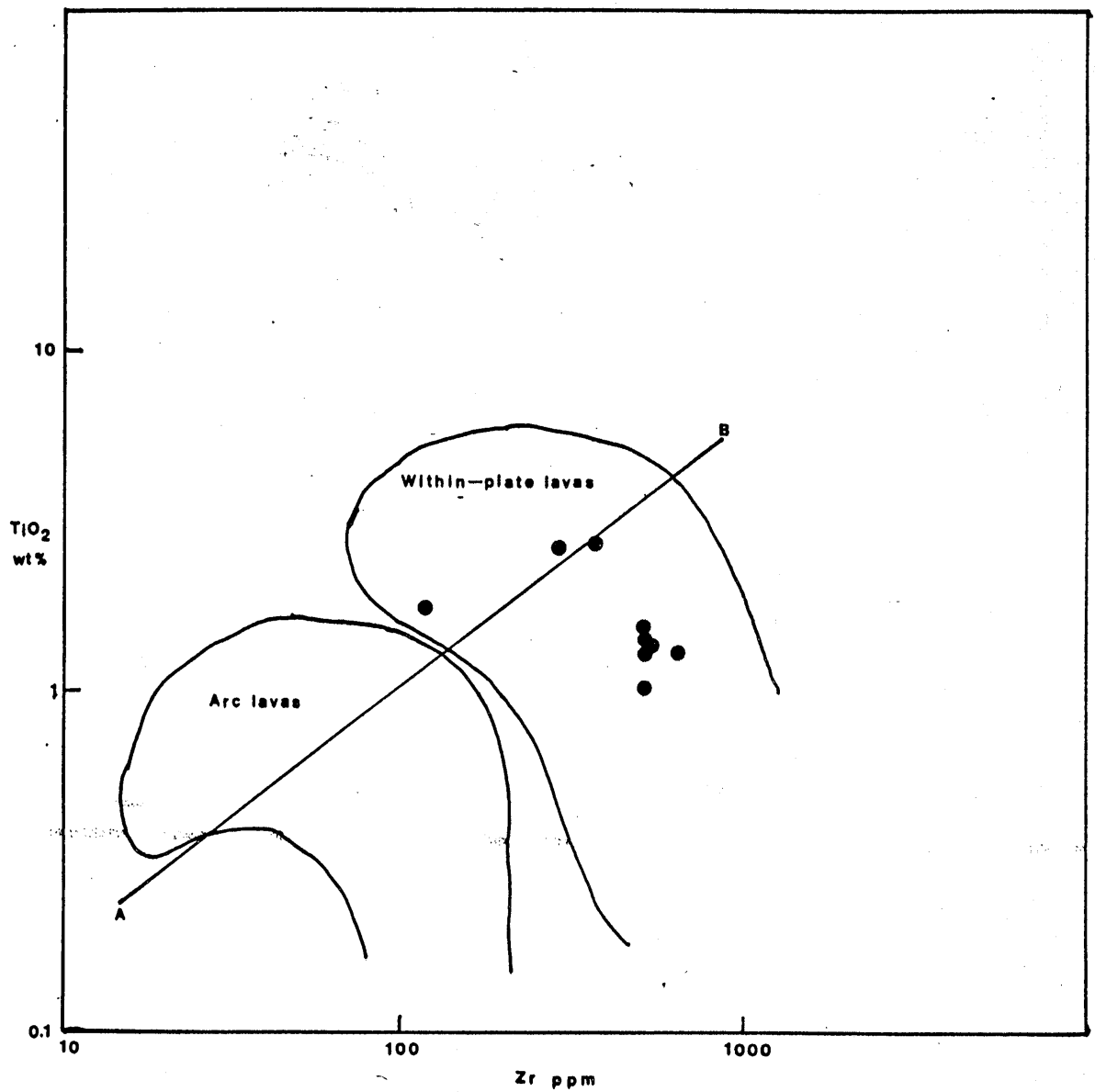


Figure 39. Plot of Zr against TiO_2 showing fields of arc and within-plate lavas (Pearce, 1980). Line A-B separates basalts from acid and intermediate rocks.

motions, are currently recognised:

- a) Ocean floor basalts (diverging plate margins);
- b) Volcanic arc basalts (converging plate margins);
- c) Oceanic island basalts (within plate - oceanic crust);
- d) Continental basalts (within plate - continental crust).

Figure 39 is divided into two fields, arc lavas i.e. volcanic arc basalts found at converging plate margins and within plate lavas, i.e. within plate oceanic or continental crust. The line A-B separates basalts from acid and intermediate lavas. The Llŷn[^] lavas plot in the within plate field. LL142 and LL156 plot above the line A-B and are therefore considered to be basalts. LL143 plots on the line while LL145, LL146, LL153 and LL154 plot under the line A-B and are considered to be acid or intermediate lavas.

Leat and Thorpe (1986) used the analyses LL142-3 and LL153-156 from this study to compare them with other lavas and rhyolites from Llŷn[^]. LL142 and LL143 are considered to be similar but chemically distinct from LL156, but all three are considered to be basalts. Leat and Thorpe (1986) considered LL153-155 to be mugearites or trachybasalts.

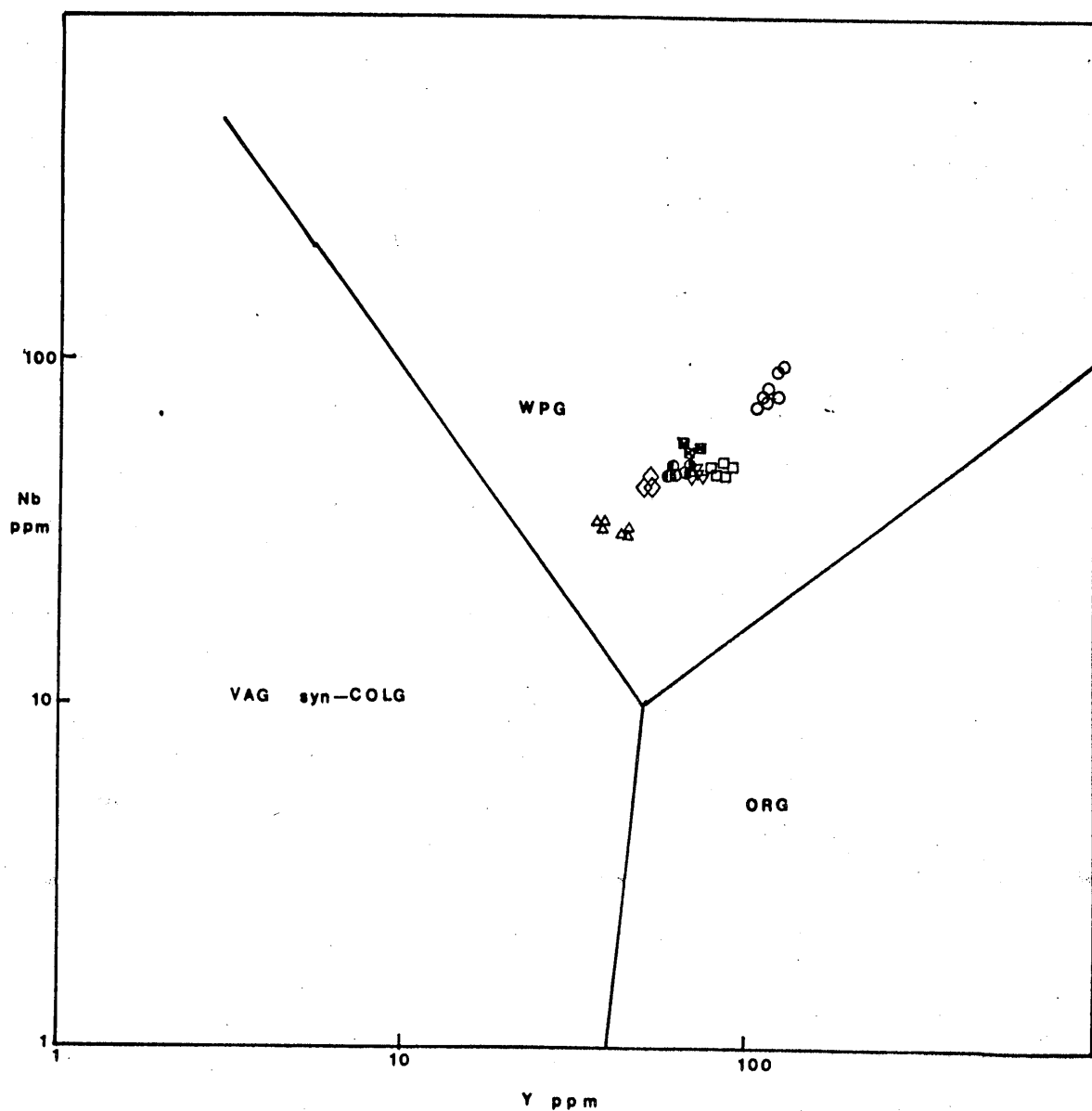


Figure 40. Plot of Y against Nb showing fields of arc, ocean ridge and within-plate granites. (Pearce et al, 1984). Symbols as in Figure 22. Data from this study only is plotted.

B. Intrusions

Granites can be subdivided according to their intrusive settings into 4 main groups. These are: ocean ridge granites (ORG), volcanic arc granites (VAG), within plate granites (WPG) and collision granites (COLG). Pearce et al (1984) used trace element discrimination diagrams to define the tectonic settings of different types of granites. The LL¹⁴² intrusions were plotted on Nb/Y and Rb/Y+Nb diagrams (Figures 40 and 41). All the intrusions plotted in the within-plate area and are comparable with the data for the lavas. The chemical similarity of the lavas and the granitic intrusions suggests that they are the same age (Caradoc) not Caledonian as suggested by Tremlett (1972). Figure 40 (Nb/Y) supports this; if the intrusions were of Caledonian age they would be more likely to plot in the SYN-COLG area, the tectonic setting most likely during the Caledonian orogeny (Nb and Y contents would be low).

Conclusions

LL142 and LL143 are similar geochemically to within-plate or transitional basalt (Pearce, 1982, 1983).

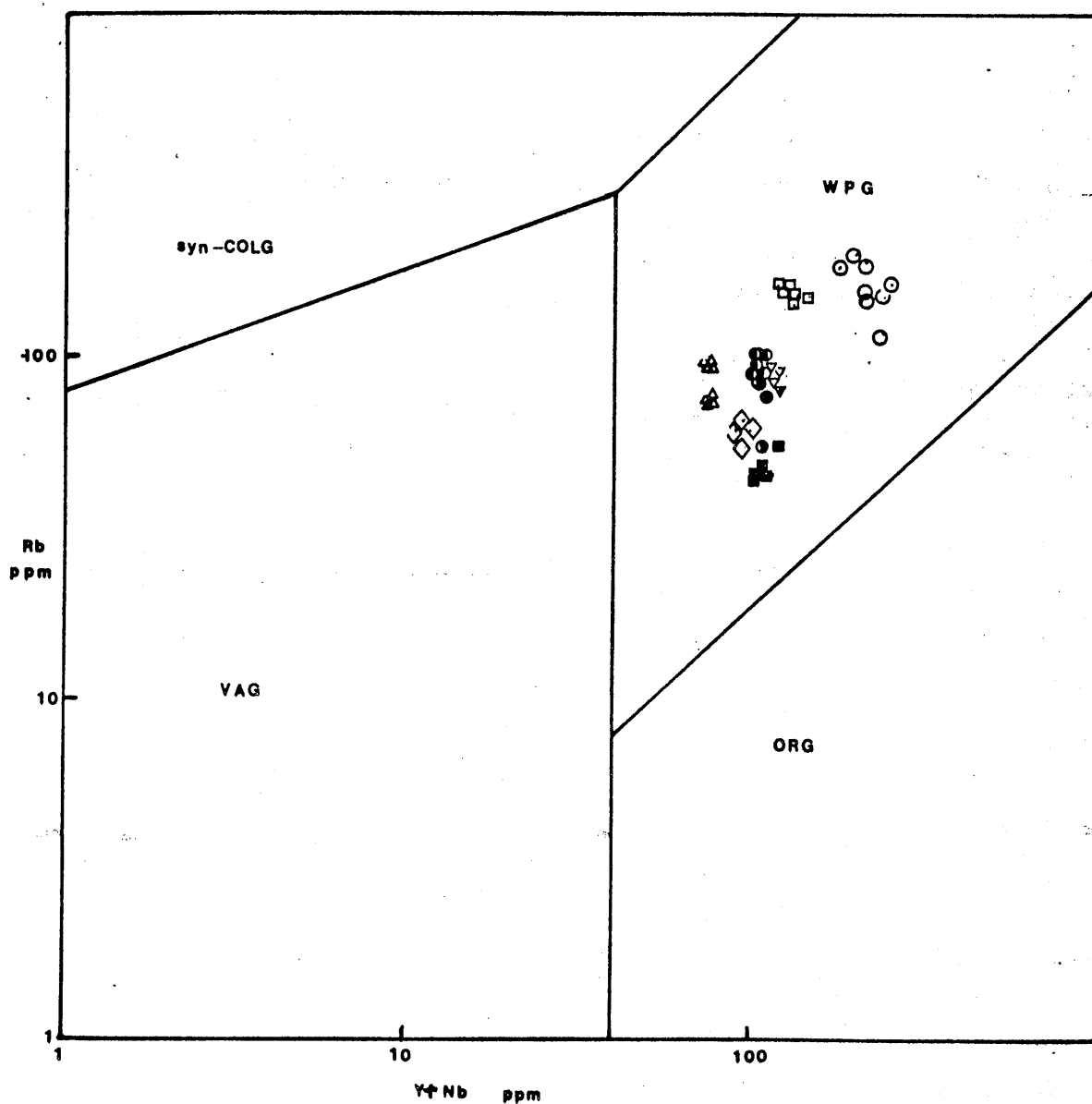


Figure 41. Plot of Y + Nb against Rb showing fields of syn-collision, within-plate, arc and ocean ridge granites' (Pearce et al, 1984). Symbols as in Figure 22. Data from this study only is plotted.

LL143 is enriched in Ba and Th relative to other elements which might indicate generation above a subduction zone; but the high Nb relative to Ce and P suggests a within-plate rather than a subduction-related origin. LL156 has concentrations of Nb, Ce, P, Zr, Ti and Y similar to those of MORB but is enriched in Sr, K, Rb and Ba; this is characteristic of an island arc tholeiitic basalt, such as are found in marginal basin environments (Pearce, 1980)

The volcanic rocks are chemically similar to the granitic intrusions which suggests a comagmatic origin and similar age. The most likely setting for the lavas and intrusions is a complex marginal basin environment dominated by E-W extension.

Chapter 8

Summary of conclusions

1. The granitic intrusions of Llyn[^] range in composition from microtonalite to sub- and peralkaline microgranite (58 - 76% SiO₂). The main minerals in the intrusions are alkali feldspar, plagioclase and quartz. Minor minerals include amphibole, ortho- and clinopyroxene and biotite. Accessory minerals are Fe-Ti oxide, apatite, zircon, allanite, epidote and sphene. The intrusions are porphyritic with phenocrysts of alkali feldspar, plagioclase and amphibole. Granophyric texture is seen in three intrusions; Nanhoron, Llanbedrog and Gurn Ddu. All the intrusions have been subject to metamorphic conditions. Microprobe analyses of pyroxene and plagioclase from the lava LL142 showed that the lava LL142 is similar in composition to the phenocrysts of the Garnfor tonalite so they may be contemporaneous. This implies that the tonalite may have been derived from a lava such as LL142 which is tholeiitic or calc-alkaline in character. The data is also consistent with the more acid intrusions and lavas being derived from such a basic/intermediate parent magma.

2. The intrusions can be divided into five chemical groups using the high field strength elements Zr and Nb.

The five groups are:-

- a). Llanbedrog and the Yr Eifl felsite, the Llanbedrog intrusion plotting near the granite minimum on the Q:Or:Ab diagram at P_{H_2O} 5kbar.
- b) Nanhoron and Foel Gron, the Nanhoron intrusion being a peralkaline granite and plotting near the granite minimum on the Q:Or:Ab diagram at 1kbar.
- c). Garnfor.
- d). Garn Boduan, Penrhyn Bodeillas, Mynydd Nefyn and the Yr Eifl microgranite.
- e). Garn Fadron, Gurn Ddu, Bwlch Mawr, Gurn Goch, Llangybi, Moel Penllechog and Penrhyn Glas (Carreg y Llam).

3. The Nanhoron and Llanbedrog intrusions could have originated by processes of fractional crystallisation of silicate liquids. This is consistent with calculations made using Figure 26 showing that the Nanhoron intrusion may have originated from a basic magma. It is also concluded that the basalt and andesites have tholeiitic tendencies as shown by their normative composition and Figures 19 and 27.

4. Petrogenetic modelling using the high field strength elements Nb and Zr suggested that the intrusions of Bwlch Mawr, Gurn Ddu and Garn Fadron and the Moel y Penmaen Lava could have resulted from 50% fractional crystallisation of plagioclase and clino/orthopyroxene from the basalt LL142.

The intrusions of Garn Boduan and Penrhyn Bodeilas could have resulted from 50% fractional crystallisation of clino/orthopyroxene from the basaltic andesite LL143. The Garnfor intrusion could have resulted from 50% or less fractional crystallisation of hornblended/ from the basaltic andesite LL143.

The lavas provide suitable parent magmas from which granite may be derived by fractional crystallisation. This is consistent with the lavas and the intrusions both being Ordovician in age.

5. The volcanic rocks are chemically similar to the granitic intrusions which suggests a comagmatic origin and similar age. The most likely setting for the lavas and intrusions is a complex marginal basin environment dominated by E-W extension.

Acknowledgements.

I am grateful to my supervisor, Dr.R.S.Thorpe for his advice and encouragement throughout my research. I am also very grateful to Dr.W.J.Wadsworth of the University of Manchester for all his advice and encouragement during the last year. The Open University and the University of Nottingham provided their excellent facilities and expertise when required. I am grateful to Mr.J.Watson, Mr.I.Chaplin, and Mr.L.Griffiths for help with sample preparation and XRF facilities, to Drs.P.Harvey and B.Atkin of the Department of Geology, Nottingham University for XRF facilities and to J.Taylor for help with the diagrams.

Appendix 1 Selected microprobe analyses

Pyroxenes	(1)	(2)	(3)	(4)	(5)
SiO ₂	52.45	52.95	51.99	52.64	50.89
TiO ₂	0.56	0.67	0.80	0.61	0.65
Al ₂ O ₃	1.31	1.40	1.82	1.39	1.92
FeO	11.62	12.08	13.30	10.98	11.68
MgO	14.25	14.60	14.14	14.64	14.59
CaO	19.76	19.41	18.15	20.05	19.08
Na ₂ O	0.31	0.44	0.46	0.35	
MnO	0.50	0.50	0.53	0.41	0.44
Total	100.76	102.05	101.19	101.07	99.20

Plagioclase	(1)	(2)	(3)	(4)	(5)	(6)	(7)
SiO ₂	53.94	54.58	57.73	56.53	56.10	56.78	56.56
Al ₂ O ₃	29.43	28.90	26.92	24.89	27.98	26.78	27.66
CaO	12.61	11.75	9.85	10.65	10.23	9.25	10.38
Na ₂ O	4.32	4.48	5.60	5.09	5.25	6.12	5.38
K ₂ O	0.28	0.59	0.70	0.70	0.72	0.58	0.47
FeO				2.19	0.49		
Total	100.58	100.30	100.80	100.05	100.77	99.51	100.45

Mineral Analyses (Croudace, 1981)

Plagioclase	(1)	(2)	(3)	(4)	(5)
SiO ₂	56.58	65.30	68.55	66.80	61.40
Al ₂ O ₃	27.38	20.44	19.84	21.17	23.99
FeO	0.47	0.20	0.14	0.25	0.24
CaO	10.07	1.15	0.27	2.94	5.59
Na ₂ O	5.57	7.12	8.65	7.66	7.13
K ₂ O	0.36	4.67	3.45	0.77	0.91
Total	100.43	98.91	100.90	100.12	99.26

Pyroxene	(6)	(7)	(8)	(9)	(10)
SiO ₂	51.98	51.22	52.13	50.64	52.86
TiO ₂	0.77	0.39	0.26	0.29	0.24
Al ₂ O ₃	2.45	0.25	0.32	0.49	0.64
FeO	10.38	17.24	23.96	31.21	14.67
MgO	14.21	10.85	19.99	12.65	11.92
CaO	20.02	17.61	1.76	1.30	18.52
Na ₂ O	0.53	0.53		0.38	0.41
P ₂ O ₅					
Total	100.82	99.00	99.43	98.78	100.15

1. Inner Garnfor plagioclase phenocryst.
2. Inner Garnfor groundmass plagioclase.
3. Inner Garnfor plagioclase phenocryst rim.
4. Penrhyn Bodeillas plagioclase phenocryst.
5. Carreg y Llam plagioclase phenocryst.
6. Inner Garnfor augite phenocryst.
7. Inner Garnfor groundmass augite.
8. Inner Garnfor hypersthene phenocryst.
9. Inner Garnfor groundmass hypersthene.
10. Penrhyn Bodeillas augite phenocryst.

Appendix 2

E.D.X.R.F. Laboratory

Department of Earth Sciences, Open University.

Preparation of Silicate Samples for Major Element Analysis

1. Sample Drying

Rock powder (2-3 g per sample) is dried overnight in an oven at 110°C using clean nickel or porcelain crucibles. Allow the samples to cool in a dessicator prior to weighing them out.

2. Loss on Ignition

Dried powder (1-2 g) is ignited for 20 min. at 1000°C in a muffle furnace using a fused silica crucible. Accurate weighing of the powder before and after ignition is essential to calculate percentage weight loss. Ignite samples in batches of eight.

Precautions:

- a) Pre-ignite silica crucibles at 1000°C for 15 minutes.
- b) Allow silica crucibles to cool for 10 minutes before commencing weighing but do not leave them longer than 20 minutes in case they absorb atmospheric moisture.
- c) Zero balance before commencing weighing.

3. Fusion

Dried rock powder (0.4 g) is mixed with (rock powder weight x 6 x Flux Factor) g. of Spectroflux 100B in a platinum / 5% gold crucible and fused in the muffle furnace at 1100°C for 12 to 15 min. The homogenous melt is poured onto a heated mould and pressed to form a glass disc. Excess glass is removed from the edge of the disc, using platinum-tipped tongs and the disc is slid onto a heated brass platten. The platten is lifted onto a heat-resistant mat, covered with a glass evaporating basin, and allowed to cool. Fragments of excess glass are put into the platinum crucible which is then placed next to the cooling glass disc. When cool, each disc is labelled on its upper surface (the side with the smallest diameter) and placed in a labelled 2"x 2" plastic bag.

Precautions:

- a) The flux correction factor* should be determined before each batch of samples is weighed out.
- b) When in use, keep the jar of flux in a dessicator to avoid absorption of atmospheric moisture. When refilling jar from stock, dry jar for one hour at 110°C; never top-up a jar without emptying residues of previous batch of flux first.

- c) A flux : rock weight ratio of exactly 6 : 1 is required. The best method to attain this is to weigh out the rock powder accurately to between 0.4000 and 0.4050 g in a platinum crucible, and then add (6 x Rock Weight x Flux loss correction factor *) g. of flux weighed exactly to within plus or minus 0.0004 g.
- d) Mix rock powder and flux thoroughly with a sharpened polythene rod before fusion.
- e) Fuse samples in batches of no more than two at a time and allow at least five minutes between each batch.
- f) Swirl melt every 3-5 minutes to produce a uniformly fluid melt, eliminating undissolved powder and bubbles so as to achieve complete homogeneity before pouring.
- g) Limit fusions to a maximum of 20 minutes if possible (12-15 minutes is ideal) to avoid significant volatilization of flux and alkali metals.
- h) Keep the press plunger in contact with platten as much as possible. If it cools prior to pressing, the disc is likely to shatter.
- i) Cool glass discs slowly on pre-heated plattens to avoid shattering.

4. General Notes

- a) Record all weighings precisely using weighing sheets provided.
- b) Clean crucibles after use:
 Silica crucibles - wash in deionized water and dry at 110°C in oven.
 Platinum crucibles - stand in cold 50/50 hydrochloric acid overnight, or warm 50/50 acid for 1-2 hours. Rinse several times in deionized water and dry in oven at 110°C.
 Nickel and porcelain crucibles should be cleaned using a dry piece of blue roll.
- c) Safety visors and leather gloves are available. Use them when accessing the furnace and pressing glass discs.

* Flux loss correction factor

To account for loss on ignition of the flux, accurately weigh about 2.5 g. of flux into a tared platinum crucible. Reweigh flux + crucible and record the weight. Ignite flux in muffle furnace for 15 minutes at 1100°C. After cooling for 10 minutes, weigh the crucible + ignited flux accurately and record the weight. Calculate the weight loss of the flux and hence the weight of the ignited flux.

The Flux Correction Factor is: $\frac{\text{Wt. of flux before fusion} - \text{Wt. of flux after fusion}}{\text{Wt. of flux before fusion}}$

Preparation of Pressed Powder Pellets

Weigh out 7 - 8 g. of rock powder in a plastic weighing boat using the Mettler top-loader balance. Transfer the powder to an agate mortar, add 6 - 12 drops of P.V.P. binding agent, then thoroughly mix using an agate pestle. The amount of binder required varies with rock type and a certain amount of experimentation may be necessary before good pellets are obtained. Assemble the two parts of the pellet mould and place a hardened steel pellet, smooth face uppermost in the bore of the mould. Return the mixture to the weighing boat and pour into the pellet mould. Shake the mould gently to level the powder, then place the second steel pellet, smooth face down, on top of the powder, followed by the steel piston.

Place the whole assembly in the hydraulic press and apply a pressure of 10 tons per sq.inch. Release the pressure, take the base off the mould, turn the mould upside down and place the perspex tube on its upper surface in line with the bore of the mould. Place the assembly, perspex tube uppermost, in the press and apply pressure until the powder pellet, sandwiched between the two steel pellets, emerges from the mould. Hold the mould carefully throughout this process to avoid it dropping suddenly when the pellet is freed.

Place the pellet on a blue paper-covered cardboard tray and write the sample name alongside it ; do not write on the pellet at this stage. Release the hydraulic pressure, and clean the mould, mortar and pestle with tissue and methylated spirit. Repeat the above procedure with the next sample. Dry the pellets on paper-covered cardboard mats, in the oven, overnight at 110°C. Label the pellets on their edges, when dry, using a felt-tip pen, and place in labelled 2"x 2" plastic bags.

Preparation of PVP/Methyl Cellulose binder

Chemicals : Polyvinylpyrrolidone ; BDH product no. 29579 4F

Methyl cellulose (high substitution) ; BDH. product no.29779 4N

Method :

Solution A

Dissolve 70 g. Polyvinylpyrrolidone (PVP) in 300 ml. methylated spirit. Add the PVP slowly in small amounts to the spirit and stir vigorously.

Solution B

Heat 400 ml. of deionized water in a 1 litre beaker. When nearly boiling remove from source of heat and slowly add 40 g.of methyl cellulose. Stir vigorously with a polythene stirring rod until the methyl cellulose is uniformly dispersed, then slowly add solution A and continue to stir vigorously until a viscose, slightly yellow liquid is produced. Bottle immediately. Clean beakers etc. with water.

Comparison of X-ray fluorescence analyses of standard samples with
usable values of Abbey (1980)

<u>Abbey</u>	AGV-1	GSP-1	G-1	STM-1
SiO ₂	59.61	67.32	69.22	59.5
Al ₂ O ₃	17.19	15.28	15.40	18.5
TiO ₂	1.06	0.66	0.48	0.13
Fe ₂ O ₃	6.59	4.02	2.51	5.0
MgO	1.52	0.97	0.75	0.1
CaO	4.94	2.03	1.96	1.1
Na ₂ O	4.32	2.81	4.06	9.0
K ₂ O	2.92	5.51	4.46	4.3
MnO	0.10	0.04	0.03	0.22
P ₂ O ₅	0.51	0.28	0.13	0.16
Ba	1200	1300	1900	550
Ce	71	360	160	nd
Nb	16	23	13	nd
Rb	67	250	170	nd
Sr	660	240	480	710
Th	64	105	25	nd
U	1.95	2.1	2.1	nd
Y	19	29	11	50
Zr	230	500	300	1200

Nottingham

	AGV-1	GSP-1	G-2	STM-1
SiO ₂	59.88	67.15	69.66	59.50
Al ₂ O ₃	17.03	14.79	15.58	18.78
TiO ₂	1.08	0.63	0.47	0.14
Fe ₂ O ₃	7.44	4.28	2.54	5.96
MgO	1.20	1.21	1.12	0.10
CaO	4.75	1.85	1.88	1.07
Na ₂ O	3.97	2.59	4.25	8.92
K ₂ O	2.95	5.60	4.59	4.29
MnO	0.11	0.04	0.03	0.27
P ₂ O ₅	0.50	0.25	0.15	0.15
Ba	1233	1245	1835	623
Ce	48	323	150	260
Nb	14	27	13	270
Pb	34	52	28	20
Rb	70	252	165	117
Sr	663	232	477	726
Th	3	103	27	31
U	0	2	2	7
Y	21	31	13	50
Zr	235	530	308	1300

The lower limits of detection (ppm) are as follows:-

Ba	8.3	U	1.4
Ce	7	Y	1.2
Nb	1.2	Zr	3.1
Pb	1.5		
Rb	0.7		
Sr	0.9		
Th	0.6		

Appendix 3

Sample localities with brief indication of mineral content

A. Intrusions

Name of Intrusion	Grid Reference	Major Minerals	Minor Minerals	Accessory Minerals
Garnfor (All porphyritic in texture)				
LL1 (Group a)	360460	Pl(E), Af(S), Q	Amph, Opx(Chl), Cpx	Fe-Ti, Ap
LL2 " "	360460	Pl(E), Af(S), Q	Amph, Opx, Cpx	Fe-Ti, Ap
LL3 " "	360459	Pl(E), Af(S), Q	Amph, Opx, Cpx(Chl)	Fe-Ti, Ap
LL4 " "	360459	Pl(E), Af(S), Q	Amph, Cpx(E)	Fe-Ti
LL5 (Group b)	361459	Pl(E), Af(S), Q	Amph, Cpx(E), Bi	Fe-Ti
LL6 " "	361459	Pl(E), Af(S), Q	Amph, Opx, Bi	Fe-Ti, Ap
LL7 (Group a)	361458	Pl(E), Af(S), Q	Amph, Cpx(Chl)	Fe-Ti, Ap
LL9 (Group b)	361458	Pl(E), Af(S), Q	Amph, Cpx, Opx	Fe-Ti
LL10 " "	361458	Pl(E), Af(S), Q	Amph, Cpx, Opx	Fe-Ti, Ap
LL11 " "	361458	Pl(E), Af(S), Q	Amph, Cpx	Fe-Ti, Ap
Nanhoron (All granophyric in texture)				
LL37	287330	Pl, Af, Q		Zr
LL38	287330	Pl, Af, Q		
LL39	287330	Pl, Af, Q		All
LL40	287330	Pl(E), Af, Q		
LL41	287330	Pl, Af, Q		
LL42	288330	Pl, Af, Q		
LL43	288330	Pl(E), Af, Q		
LL44	288330	Pl(E), Af, Q		
LL45	288330	Pl, Af, Q		
LL46	288330	Pl, Af, Q		
LL47	288330	Pl, Af, Q		Sph

Key:

Pl	Plagioclase	(E)	Epidotised	All	Allanite	Opx	Orthopyroxene
Af	Alkali feldspar	Cpx	Clinopyroxene	(S)	Sericitised	Bi	Biotite
Q	Quartz	Fe-Ti	Fe-Ti oxide	(Chl)	Chloritised	Ep	Epidote
Amph	Amphibole	Ap	Apatite	Zr	Zircon	Sph	Sphene

A. Intrusions

Name of Intrusion	Grid Reference	Major Minerals	Minor Minerals	Accessory Minerals
-------------------	----------------	----------------	----------------	--------------------

Llanbedrog (All granophyric in texture)

LL54	330304	Pl(S), Af, Q	Amph(Chl)	
LL55	330304	Pl(E), Af(S), Q	Amph(Chl)	
LL56	330304	Pl(E), Af(S), Q	Amph(Chl)	
LL57	331304	Pl(E), Af(S), Q	Amph	Zr
LL58	331304	Pl, Af(S), Q	Amph	Zr
LL59	331304	Pl, Af, Q	Amph	
LL60	331305	Pl, Af, Q	Amph	
LL61	331305	Pl, Af(S), Q	Amph	
LL62	331305	Pl, Af(S), Q	Amph	Zr
LL63	331305	Pl, Af(S), Q	Amph	Zr
LL132	332304	Pl, Af(S), Q	Amph	
LL133	332304	Pl, Af(S), Q	Amph	
LL134	335305	Pl, Af(S), Q	Amph	Zr, Ep
LL135	335305	Pl, Af(S), Q	Amph	Zr

Penrhyn Bodeilas (All slightly granophyric)

LL64	319421	Pl, Af(S), Q	Amph, Cpx(Chl)	Zr, Ap, Fe-Ti
LL65	319421	Pl, Af(S), Q	Amph, Cpx(Chl)	Zr, Ap, Fe-Ti
LL66	319420	Pl, Af(S), Q	Amph, Cpx(Chl)	Zr, Fe-Ti
LL67	319420	Pl, Af(S), Q	Amph, Cpx(Chl)	Zr, Ap, Fe-Ti
LL68	319420	Pl, Af(S), Q	Amph, Cpx(Chl)	Zr, Ap, Ep, Fe-Ti

Gurn Ddu (All with Granophyric patches)

LL69	393466	Pl, Af(S), Q	Amph(Chl), Opx	Ep, Ap, Zr, Fe-Ti
LL70	393466	Pl(E), Af(S), Q	Amph(Chl)	Ap, Zr, Fe-Ti
LL71	394466	Pl(E), Af(S), Q	Amph(Chl)	Ap, Zr, Fe-Ti
LL72	394466	Pl(E), Af(S), Q	Amph(Chl), Opx	Ap, Zr, Fe-Ti
LL73	395469	Pl(E), Af(S), Q	Amph(Chl)	Ap, Zr, Fe-Ti

Key:

Pl	Plagioclase	(E)	Epidotised	All	Allanite	Opx	Orthopyroxene
Af	Alkali feldspar	Cpx	Clinopyroxene	(S)	Sericitised	Bi	Biotite
Q	Quartz	Fe-Ti	Fe-Ti oxide	(Chl)	Chloritised	Ep	Epidote
Amph	Amphibole	Ap	Apatite	Zr	Zircon	Sph	Sphene

A. Intrusions

Name of Intrusion	Grid Reference	Major Minerals	Minor Minerals	Accessory Minerals
Gurn Ddu (All Porphyritic in Texture)				
LL74	395469	Af(S), Pl, Q	Anph(Ep, Chl)	Zr, Fe-Ti
LL75	395468	Pl, Af(S), Q	Anph, Opx(Ep)	Fe-Ti, Ap, Zr
LL76	395468	Pl, Af(S), Q	Anph, Opx	Fe-Ti, Ap, Zr
LL77	399470	Pl, Af(S), Q	Anph, Opx(Ep)	Sph, Fe-Ti, Ap, Zr
LL78	399471	Pl, Af(S), Q	Opx(Chl)	Ap, Fe-Ti, All
LL79	399471	Pl, Af(S), Q	Anph, Opx(Ep)	Ap, Fe-Ti
Bwlch Mawr (All porphyritic in texture)				
LL80	432478	Af(S), Pl(E), Q	Opx(Chl, E)	Ap, Fe-Ti
LL81	432478	Af(S), Pl(E), Q		Zr, Ap, Fe-Ti
LL82	432479	Af(S), Pl(E), Q		
LL83	432479	Af(S), Pl(E), Q		
LL84	432480	Af(S), Pl(E), Q	Opx(Chl, E)	
LL85	432480	Af(S), Pl(E), Q		
Garn Fadron (All porphyritic in texture)				
LL101	279348	Q, Af(S), Pl(E)	Opx, Cpx	Fe-Ti
LL102	279348	Q, Af(S), Pl(E)	Opx, Cpx	Fe-Ti, Ap
LL103	278350	Q, Af(S), Pl(E)		Fe-Ti, Ap, Zr
LL104	278350	Q, Af(S), Pl(E)		Fe-Ti, Ap, Zr
LL105	278351	Q, Af(S), Pl(E, Chl)		Fe-Ti, Ap
LL106	278351	Q, Af(S), Pl(Chl)		Fe-Ti, Ap
LL107	278351	Q, Af(S), Pl(Chl)		Fe-Ti, Ap
LL157	278350			
LL158	278350			
LL159	278350			
LL160	277351			
LL161	277351			
LL162	277351			

Key:

Pl	Plagioclase	(E)	Epidotised	All	Allanite	Opx	Orthopyroxene
Af	Alkali feldspar	Cpx	Clinopyroxene	(S)	Sericitised	Bi	Biotite
Q	Quartz	Fe-Ti	Fe-Ti oxide	(Chl)	Chloritised	Ep	Epidote
Anph	Amphibole	Ap	Apatite	Zr	Zircon	Sph	Sphene

A. Intrusions

Name of Intrusion	Grid Reference	Major Minerals	Minor Minerals	Accessory Minerals
Garn Penttyrch (All porphyritic in texture)				
LL125	424417	Af, Pl, Q	Opx(Chl)	Ep, Zr, Bi
LL173	425418			
LL174	425418			
LL175	425419	Af(S), Pl(E, Chl)	Opx(E)	
LL176	425419			
LL126		Q, Af(S), Pl(E)	Opx, Cpx	Fe-Ti
LL127		Q, Af(S), Pl(E)	Opx, Cpx	Fe-Ti
LL128		Q, Af(S), Pl(E)	Opx, Cpx	Fe-Ti, Zr
LL129		Q, Af(S), Pl	Opx	
LL130		Q, Af(S), Pl(E)	Opx, Cpx	Fe-Ti, Zr
LL131		Q, Af(S), Pl(E)	Opx, Cpx	Fe-Ti, Zr
LL137	310394	Af(S), Pl(E), Q	Opx(Chl)	Ap
LL138	310394			
LL139	310394			
LL140	311394			
LL141	311394			

Key:

Pl	Plagioclase	(E)	Epidotised	All	Allanite	Opx	Orthopyroxene
Af	Alkali feldspar	Cpx	Clinopyroxene	(S)	Sericitised	Bi	Biotite
Q	Quartz	Fe-Ti	Fe-Ti oxide	(Chl)	Chloritised	Ep	Epidote
Amph	Amphibole	Ap	Apatite	Zr	Zircon	Sph	Sphene

B. Lavas

Name of Lavas	Grid Reference	Major Minerals	Minor Minerals	Accessory Minerals
Moel-y-Pennaen				
LL145	338388	Pl(E)	Amph, Cpx	
LL146	338388			
LL147	338388			
LL148	338388			
LL149	337388			
LL150	337388			
LL151	337388	Pl(S, Chl)	Cpx	Fe-Ti
All Porphyritic in Texture				
LL142 (1)	315386	Pl, Af(S)	Opx(E), Cpx	Fe-Ti, Ap
LL143 (2)	314385			
LL153 (3)	292335		Cpx	Ap
LL154 (4)	298372	Pl(S)		Fe-Ti
LL155 (5)	298371	Pl(S)		
LL156 (6)	311360	Pl		
LL163 (7)	375376			

- | | |
|---------------------|---------------------|
| (1) Near Boduan | (5) Near Fridd Farm |
| (2) Near Boduan | (6) Near Bodgadle |
| (3) Near Nanhoron | (7) Near Pwllheli |
| (4) Near Fridd Farm | |

Key:

Pl	Plagioclase	(E)	Epidotised	All	Allanite	Opx	Orthopyroxene
Af	Alkali feldspar	Cpx	Clinopyroxene	(S)	Sericitised	Bi	Biotite
Q	Quartz	Fe-Ti	Fe-Ti oxide	(Chl)	Chloritised	Ep	Epidote
Amph	Amphibole	Ap	Apatite	Zr	Zircon	Sph	Sphene

Appendix 4
Analytical Data

Nottingham

	LL1 (a)	LL2 (a)	LL3 (a)	LL4 (a)	LL5 (b)	LL6 (b)	LL7 (a)	LL9 (b)	LL10 (b)	LL11 (b)
SiO ₂	61.59	60.85	61.69	61.92	66.70	67.02	62.28	66.12	66.43	67.22
TiO ₂	1.39	1.44	1.47	1.42	0.51	0.52	1.36	0.51	0.49	0.50
Al ₂ O ₃	15.06	14.87	15.36	15.35	15.91	16.23	15.45	15.41	15.78	16.08
Fe ₂ O ₃	1.74	1.79	1.86	1.80	0.90	0.92	1.73	0.83	0.89	0.90
FeO	4.64	4.77	4.96	4.81	2.40	2.45	4.62	2.21	2.36	2.40
MnO	0.14	0.14	0.15	0.15	0.08	0.09	0.14	0.07	0.09	0.08
MgO	1.64	1.54	1.83	1.67	0.89	0.84	1.76	0.80	0.96	0.90
CaO	3.82	3.96	3.89	3.93	1.75	1.75	3.88	1.88	1.66	1.79
Na ₂ O	4.58	4.56	4.78	4.70	5.00	5.24	4.55	4.89	5.13	5.19
K ₂ O	3.20	3.05	3.08	3.13	4.31	4.26	3.21	4.22	4.33	4.26
P ₂ O ₅	0.54	0.55	0.57	0.57	0.18	0.18	0.58	0.17	0.18	0.18
Total	98.34	97.52	99.64	99.45	98.63	99.50	99.56	97.11	98.30	99.50
Ba	573	517	502	508	578	568	565	596	539	577
Ce	92	90	104	92	76	83	98	83	86	85
Cr	9	13	15	12	13	10	12	13	12	20
Cu	11	10	12	9	4	5	8	4	6	5
Ni	0	3	0	2	0	0	0	0	0	0
Nb	32	31	32	33	35	34	31	35	34	35
Pb	14	16	16	18	19	20	17	21	21	18
Rb	73	70	71	70	94	89	74	94	97	90
Sr	381	391	377	382	209	217	378	221	210	206
Th	7	4	2	2	10	14	6	8	8	7
U	0	0	3	2	3	2	2	2	2	2
Y	45	43	42	45	39	38	44	37	41	36
Zn	75	74	78	79	49	53	77	50	57	54
Zr	509	508	510	511	545	538	510	557	537	555
Biz	12.23	12.14	11.08	11.81	15.20	14.35	12.61	15.70	14.19	14.70
C	0	0	0	0	0.27	0.25	0	0	0.07	0.11
Or	18.91	15.03	15.20	18.50	25.47	25.18	18.97	24.94	25.59	25.18
Ab	38.76	38.58	40.44	39.77	42.30	44.24	38.50	41.38	43.40	43.91
An	11.09	11.10	11.36	11.55	7.51	7.51	12.26	7.64	7.06	7.71
Di	3.61	4.14	3.51	3.53	0	0	2.66	0.48	0	0
Hy	7.33	6.93	8.23	7.68	5.19	5.14	8.12	4.41	5.35	5.23
Mt	2.52	2.60	2.70	2.61	1.31	1.33	2.51	1.20	1.29	1.31
Il	2.64	2.73	2.79	2.70	0.97	0.99	2.58	0.97	0.93	0.95
Ap	1.27	1.30	1.35	1.35	0.43	0.43	1.37	0.40	0.43	0.43

Key:

- 0 Element or oxide was below detection limits
- nd not detected
- < below detection limit

Nottingham

	LL37	LL38	LL39	LL40	LL41	LL42	LL43	LL44	LL45	LL46	LL47
SiO ₂	73.58	74.05	74.01	73.50	74.37	74.04	74.09	75.06	74.99	73.72	73.36
TiO ₂	0.25	0.26	0.24	0.27	0.25	0.25	0.22	0.24	0.26	0.26	0.26
Al ₂ O ₃	10.60	10.47	10.51	10.29	10.20	10.45	13.07	10.66	10.18	10.48	10.19
Fe ₂ O ₃	1.05	1.05	1.06	1.07	1.09	1.07	0.97	1.02	1.13	1.03	1.12
FeO	2.81	2.81	2.83	2.85	2.90	2.85	2.58	2.71	3.01	2.75	3.00
MnO	0.11	0.11	0.11	0.11	0.11	0.12	0.12	0.10	0.11	0.10	0.12
MgO	0.06	0.04	0.07	0.06	0.06	0.07	0.02	0.03	0.05	0.04	0.07
CaO	0.31	0.25	0.26	0.28	0.30	0.27	0.34	0.23	0.27	0.22	0.18
Na ₂ O	3.99	4.50	4.38	4.27	4.39	4.40	3.52	3.96	5.09	4.38	4.39
K ₂ O	5.10	4.57	4.71	4.64	4.64	4.62	5.48	5.13	3.75	4.65	4.61
P ₂ O ₅	0.02	0.02	0.02	0.02	0.01	0.02	0.01	0.02	0.02	0.02	0.02
Total	97.88	98.13	98.20	97.36	98.32	98.16	100.42	98.93	98.86	97.65	97.32
Ba	49	41	58	37	63	49	45	44	67	52	59
Ce	172	226	189	189	217	207	184	218	245	246	239
Cr	1	1	3	8	4	3	11	4	1	4	2
Cu	<	<	<	2	<	3	3	<	<	3	<
Ni	6	6	5	7	7	5	2	5	6	8	7
Nb	76	85	78	80	81	79	78	84	96	97	96
Pb	23	32	31	29	28	25	15	15	21	29	30
Rb	190	159	156	156	154	155	213	199	120	177	165
Sr	14	12	7	8	8	10	14	15	8	11	9
Th	16	18	16	19	14	16	25	24	26	32	30
U	2	1	2	<	3	<	2	3	3	4	1
Y	117	137	126	124	129	131	122	140	153	155	150
Zn	150	160	151	143	148	160	139	143	155	161	172
Zr	881	1010	947	884	990	949	892	1042	1116	1144	1136
Qtz	31.39	32.19	31.96	32.23	33.14	32.16	30.18	32.95	33.64	32.00	32.18
C	0	0	0	0	0	0	0.76	0	0	0	0
Or	30.14	27.01	27.84	27.43	27.43	27.31	32.39	30.32	22.16	27.48	27.25
Ab	26.13	28.41	27.84	27.10	26.63	28.03	29.78	26.27	31.49	28.02	26.75
An	0	0	0	0	0	0	1.62	0	0	0	0
Di	1.25	0.99	1.03	1.12	1.26	1.07	0	0.90	1.07	0.85	0.68
Hy	4.44	4.51	4.63	4.55	4.60	4.65	3.85	4.36	4.86	4.45	5.12
Mt	0	0	0	0	0	0	1.41	0	0	0	0
Il	0.48	0.49	0.46	0.51	0.48	0.48	0.42	0.46	0.49	0.49	0.49
Ap	0.05	0.05	0.05	0.05	0.02	0.05	0.02	0.05	0.05	0.05	0.05
Ac	3.04	3.04	3.07	3.10	3.15	3.10	0	2.95	3.27	2.98	3.24
Ns	0.97	1.45	1.34	1.28	1.61	1.32	0	0.90	1.83	1.32	1.56

Key:

- 0 Element or oxide was below detection limits
- nd not detected
- < below detection limit

	LL54	LL55	LL56	LL57	LL58	LL59	LL60	LL61	LL62	LL63
SiO ₂	74.03	73.81	73.31	74.37	70.37	74.35	73.00	74.26	73.55	74.63
TiO ₂	0.19	0.18	0.18	0.16	0.17	0.16	0.16	0.16	0.16	0.16
Al ₂ O ₃	12.60	14.32	14.26	12.91	11.73	13.80	14.04	14.10	13.70	14.26
Fe ₂ O ₃	0.49	0.43	0.47	0.44	0.46	0.42	0.42	0.44	0.39	0.37
FeO	1.30	1.14	1.26	1.18	1.22	1.11	1.13	1.16	1.03	0.99
MnO	0.06	0.10	0.14	0.06	0.05	0.07	0.04	0.04	0.04	0.04
HgO	0.17	0.12	0.11	0.13	0.17	0.14	0.13	0.14	0.12	0.08
CaO	0.81	0.85	1.02	0.50	0.28	0.58	0.20	0.18	0.19	0.28
Na ₂ O	4.09	4.08	3.82	4.17	3.86	4.24	4.39	4.32	4.24	4.20
K ₂ O	4.97	5.15	5.16	5.21	5.24	5.34	5.43	5.47	5.41	5.22
P ₂ O ₅	0.03	0.02	0.03	0.03	0.03	0.02	0.03	0.03	0.03	0.02
Total	98.74	100.20	99.76	99.16	93.58	100.23	98.97	100.30	98.86	100.25
Ba	480	489	476	483	441	478	482	503	476	473
Ce	139	159	141	139	143	142	139	166	152	131
Cr	<	24	0	<	19	2	1	<	<	8
Cu	1	0	4	1	<	<	3	<	1	4
Ni	6	0	0	5	7	4	5	5	5	0
Nb	48	50	51	50	47	48	43	43	46	52
Pb	20	28	29	27	24	27	27	26	26	20
Rb	152	166	165	169	166	166	167	163	162	171
Sr	39	37	41	33	18	24	14	16	18	21
Th	18	16	16	17	13	17	8	14	6	16
U	2	3	3	<	<	3	5	1	3	0
Y	87	79	85	90	89	89	83	88	90	84
Zn	40	54	68	51	52	49	57	61	46	51
Zr	232	250	252	241	224	214	220	210	232	238
Qtz	29.03	27.68	28.71	28.49	26.75	27.14	25.44	26.96	27.05	28.95
C	0	0.53	0.60	0	0	0.04	0.65	0.81	0.59	0
Or	29.37	20.43	30.49	30.79	30.97	31.56	32.09	32.33	31.97	30.85
Ab	34.65	34.51	32.32	35.28	31.16	35.87	37.14	36.50	35.87	35.53
An	1.34	4.08	4.86	1.12	0	2.74	0.79	0.69	0.74	1.25
Di	2.14	1.00	1.03	0	0	0	0	0	0	0
Hy	1.09	1.92	2.16	1.45	1.93	1.90	1.86	1.92	1.67	1.52
Mt	0.71	0.62	0.68	0.63	0	0.60	0.60	0.63	0.56	0.53
Il	0.36	0.34	0.34	0.30	0.32	0.30	0.30	0.30	0.30	0.30
Ap	0.07	0.04	0.07	0.07	0.07	0.04	0.07	0.07	0.07	0.04
Ac	0	0	0	0	1.31	0	0	0	0	0
Na	0	0	0	0	0	0	0	0	0	0

Key:
 0 Element or oxide was below detection limits
 nd not detected
 < below detection limit

	LL65	LL66	LL67	LL68	LL163	LL125	LL140	LL155	LL156
SiO ₂	62.77	63.22	62.67	62.84	63.40	65.52	64.67	56.08	46.16
TiO ₂	0.84	0.74	0.81	0.84	0.96	0.48	0.36	1.41	1.81
Al ₂ O ₃	16.27	16.49	15.96	16.03	14.55	14.05	16.49	15.14	15.24
Fe ₂ O ₃	1.60	1.50	1.56	1.62	2.37	1.63	1.42	3.16	3.44
FeO	4.30	4.02	4.19	4.34	6.31	4.34	3.78	8.42	9.18
MnO	0.17	0.15	0.16	0.17	0.24	0.17	0.21	0.27	0.15
MgO	1.56	1.33	1.47	1.39	1.54	0.61	1.17	1.73	8.01
CaO	2.84	2.50	2.70	2.75	3.11	1.06	1.26	3.70	9.86
Na ₂ O	5.63	5.81	5.92	5.86	3.78	4.51	6.03	4.19	2.44
K ₂ O	3.41	3.45	3.47	3.35	3.48	4.19	3.58	1.36	0.38
P ₂ O ₅	0.39	0.35	0.37	0.40	0.39	0.16	0.09	0.58	0.15
Total	99.78	99.56	99.28	99.59	100.13	96.72	99.06	96.04	96.82

Ba	574	627	595	598	858	650	622	712	328
Ce	129	102	107	126	122	124	127	115	9
Cr	10	11	11	8	11	5	14	13	422
Cu	11	6	8	5	11	7	2	8	79
Ni	0	2	2	0	3	0	0	0	168
Nb	47	45	48	47	48	51	55	50	2
Pb	14	14	19	11	14	24	15	23	7
Rb	61	65	64	57	87	109	62	26	11
Sr	323	293	296	295	276	121	251	732	477
Th	2	3	5	2	5	12	5	9	0
U	2	2	3	1	2	3	3	3	0
Y	53	49	51	51	68	73	62	65	24
Zn	88	84	91	83	144	103	117	166	88
Zr	745	696	730	745	527	573	796	612	114

Qtz	7.69	7.79	6.49	7.31	16.45	17.72	9.16	12.22	0
C	0	0	0	0	0	0.55	0.62	1.33	0
Or	20.15	20.39	20.50	19.80	20.56	24.76	21.16	8.62	2.24
Ab	47.63	49.15	50.08	49.58	31.98	35.15	51.01	35.45	35.45
An	9.05	8.73	6.73	7.54	12.46	4.21	5.66	14.56	29.51
Di	2.08	1.16	3.55	2.92	0.35	0	0	0	14.97
Hy	8.34	7.92	7.24	7.54	12.14	7.66	8.47	15.33	11.89
Ms	2.31	2.17	2.26	2.34	3.43	2.36	2.05	4.58	4.98
Il	1.59	1.40	1.53	1.59	1.82	0.99	0.68	2.67	3.43
Ap	0.92	0.82	0.87	0.94	0.92	0.37	0.68	2.67	0.35
Ac	0	0	0	0	0	0	0	0	0
Ns	0	0	0	0	0	0	0	0	0

Key:

0 Element or oxide was below detection limits
nd not detected
< below detection limit

	LL70	LL72	LL74	LL75	LL76	LL77	LL78	LL79	LL80	LL81	LL83
SiO ₂	63.22	63.36	63.92	63.69	65.39	65.06	64.92	64.87	64.06	65.83	66.42
TiO ₂	0.94	0.88	0.75	0.71	0.67	0.71	0.74	0.75	0.44	0.50	0.47
Al ₂ O ₃	15.26	14.68	14.77	14.20	15.02	15.08	15.19	14.99	17.88	16.34	18.11
Fe ₂ O ₃	1.95	1.96	1.71	1.79	1.61	1.64	1.74	1.76	1.34	1.45	1.38
FeO	5.19	5.23	4.56	4.78	4.30	4.38	4.64	4.68	3.57	3.87	3.68
MnO	0.24	0.26	0.22	0.22	0.20	0.20	0.21	0.20	0.18	0.23	0.20
MgO	1.12	1.13	0.98	0.95	0.94	0.91	0.93	0.99	0.50	0.44	0.50
CaO	2.65	2.41	2.58	2.44	2.23	2.24	2.35	2.29	4.11	3.38	3.55
Na ₂ O	5.05	5.17	4.70	4.83	5.20	5.08	4.97	4.95	1.88	4.43	2.37
K ₂ O	3.68	3.47	3.67	3.43	3.78	3.74	3.63	3.64	3.01	1.79	2.90
P ₂ O ₅	0.35	0.40	0.30	0.33	0.29	0.28	0.26	0.27	0.11	0.13	0.11
Total	99.65	98.95	98.16	97.37	99.63	99.32	99.58	99.39	97.08	98.89	99.69
Ba	759	599	738	627	710	695	669	683	387	313	375
Ce	138	139	128	112	118	111	130	133	114	120	127
Cr	12	10	7	19	9	6	10	12	8	8	7
Cu	7	8	5	3	6	5	7	5	2	5	2
Ni	0	2	2	3	0	0	2	2	0	0	3
Nb	49	44	47	48	48	49	50	49	50	54	49
Pb	18	15	28	16	17	20	20	21	18	22	20
Rb	95	80	95	91	99	98	96	101	88	52	79
Sr	301	262	287	247	266	246	239	238	141	206	137
Th	4	3	7	4	10	12	11	13	8	6	6
U	2	2	2	2	0	2	3	0	2	3	2
Y	61	61	59	64	62	62	65	63	69	69	68
Zn	129	109	115	113	110	108	114	114	101	110	104
Zr	582	570	551	567	585	572	600	591	532	559	536
Qtz	10.89	11.68	14.13	14.43	12.24	13.58	13.91	14.03	30.06	23.17	31.12
C	0	0	0	0	0	0	0	0	4.32	1.28	4.88
Or	21.75	20.51	21.69	20.27	23.34	22.11	21.46	21.51	17.79	10.58	17.14
Ab	42.72	43.74	29.76	40.87	44.00	42.98	42.05	41.88	15.91	37.48	20.05
An	8.10	6.61	8.37	6.94	6.48	7.30	8.42	7.94	19.67	15.92	16.89
Di	2.34	2.33	2.11	2.57	2.29	1.69	1.31	1.42	0	0	0
Hy	8.40	8.64	7.50	7.58	7.00	7.29	7.89	8.01	6.30	6.07	6.46
Mt	2.82	2.84	2.48	2.60	2.32	2.38	2.52	2.55	1.94	2.10	2.00
Il	1.78	1.67	1.42	1.35	1.27	1.35	1.41	1.42	0.84	0.95	0.89
Ap	0.82	0.94	0.71	0.78	0.68	0.66	0.61	0.64	0.26	0.31	0.26
Ac	0	0	0	0	0	0	0	0	0	0	0
Ns	0	0	0	0	0	0	0	0	0	0	0

Key:

0 Element or oxide was below detection limits
nd not detected
< below detection limit

	LL101	LL102	LL103	LL104	LL105	LL157	LL158	LL159	LL160	LL161
SiO ₂	59.69	57.50	56.93	58.37	59.81	62.92	62.39	62.56	61.84	59.57
TiO ₂	0.91	0.83	0.82	0.92	0.98	0.96	0.97	0.90	0.98	0.96
Al ₂ O ₃	13.84	13.86	13.22	14.26	15.46	14.25	14.23	14.38	14.27	13.81
Fe ₂ O ₃	2.53	2.75	2.68	2.75	2.46	2.46	2.49	2.39	2.45	2.51
FeO	6.74	7.33	7.15	7.33	6.55	6.56	6.64	6.37	6.53	6.69
MnO	0.24	0.29	0.30	0.25	0.31	0.28	0.27	0.24	0.28	0.26
MgO	1.42	1.43	1.25	1.67	1.48	1.50	1.43	1.40	1.59	1.48
CaO	3.43	3.58	4.21	3.94	5.49	2.65	2.33	2.94	2.99	3.96
Na ₂ O	3.43	3.66	3.13	3.49	2.63	4.21	4.55	3.73	3.79	3.44
K ₂ O	3.27	3.18	3.58	3.21	2.07	3.50	3.48	3.74	3.29	3.38
P ₂ O ₅	0.44	0.48	0.57	0.48	0.34	0.39	0.40	0.43	0.38	0.46
Total	95.94	94.89	93.84	96.67	97.58	99.68	99.18	99.08	98.49	96.52
Ba	702	795	940	710	455	845	968	1081	871	807
Ce	118	124	112	141	114	117	129	110	122	127
Cr	15	8	8	15	13	9	13	16	7	14
Cu	11	10	12	11	5	10	9	6	8	10
Ni	4	3	5	0	0	3	2	3	2	3
Nb	47	45	43	47	42	47	46	47	48	47
Pb	17	19	19	16	14	18	15	17	18	16
Rb	97	81	97	84	55	79	76	100	81	91
Sr	285	213	311	281	177	190	188	411	334	405
Th	4	4	6	0	4	6	6	7	10	6
U	2	0	2	0	2	0	0	2	0	2
Y	69	69	80	69	63	68	70	66	68	70
Zn	138	153	149	144	133	146	145	140	139	146
Zr	521	487	496	523	492	529	524	528	536	522
Qtz	15.10	11.44	12.37	12.16	19.66	14.35	12.35	15.49	15.33	14.02
C	0	0	0	0	0	0	0	0	0	0
Or	19.33	18.80	21.16	18.97	12.24	20.69	21.16	22.10	19.44	19.97
Ab	29.62	30.97	26.48	29.53	22.25	35.62	35.49	31.55	32.06	29.10
An	12.71	12.00	11.45	13.77	24.27	9.65	7.83	11.45	12.21	12.26
Di	1.22	2.25	4.91	2.25	0.64	0.81	0.94	0.27	0.11	3.73
Hy	12.14	12.77	10.71	13.14	12.31	12.27	12.11	12.02	13.01	10.88
Ms	3.67	2.99	3.89	3.99	3.57	3.57	3.61	3.46	3.55	3.63
Il	1.73	1.58	1.56	1.75	1.86	1.82	1.84	1.70	1.86	1.82
Ap	1.04	1.13	1.35	1.13	0.80	0.92	0.94	1.01	0.89	1.08
Ac	0	0	0	0	0	0	0	0	0	0
Ns	0	0	0	0	0	0	0	0	0	0

Key:

- 0 Element or oxide was below detection limits
- nd not detected
- < below detection limit

	LL142	LL143	LL145	LL146	LL147	LL148	LL150	LL151	LL153	LL154
SiO ₂	52.29	54.66	57.33	56.36	55.56	55.65	56.48	56.27	52.64	53.28
TiO ₂	2.71	2.77	1.47	1.57	1.63	1.58	1.57	1.49	1.05	1.48
Al ₂ O ₃	14.31	13.72	15.01	14.36	14.47	14.76	14.61	14.70	18.73	15.64
Fe ₂ O ₃	2.97	3.05	2.78	2.96	3.11	3.01	2.96	2.90	2.86	3.27
FeO	7.92	8.15	7.41	7.88	8.29	8.04	7.90	7.73	7.62	8.73
MnO	0.17	0.19	0.21	0.24	0.23	0.23	0.23	0.24	0.38	0.34
MgO	4.79	4.25	2.46	2.91	3.09	3.14	2.98	2.88	2.17	2.17
CaO	7.77	4.99	4.87	5.50	5.59	5.50	5.58	5.35	9.69	4.51
Na ₂ O	2.93	2.71	4.13	4.61	4.38	4.62	4.56	3.73	0.79	4.19
K ₂ O	0.90	1.06	2.84	1.07	1.06	0.97	1.22	2.11	1.61	1.50
P ₂ O ₅	0.42	0.44	0.88	0.94	0.92	0.90	0.91	0.90	0.61	0.64
Total	97.18	95.99	99.39	98.40	98.33	99.40	99.00	98.30	98.15	95.75
Ba	441	758	619	401	386	325	401	581	277	686
Ce	72	72	122	111	114	109	134	116	99	117
Cr	45	40	10	11	10	9	10	13	25	27
Cu	16	16	7	8	8	10	10	5	5	6
Ni	15	8	0	2	2	0	2	0	2	2
Nb	24	29	45	44	46	45	44	44	43	52
Pb	11	16	9	14	12	10	14	17	7	10
Rb	21	20	43	16	17	17	21	32	59	30
Sr	658	583	542	545	548	537	515	590	436	775
Th	0	4	2	0	5	2	2	5	0	3
U	0	3	0	0	0	0	0	0	0	0
Y	34	41	61	60	60	60	61	61	59	67
Zn	84	101	146	144	144	143	140	140	139	208
Zr	289	371	513	518	516	518	518	509	501	632
Qtz	11.16	15.30	7.53	8.73	8.39	8.56	8.23	9.58	15.04	6.82
C	0	0.09	0	0	0	0	0	0	0	0.45
Or	0	6.26	16.78	6.32	6.26	5.73	7.21	12.47	9.51	8.86
Ab	24.79	22.92	34.94	39.00	37.05	39.08	38.58	31.55	6.65	35.45
An	25.85	21.88	14.03	15.33	16.69	16.67	15.79	17.14	42.80	18.19
Di	8.08	0	3.67	4.85	4.20	3.94	4.96	2.94	1.08	0
Hy	15.90	18.80	13.55	14.69	15.98	15.94	14.83	15.48	15.45	16.92
Mt	4.30	4.42	4.03	4.29	4.50	4.36	4.29	4.20	4.14	4.74
Il	5.14	5.26	2.79	2.98	3.09	2.00	2.98	2.82	1.99	2.81
Ap	0.99	1.03	2.07	2.21	2.17	2.12	2.14	2.12	1.43	1.51
Ac	0	0	0	0	0	0	0	0	0	0
Ns	0	0	0	0	0	0	0	0	0	0

Key:

- 0 Element or oxide was below detection limits
- nd not detected
- < below detection limit

References

Abbey, S. (1980) Studies in 'standard examples' for use in the general analysis of silicate rocks and minerals. *Geostandards Newsletter*, Vol.4, No.2, p.163-190.

Alberquerque, C.A.R. De (1977) Geochemistry of the tonalitic and granitic rocks of the Nova Scotia southern plutons. *Geochim. Cosmochim. Acta* 41, p.1-13.

Arth, J.G. (1976) Behaviour of trace elements during magmatic processes - a summary of theoretical models and their application. *J. Res. US. Geol. Surv.* 4, p.41-49.

Beckinsale, R.D., Evans, J.A., Thorpe, R.S., Gibbons, W. and Harmon, R. (1984) Rb-Sr whole-rock isochron ages SiO_2 values and geochemical data from the Sarn Igneous Complex and the Parwyd gneisses of the Mona Complex of Llyn, N. Wales. *J. Geol. Soc. London* 141, p.701-9

Bevins, R.E., Kokelaar, B.P. and Dunkley, P.N. (1984) Petrology and geochemistry of lower to middle Ordovician igneous rocks in Wales: a volcanic arc to marginal basin transition. *Proc. Geol. Ass.* 95, p.337-347.

Bowden, R., Bennet, J.N., Whitley, J.E. and Moyes, A.B. (1979) Rare earths in Nigerian Mesozoic granites and related rocks. *Phys.Chem.Earth*, 11, p.479-492.

Campbell, S.D.G., Howells, M.F., Smith, M. and Reedman, A.J. (1988) A Caradoc failed-rift within the Ordovician marginal basin of Wales. *Geol.Mag.*

Carmichael, I.S.E. (1960) The pyroxenes and olivines from some Tertiary acid glasses. *J.Petrol.* 1, p.309-336.

Cattermole, P.J. and Romano, M. (1981) Llŷn Peninsula. The Geologists Association Guide No.39, London, 39pp.

Chappell, B.W. and White, A.J.R. (1974) Two contrasting granite types. *Pacific Geol.* 8, p.173-174.

Cox, K.G., Bell, J.D. and Pankhurst, R.J. (1979) The interpretation of igneous rocks. George Allen and Unwin, London.

Croudace, I.W. (1980) The geochemistry and petrogenesis of the Lower Palaeozoic granitoids of N.Wales. Unpublished Ph.D.thesis, University of Birmingham.

Croudace, I.W. (1981) The geochemistry and petrogenesis of the Lower Palaeozoic granitoids of the Llŷn Peninsula, North Wales. *Geochim,et Cosmochim Acta* 46, p.609-622.

Fitch, F.J. (1967) Ignimbrite volcanism in North Wales. *Bull. Volcanol.* 30, p.199-219.

Fitton, J.G. and Hughes, D.J. (1970) Volcanism and plate tectonics in the British Ordovician. *Earth, Planet. Sci. Lett.* 8, p.223-228.

Gast, P.W. (1968) Trace element fractionation and the origin of tholeiitic and alkaline magma types. *Geochim. Cosmochim. Acta* 32, p.1057-1086.

Hanson, G.N. (1978) The application of trace elements to the petrogenesis of igneous rocks of granitic composition. *Earth and Planet. Sci. Lett.* 38, p.26-43.

Harker, A. (1888) Eruptive rocks in the neighbourhood of Sarn. *Q.J.G.S.*

Harris, A.L., Holland, C.H. and Leake, B.E. (eds) (1979) The Caledonides of the British Isles - Reviewed. *Spec. Pub. Geol. Soc. London* 8, 768pp.

Harris, P.G. (1957) Zone refining and the origin of potassic basalts. *Geochim. Cosmochim. Acta* 12, p.195-208.

Irvine, T.N. and Baragar, W.R. (1971) A guide to the chemical classification of the common igneous rocks. *Canadian J. Earth Sci.* 8, p.523-548.

Kokelaar, B.P. (1988) Tectonic controls of Ordovician arc and marginal basin volcanism in Wales. *J. Geol. Soc. London* 145, p.759-775.

Kokelaar, B.P., Howells, M.F., Bevins, R.E., Roach, R.A. and Dunkley, P.N. (1988) The Ordovician marginal basin of Wales. In Kokelaar, B.P. and Howells, M.F. (eds) *Marginal Basin Geology*. Spec. Pub. Geol. Soc. London, 16, p.245-269.

Leat, P.T. and Thorpe, R.S. (1986) Geochemistry of an Ordovician basalt-tracybasalt-subalkaline/peralkaline rholite association from the Llyn Peninsula, N. Wales, UK. *Geol. J.* Vol. 21, p.29-43.

Le Bas, M.J. (1962) The role of aluminium in igneous clinopyroxenes with relation to their parentage. *Am. J. Sci.* 260, p.267-288.

Matley, C.A. (1938) The geology of the country around Pwllheli, Llanbedrog and Madryn, S.W. Caerns. *W. J. G. S. SCIV*, p.555-606.

Matley, C.A. and Heard, A. (1930) The geology of the country around Bodfean. *Q. J. G. S. Lond.* 86, p.130-168.

O'Hara, M.J. (1977) Geochemical evolution during fractional crystallisation of a periodically refilled magma chamber. *Nature* 266, p.503-507.

Pearce, J.A. and Cann, J.R. (1973). Tectonic setting of basic volcanic rocks investigated using trace element analyses. *Earth Planet. Sci. Letts.* 19, 290-300.

Pearce, J.A., Harris, N.B.W. and Tindle, A.G. (1984) Trace element discrimination diagrams for the tectonic interpretation of granitic rocks. *J. Petrol.* 25, p.956-983.

Pearce, J.A. and Norry, M.J. (1979) Petrogenetic implications of Ti, Zr, Y and Nb variations in volcanic rocks. *Contrib. Mineral. Petrol.* 69, p.33-47.

Potts, P.J., Webb, P.C. and Watson, J.S. (1984) Energy-dispersive X-ray fluorescence analysis of silicate rocks for major and trace elements. *X-Ray Spectrometry*, Vol.13 No.1.

Rayleigh, J.W.S. (1896) Theoretical considerations respecting the separation of gases by diffusion and similar processes. *Philos. Mag.* 42, p.77.

Roberts, B. (1979) The geology of Snowdonia and Llyn: an outline and field guide. Adam Hilger Ltd., Bristol.

Roberts, B. (1981) Low grade and very low grade regional metabasic Ordovician rocks of Llyn and Snowdonia. *Geol. Mag.* 118 (2), p.189-200.

Sedgwick, A. (1843) Outline of the geological structure of North Wales. Q.J.G.S. 4, p.212-224.

Smith, I.E.M., Chappel, B.W., Ward, G.K. and Freeman, R.S. (1977) Peralkaline rholites associated with endesitic arcs of the S.W. Pacific. Earth Planet. Sci. Lett. 37, p.230-236.

Stillman, C.J., Downes, K. and Schiener, E.J. (1974) Caradocian volcanic activity in east and southeast Ireland. Sci. Proc. R. Dubl. Soc. SA., p.87-98.

Stillman, C.J. and Francis, E.H. (1979) Caledonide volcanism in Britain and Ireland. In Harris, A.L., Holland, C.H. and Leake, B.E. (eds). The Caledonides of the British Isles = Reviewed. Spec. Pub. Geol. Soc. London 8, p.557-577.

Stillman, C.J. and Williams, C.T. (1978) Geochemistry and tectonic setting of some Upper Ordovician volcanic rocks in East and Southeast Ireland. Earth, Plan. Sci. Lett. 41, p.288-310.

Thomas, C. and Briden, J.C. (1976) Anomalous geomagnetic field during the late Ordovician. Nature 259, p.380-382.

Tremlett, W.E. (1962) The geology of the Nefyn-Llanaelhaearn area of North Wales. Lpool. Manch. Geol. J. 3, p.157-176.

Tremlett, W.E. (1964) The geology of the Clynog Fawr district and Gurn Ddu hills of Northwest Llyn. Geol. J. 4, p.207-223.

Tremlett, W.E. (1965) The geology of the Chwilog area of southeastern Llyn (Caernarvonshire). Geol. J. 4, p.435-448.

Tremlett, W.E. (1970) The Caledonoid faults of northern Llyn (North Wales). Geol. Mag. 107, p.235-247.

Tremlett, W.E. (1972) Some geochemical characteristics of Ordovician and Caledonian acid intrusions of Llyn, North Wales. Proc. Yorks. Geol. Soc. 39, p.33-57.

Weaver, S.D., Sceal, J.S.C., Gibson, I.L. (1972) Trace element data relevant to the origin of trachytic and pantelleritic lavas in the East African Rift System. Contrib. Mineral. Petrol. 36, p.181-194.

Wood, D.A., Joron, J-L., Marsh, N.G., Tarney, J. and Treuil, M.
(1980) Major and trace element variations in basalts
from the North Philippine sea drilled by IPOD, leg 58. In
Klein, G., Kobayashi, K. et al. Init.Rept.D.S.D.P., 58,
U.S.Govnt.Printing Office, Washington.

Zanettin, B. (1984) Proposed new chemical classification
of volcanic rocks. Episodes, Vol.7 No.4.